

Republic of Iraq  
Ministry of Higher Education  
and Scientific Research  
Al-Nahrain University  
College of Science  
Department of Physics



# **Digital Processing and Analysis for the Tracks Produced From the Irradiation with Neutrons Source $^{241}\text{Am}$ - $^9\text{Be}$ on Some of Solid State Nuclear Track Detectors**

## **A Thesis**

Submitted to the College of Science/ Al-Nahrain University as a Partial  
Fulfillment of the Requirements for the Degree of Master of Science in Physics

**By**

**Mustafa Yousuf Rajab**

B.Sc. Physics / College of Science / Al-Nahrain University

**Supervised by**

**Dr. Hussain Ali Al-Jobouri**

(Assist. Professor)

January 2016 A. D.

Raby` Al-Thaany 1437 A. H.

بِسْمِ اللَّهِ الرَّحْمَنِ الرَّحِيمِ

وَيَسْأَلُونَكَ عَنِ الرُّوحِ قُلِ الرُّوحُ مِنْ أَمْرِ رَبِّي وَمَا أُوتِيتُمْ مِنْ

مِنْ أَمْرِ رَبِّي وَمَا أُوتِيتُمْ مِنْ

الْعِلْمِ إِلَّا قَلِيلًا

"سُورَةُ الْأَسْرَاءِ ٨٥"

# **Supervisors Certification**

We certify that this thesis entitled " **Digital Processing and Analysis for the Tracks Produced From the Irradiation with Neutrons Source  $^{241}\text{Am}$ - $^9\text{Be}$  on Some of Solid State Nuclear Track Detectors** " under our supervision at College of Science / Al-Nahrian University as a partial fulfillment of requirements for the Degree of Master of Science in Physics.

Signature:

Name: **Dr. Hussain Ali Al-Jobouri**

Scientific Degree: **Assist. Prof.**

Date: 21 / 2 /2016

---

In view of the available recommendations, I forward this thesis for debate by the Examination Committee.

Signature:

Name: **Dr. Alaa Jabbar Ghazai**

Title: **Assist. Prof.**

Title: Head of the department of Physics

College of Science / Al-Nahrian University.

Date: 21 / 2 /2016

# Committee Certification

We, the examining committee certify that we have read this thesis entitled " **Digital Processing and Analysis for the Tracks Produced From the Irradiation with Neutrons Source  $^{241}\text{Am}$ - $^9\text{Be}$  on Some of Solid State Nuclear Track Detectors** " and examined the student "**Mustafa Yousuf Rajab**" in its contents and that in our opinion , it is accepted for the Degree of Master of Science in Physics.

Signature:

Name:

Scientific Degree:

Date: 21 / 2 /2016

*(Chairman)*

Signature:

Name:

Scientific Degree:

Date: 21 / 2 /2016

(Member)

Signature:

Name:

Scientific Degree:

Date: 21 / 2 /2016

(Member)

Signature:

Name:

Scientific Degree:

Date: / /2015

(Member/ Supervised)

---

I, hereby certify upon the decision of the examining committee.

Signature:

Name: **Dr. Hadi M. A. Abood**

Title: Assistant Professor

Address: Dean of the College of Science

Date: / /2015

## *Dedication*

 To the big heart my *Dear Father*

 To the fountain of patience and optimism and the hope  
which in existence after Allah and His Messenger, *My  
Dear Mother*

 To those who have demonstrated to me what is the most  
beautiful of life *My Brothers and My Sister*

 To the people who paved our way of science and  
knowledge *Our Teachers Distinguished*

 To whom the tasted of the most beautiful moments with  
*My Friends*

*Mustafa*

# **Acknowledgments**

*Praise be to "ALLAH" , Lord of the whole and peace be upon his messenger Mohammad And his family and companions.*

*I would like to express great my thanks and Gratitude for our god and our Creator "ALLAH" for his graces that enabled me to finish the requirements of this thesis and overcoming all the difficulties and obstacles that encountered in my study.*

*I wish to extend my appreciation and deep thanks to my supervisor **Dr. Hussain Ali Al-Jobouri** for the suggest the project of research, helpful discussions and comments throughout this work, and for reading of this thesis.*

*I would like to express my thanks to all the staff of physics department, for their assistance during the preparation of the thesis . And special mention **Dr. Nada F. Tawfiq** for helping me to solve many problems, also I thanks **Dr. Laith A. Najam** .*

*I would like to express my deep thank to **Dr. Khaled Hadi** in department of physics / college of education for pure sciences / Ibn Al-Haitham / Baghdad University for helping me in Irradiation process*

*My deep thanks to my father , my mother , my brothers , my sisters and my friends , (Ali , Marwa , Rasha , Ula , Fala) for their help me during the work.*

*Mustafa*

# Summary

Image processing technique was used in a lot of studies and research and it concluded, including a number of mathematical relations. In this study, two programs were used, the first one; MATLAB program and second Image-J program. These programs were used to tracks analysis of  $\alpha$  - particles on the nuclear track detectors type CR-39 and CN-85. Where irradiated detectors by thermal neutrons from ( $^{241}\text{Am}$ - $^9\text{Be}$ ) source with activity 12Ci and neutron flux  $10^5 \text{ n.cm}^{-2}.\text{s}^{-1}$ . Which obtained on incident  $\alpha$ -particles for detectors through  $^{10}\text{B}(n, \alpha)^7\text{Li}$  interaction after covered it with boric acid  $\text{H}_3\text{BO}_3$  pellets. The irradiation times -  $T_D$  for both detectors were 4h, 8h, 16h and 24h.

Through the analyze irradiated detectors of using MATLAB outputs for found the following relationships: a)The irradiation time - $T_D$  has behavior linear relationships with following nuclear track parameters, Total track number -  $N_T$ , Maximum track number -  $M_{RD}$  (with depended on track diameter -  $D_T$  at range of radiation response region  $2.5\mu\text{m} - 4\mu\text{m}$  and  $2.5\mu\text{m} - 5\mu\text{m}$  for CR-39 and CN-85 detector respectively) and Maximum track number -  $M_D$  (without depending on track diameter -  $D_T$ ). b) The irradiation time - $T_D$  has behavior exponential relationship with maximum track number -  $M_{RA}$  (with depended on track area -  $A_T$ ) at range of radiation response region  $7\mu\text{m}^2 - 24\mu\text{m}^2$  and  $9\mu\text{m}^2 - 35\mu\text{m}^2$  for both CR-39 and CN-85 detector respectively. c) The irradiation time - $T_D$  has behavior a logarithmic relationship with maximum track number -  $M_A$  (without depending on track area -  $A_T$ ).

While through the analyze of outputs Image-J program for irradiated detectors found the irradiation time -  $T_D$  has behavior linear relationships with following nuclear track detector parameters: a) Total track number -  $N_T$ . b) Maximum track number -  $M_{RA}$  (with depended on track area -  $A_T$ ) at range of radiation response region  $12 \mu\text{m}^2 - 24\mu\text{m}^2$  and  $5 \mu\text{m}^2 - 27\mu\text{m}^2$  for both CR-39 and CN-85 detector respectively. c) Maximum track number -  $M_A$  (without depending on track area -  $A_T$ )

This study show that MATLAB program was more analytical and accuracy from Image-J program, through the logarithmic behavior for both detectors between irradiation time -  $T_D$  with the maximum track number -  $M_A$  (without depending on track area -  $A_T$ ). There is the possibility of future use image analysis of MATLAB program in the other nuclear track parameters analysis, including; etched velocity-  $V_t$ , track diameter-  $D_t$ , critical angle of nuclear track -  $\theta_t$ , nuclear track depth -  $D_p$ .

The image analyze technique for nuclear track detector which obtained from this study especially with regard to track diameter -  $T_D$  can be take into account for classification of  $\alpha$ -particle emitters, In addition to introduce this technique in preparation of nano-filters and nono-membrane in nanotechnology fields.

# *List of Contents*

Subject		Page
List of Contents		I
List of Figures		II
List of Tables		III
List of Abbreviations		IV
Chapter One Introduction and Literature Review		
1.1	A brief history of solid-state nuclear track detectors-SSNTDs	2
1.2	Type of solid state nuclear track detector	3
1.2.1	Inorganic detectors	3
1.2.2	Organic detectors	3
1.3	Radiation	4
1.4	Types of radiation	5
1.4.1	Non ionization radiation	5
1.4.2	Ionization radiation	5
1.5	Some properties of SSNTDs used in this study	6
1.5.1	CR-39 Track detector	6
1.5.2	CN-85 Track detector	7
1.6	Thermal neutron source	7
1.7	Application of SSNTDs	8
1.8	Techniques used with SSNTDs	8
1.8.1	Techniques used with SSNTDs in non-particle radiation	9
1.8.2	Techniques used with SSNTDs in particle radiation	11
1.9	Image processing software for SSNTDs	12
1.10	The aim of study	15

Chapter Two			Materials and Methods		
2.1	Materials	18			
2.1.1	Nuclear track detector	18			
2.1.2	Sensitive balance	18			
2.1.3	pressing	18			
2.1.4	Boric acid	18			
2.1.5	Thermal neutron	19			
2.1.6	Water bath	19			
2.1.7	Optical microscope	19			
2.1.8	Digital Eyepiece for Microscope	19			
2.1.9	Image analysis programs	20			
2.1.9.1	MATLAB program	20			
2.1.9.2	Image-J program	20			
2.2	Method	21			
2.2.1	Preparation of SSNTDs	21			
2.2.2	Preparation the boric acid plate	21			
2.2.3	Thermal neutron irradiation	21			
2.2.4	Chemical etching	22			
2.2.5	Preparation of images	23			
2.2.6	Preparation programs	24			
Chapter Three			Results and Discussion		
3.1	Image processing by using MATLAB program	27			
3.1.1	For CR-39 detector	27			
3.1.2	For CN_85 detector	38			
3.2	Image processing and analysis by using Image-J program	53			
3.2.1	For CR-39 detector	53			
3.2.1	For CN-85 detector	58			
Chapter Four			Conclusions		
4.1	Conclusions	68			
Reference		71			

# *List of Figures*

<b>Figure</b>	<b>Caption</b>	<b>Page</b>
1-1	Chemical form of CR-39 detector	6
1-2	Application fields of solid state nuclear track detector - SSNTDs	9
2-1	The irradiation by thermal neutron on CR-39 and CN-85 detector which covered with boric acid pellets	22
2-2	Sketch of digital system which show optical microscope , video camera and personal computer	24
2-3	Show the flowchart of image processing and analysis in MATLAB after take image from microscope	25
3-1	Images by optical microscope of CR-39 detector irradiated with thermal neutrons for different irradiation times ( un-irradiated , 4h , 8h , 16h and 24h)	27
3-2	First step from image processing of MATLAB program which obtained the track image in CR-39 detector after 24h irradiated time - $T_D$ a) Before image analysis b) After image analysis	28
3-3	Second step from image processing of MATLAB program which obtained the convert to binary system in CR-39 detector after 24h irradiated time - $T_D$	28
3-4	Third step from image processing of MATLAB program which obtained the track intensity - $I_T$ (in pixel) varies with track radius - $R_T$ (in pixel) for CR-39 detector after 24h irradiated time - $T_D$	29
3-5	Forth step from image processing of MATLAB program which appear the pseudo coloring map for tracks of irradiated CR-39 detector at 24h	30

3-6	Fifth step from image processing of MATLAB program which obtained the histogram between the tracks number - $N$ and the tracks diameter - $D_T$ for irradiated CR-39 detector at 24h	30
3-7	Six step from image processing of MATLAB program which obtained the histogram between the tracks number - $N$ and the tracks area - $A_T$ for irradiated CR-39 detector at 24h	31
3-8	Relation between track intensity - $I_T$ (pixel) for CR-39 with track radius - $R_T$ ( $\mu\text{m}$ ) at different irradiation time - $T_D$ (h) for 4h, 8h, 16h, and 24h	31
3-9	Relation between track intensity - $I_T$ for CR-39 with irradiation time - $T_D$ for different track radius - $R_T$ (0.4225, 0.845, 1.2675 and 1.69) $\mu\text{m}$	32
3-10	Relation between the tracks number - $N$ for CR-39 with tracks diameter - $D_T$ ( $\mu\text{m}$ ) at irradiation time - $T_D$ (h) 4h , 8h , 16h and 24h	32
3-11	Calibration curve between irradiation time - $T_D$ (h) with maximum count of track - $M_{RD}$ (relative to track diameter - $D_T$ ) for limited response region between 2.7 $\mu\text{m}$ to 4 $\mu\text{m}$	33
3-12	Relation between maximum track number - $M_D$ (without depending on track diameter - $D_T$ ) with irradiation time - $T_D$ (h)	34
3-13	Relation between the track number - $N$ for CR-39 with area of track- $A_T$ ( $\mu\text{m}^2$ ) at irradiation time - $T_D$ (h) 4h , 8h , 16h and 24h	35
3-14	Calibration curve between irradiation time - $T_D$ (h) with maximum count of track - $M_{RA}$ (relative to track area - $A_T$ ) at limited response region of $A_T$ , starting from 7 $\mu\text{m}^2$ to 23 $\mu\text{m}^2$	35
3-15	Relation between maximum value for track number - $M_A$ (without depending on area of track - $A_T$ ) with irradiation time $T_D$ (h)	36
3-16	Linear relation between the total track numbers- $N_T$ with irradiation time- $T_D$ (h)	37

3-17	Images by optical microscope of CN-85 detector irradiated with thermal neutrons for different irradiation times - $T_D$ ( un-irradiated , 4h , 8h , 16h and 24h)	38
3-18	First step from image processing of MATLAB program which obtained the track image in CN-85 detector after 24h irradiated time - $T_D$ a) Before image analysis b) After image analysis	39
3-19	Second step from image processing of MATLAB program which obtained the convert to binary system in CN-85 detector after 24h irradiated time - $T_D$	39
3-20	Third step from image processing of MATLAB program which obtained the track intensity - $I_T$ (in pixel) varies with track radius - $R_T$ (in pixel) for CN-85 detector after 24h irradiated time - $T_D$	40
3-21	Forth step from image processing of MATLAB program which appear the pseudo coloring map for tracks of irradiated CN-85 detector at 24h	41
3-22	Fifth step from image processing of MATLAB program which obtained the histogram between the tracks number - $N$ and the track diameter - $D_T$ for irradiated CN-85 detector at 24h	41
3-23	Six step from image processing of MATLAB program which obtained the histogram between the track numbers - $N$ and the area of tracks - $A_T$ for irradiated CN-85 detector at 24h	42
3-24	Relation between track intensity - $I_T$ (pixel) for CN-85 with track radius - $R_T$ at different irradiation time - $T_D$ for 4h , 8h , 16h and 24h	42
3-25	Relation between track intensity - $I_T$ for CN-85 with irradiation time - $T_D$ (h) for different radius of track - $R_T$ (0.4225, 0.845, 1.2675, 1.69 and 2.11 $\mu$ m)	43
3-26	Relation between the tracks number - $N$ for CN-85 with track diameter - $D_T$ ( $\mu$ m) at irradiation time - $T_D$ (h) 4h , 8h , 16h and 24h	44

3-27	Calibration curve between irradiation time - $T_D$ (h) with maximum count of track - $M_{RD}$ (relative to track diameter - $D_T$ ) for limited response region between 2.5 $\mu\text{m}$ and 5 $\mu\text{m}$ .	44
3-28	Relation between maximum value for track number- $M_D$ (without depending on track diameter - $D_T$ ) with irradiation time - $T_D$ (h)	45
3-29	Relation between the track number - $N$ for CN-85 with track area - $A_T$ ( $\mu\text{m}^2$ ) at irradiation time - $T_D$ (h) for 4h , 8h , 16h and 24h	46
3-30	Calibration curve between irradiation time - $T_D$ (h) with maximum count of track - $M_{RA}$ (relative to area track - $A_T$ ) at limited response region of $A_T$ , from 9 $\mu\text{m}^2$ and 35 $\mu\text{m}^2$	47
3-31	Relation between maximum count of track - $M_A$ with irradiation time - $T_D$ (h)	48
3-32	Linear relation between the total track numbers- $N_T$ with irradiation time- $T_D$ (h)	49
3-33	Final relation of irradiation time - $T_D$ for nuclear track detector type CR-39 and CN-85 with following nuclear track parameter, a) Maximum track number - $M_D$ (without depended on track diameter) b) Maximum track number - $M_A$ (without depended on track area) c) Total number of track - $N_T$	51
3-34	First step from image processing of Image-J program which obtained the track image in CR-39 detector after 24h irradiated time - $T_D$	53
3-35	Second step from image processing of Image-J program which obtained the convert to binary system in CR-39 detector after 24h irradiated time - $T_D$	53
3-36	Third step from image processing of Image-J program between the track number - $N_T$ and the tracks area- $A_T$ for irradiated CR-39 detector at 24h	54
3-37	Relation between the track number – $N$ for CR-39 with track diameter - $D_T$ at irradiation time - $T_D$ for 4h , 8h , 16h and 24h	55

3-38	Calibration curve between irradiation time - $T_D$ with maximum count of track - $M_{RA}$ (relative to track area - $A_T$ ) at limited response region of $A_T$ , from $12\mu m^2$ and $24\mu m^2$	55
3-39	Relation between maximum track number - $M_A$ for each irradiation time - $T_D$ with irradiation time - $T_D$	56
3-40	Linear relation between the total track numbers - $N_T$ with irradiation time - $T_D$	57
3-41	First step from image processing of Image-J program which obtained the track image in CN-85 detector after 24h irradiated time - $T_D$	58
3-42	Second step from image processing of Image-J program which obtained the convert to binary system in CN-85 detector after 24h irradiated time - $T_D$	58
3-43	Third step from image processing of Image-J program between the track numbers - $N$ and the track area - $A_T$ for irradiated CN-85 detector at 24h	59
3-44	Relation between the track number - $N$ for CR-39 with track area - $A_T$ at irradiation time - $T_D$ for 4h , 8h , 16h and 24h	60
3-45	Calibration curve between irradiation time - $T_D$ (h) with maximum track number - $M_{RA}$ (relative to track area) at limited response region of $A_T$ , starting from $5\mu m^2$ and $27\mu m^2$	61
3-46	Relation between maximum track number - $M_A$ with irradiation time - $T_D$ (h)	61
3-47	Linear relation between the total track numbers - $N_T$ with irradiation time- $T_D$	62
3-48	Final relation of irradiation time - $T_D$ for nuclear track detector type CR-39 and CN-85 with following nuclear track parameters, a) Maximum track number - $M_A$ (without depended on track area) b) Total number of track - $N_T$	64
3-49	Relation between irradiation time - $T_D$ and maximum number of track - $M_A$ for nuclear track detector type CR-39 and CN-85 by using of MATLAB and Image-J programs	65

# *List of Tables*

<b>Table</b>	<b>Caption</b>	<b>Page</b>
1-1	Chemical composition of inorganic nuclear track detectors	3
1-2	Chemical composition of organic nuclear track detectors	4
2-1	show the information about chemical etching for detectors	23
3-1	The final equation which calculated by output of MATLAB program for the relation between irradiation time- $T_D$ with $M_{TD}$ (deepened on diameter), $M_{TA}$ (deepened on area), maximum track number - $M_D$ (without depended on track diameter) , maximum track number - $M_A$ (without depended on track area), and total number of track - $N_T$ .	50
3-2	The final equations which calculated by output of Image-J program for the relation between irradiation time - $T_D$ with MTA (deepened on area), maximum track number - $M_T$ (without depended on track diameter or track area) , and total number of track - $N_T$	63

## *List of Abbreviations*

Abbreviations	Definition
SSNTDs	Solid State Nuclear Track Detectors
TEM	Transmission Electron Microscope
PADC	Polyallyl Diglycol Carbonate
FTIR	Fourier Transform Infrared
SUV	Solar Ultraviolet
TGA	Thermo - Gravimetric Analysis
PL	Photoluminescence
AFM	Atomic Force Microscope
SEM	Scanning Electron Microscope
EDS	Energy-Dispersed Spectrometry
$T_D$	Irradiation Time
$I_T$	Pixel Value Sum of Opened Tracks (intensity)
$R_T$	Track Radius
$D_T$	Track Diameter
$A_T$	Area Track
$M_{RD}$	Maximum Track Number (relative to track diameter - $D_T$ )
$M_D$	Maximum Track Number (without depending on track diameter - $D_T$ )
$M_{RA}$	Maximum Track Number (relative to track area - $A_T$ )
$M_A$	Maximum Track Number (without depending on track area - $A_T$ )
$N_T$	Total Track Number (without depended on track area - $A_T$ or track diameter - $D_T$ )
$D_P$	Depth of Tracks



*Chapter One*  
*Introduction*  
*and Literature Review*

# **Chapter One**

## **Introduction and Literature Review**

### ***1.1 A brief history of solid-state nuclear track detectors-SSNTDs***

During the last 60 years the method generally known as solid state nuclear track detector-SSNTD has grown and is now a distinct branch of science and technology. The science of solid-state nuclear track detectors was born in 1958 when D.A. Young discovered the first tracks in a crystal of LiF. The etch pits, later called “tracks”, were found in a LiF crystal which was previously placed in contact with a uranium foil, irradiated with slow neutrons and treated with a chemically aggressive solution. The thermal neutrons led to fission of the uranium nuclei and the fission fragments bombarded the LiF crystal and damaged it. The damaged regions constituted more chemically active zones than the surrounding undamaged areas, so several books and many articles published in scientific journals and were published on the field of solid state nuclear track detectors - SSNTDs [1, 2].

The First conference on this field was named, International Colloquium on Corpuscular Photography in 1957 in Strasbourg, France. Silk and Barnes (1959) reported the finding of damaged regions in mica. They used the Transmission Electron Microscope - TEM to investigate tracks of heavy charged particles in mica. Fleischer in 1965 conducted extensive investigations of this technique and using in this materials like minerals, plastics and glasses for this technique. CR-39 Polyallyl diglycol carbonate was discovered as nuclear track detector - NTD in 1978 by Cartwright et al. CR stand for Columbia Resin [2-4].

And the final conference was 25st International Conference on Nuclear Tracks in Solids held in Puebla, México in 2011, and the coming one will be the 26<sup>nd</sup> International Conference on nuclear tracks in solids to be held in Kobe, Japan in 2014.

## 1.2 Types of solid state nuclear track detector

### 1.2.1 Inorganic detectors

Inorganic detectors are compounds where carbon and hydrogen do not enter in its structure, and created a "ionic bond" between its atoms. Table (2-1) displays some kinds of the inorganic nuclear track detectors and their chemical composition [5].

**Table(1-1)** Chemical composition of inorganic nuclear track detectors [5]

No.	Detectors	Chemical Composition
1	Zircon	$ZrSiO_4$
2	Quartz	$SiO_2$
3	Mica( Biotite ) Mica (Muscovite)	$K(Mg, Fe)_3 AlSi_3O_{10} (OH)_2$ $KAl_3Si_3O_{10} (OH)_2$
4	Fluorite	$CaF_2$
5	Soda Lime Glass	$23SiO_2 5Na_2O 5CaO Al_2O_3$
6	Olivine	$MgFeSiO_4$
7	Calcite	$CaCO_3$

### 1.2.2 Organic detectors

Organic detectors are compounds where carbon and hydrogen enter in their structures, and created a "covalent bond" between its atoms, this type of SSNTDs has a sensitivity larger than inorganic detectors because the bonds of C-C, C-H which are easily broken after exposure to the radiation, also the organic detectors have a high analytic power larger than inorganic detectors, the threshold energy for organic detectors is less than inorganic detectors. Table (2-2) shows some kinds of the organic detectors and their chemical composition [6].

**Table (2-2)** Chemical composition of organic nuclear track detectors [6].

No.	Detectors	Chemical Composition	
1	Polyester ( HB Pa IT)	$C_{17}H_9O_2$	---
2	Polyimide	$C_{11}H_4O_4N_2$	---
3	Cellulose, <b>Cellulose Nitrate</b> Cellulose Triacetate	$C_6H_8O_9N_2$ $C_3H_4O_2$	(CN ) ( CT )
4	Polycarbonate ( Lexan, Makrofol )	$C_{16}H_{14}O_3$	( PC)
5	Plexiglass	$C_5H_8O_2$	---
6	<b>Polyallyl diglycol Carbonate</b>	$C_{12}H_{18}O_7$	<b>(CR-39)</b>

### 1.3 Radiation

[Radiation](#) is energy given off by matter in the form of rays or high-speed particles. Radiation travels from its source in the form of energy waves or energized particles. These atoms constantly seek a strong, stable state. As they convert from an unstable to stable form they release excess atomic energy in the form of radiation. All matter is composed of [atoms](#), atoms are made up of various parts, the [nucleus](#) contains minute particles called [protons](#) and [neutrons](#), and the atom's outer shell contains other particles called [electrons](#). The nucleus carries a positive electrical charge, while the electrons carry a negative electrical charge. Radiation is part of our environment, It comes from both natural and man-made sources. Natural sources include cosmic radiation from space, radioactive rocks and soils, and other radioactive materials found in food and water. Humans have been exposed to these natural radiation sources since the dawn of humanity. Man-made sources of radiation include medical diagnosis and treatment, nuclear power industry, scientific research, consumer products, and nuclear weapons testing [7, 8] .

Radiation can come from as far away as outer space and from as near as the ground that you are standing on. Because it is naturally all around us, we cannot eliminate radiation from our environment. We can, however, reduce our health risks by controlling our exposure to it [9].

## ***1.4 Types of radiation***

Radiation has so much energy it can knock electrons out of atoms, a process known as ionization, but There is another radiation has no much energy to knock electrons out of atoms known as non-ionization radiation.

### ***1.4.1 Non ionization radiation***

Non-ionizing radiation has less energy than ionizing radiation ; it does not possess enough energy to produce ions. The non-ionizing radiation spectrum is divided into two main regions, optical radiations and electromagnetic fields. The optical can be further sub-divided into ultraviolet, visible, and infra-red. The electromagnetic fields are further divided into radiofrequency (microwave, very high frequency and low frequency radio wave). Non-ionizing radiation originates from various sources: natural origin (such as sunlight or lightning discharges etc.) and man-made (seen in wireless communications, industrial, scientific and medical applications) [7, 10].

### ***1.4.2 Ionization radiation***

Ionizing radiation is capable of knocking electrons out of their orbits around atoms, upsetting the electron / proton balance and giving the atom a positive charge. Electrically charged molecules and atoms are called ions. Ionizing radiation includes the radiation that comes from both natural and man-made radioactive materials. There are several types of ionizing radiation Alpha radiation  $\alpha$ , Beta radiation  $\beta$ , photon radiation (gamma  $\gamma$  and x-ray) and neutron radiation n. These were

collectively called ionizing radiation because of their ability to strip one or more electrons away from atoms in whatever material they pass through [7, 11].

### ***1.5 Some properties of SSNTDs used in this study***

There are several type of solid state nuclear track detectors but in this study, two types of organic detector were used ; CR-39 and CN-85 track detectors.

#### ***1.5.1 CR-39 track detector***

Polyallyl diglycol carbonate - PADC which is generally referred as CR-39 the most sensitive of the nuclear track recording plastics. It was first discovered by Cartwright, this detector consists of short polyallyle chains joined by links containing carbonate and die ethylene glycol groups into a dense three dimensional network [12]. The chemical form of CR-39 is  $C_{12}H_{18}O_7$  it is illustrated in figure (1-1) [13].

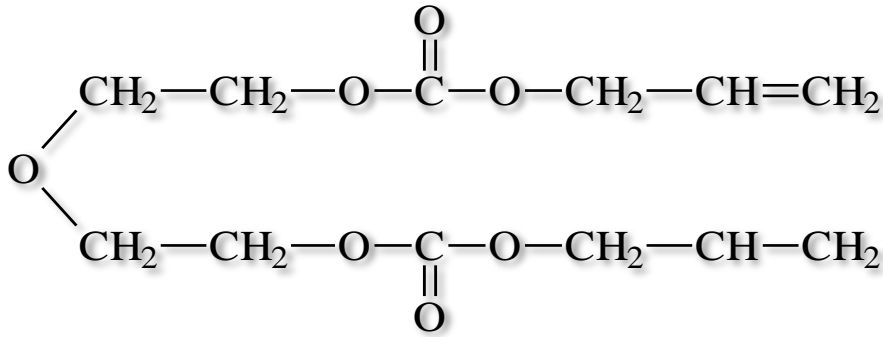


**Figure (1-1)** Chemical form of CR-39 detector [13]

The general characteristics of CR-39 can be summarized as [14]:

1. Amorphous polymer.
2. Optically clear.
3. Environmentally very stable.
4. Having a closed packed and uniforms molecular structure.
5. Having non – solvent chemical etchant.

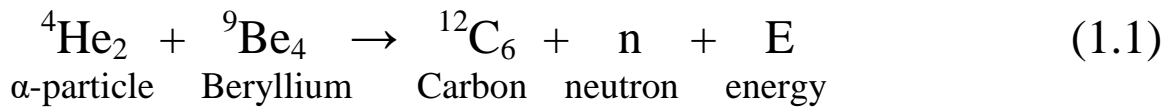
6. Highly cross – linked thermoset.
7. Sensitive to heavy ion damage.

### ***1.5.2 CN-85 track detector***

This detector contains in chemical composition on nitrogen which has a chemical structure  $C_6H_{18}O_5N_2$ , and it is one of the good detectors for the detection of neutrons and charged particles such as protons, alpha particles, fission fragments and heavy ions. Detector estimated thickness of about 100  $\mu m$ , for detection of neutrons the detector covered by boric acid  $H_3BO_3$  to get on  $(n,\alpha)$ , for the interaction the thermal neutron with boron and get the interaction  $^{10}B (n,\alpha) ^7Li$  [15, 16].

### ***1.6 Thermal neutron source***

Neutron sources vary in intensity and in the energy of the neutrons emitted. They can be classified into three groups: nuclear fission reactors, radioisotopes, and particle accelerators. Nuclear reactors are obviously not portable, and not suitable for nuclear well logging sources. Radioisotopes are the most commonly used neutron source in well logging applications. Particle accelerators have seen relatively limited (although growing) use in well logging. The  $(n, \alpha)$  neutron sources contain an  $\alpha$ -emitting radioisotope, with low mass nuclei as a target. As compared to other isotopes, where the Beryllium  $^9Be_4$  is the most important target, because it has the highest neutron yield. The long half-life ( $\sim 433$  years) of  $^{241}Am-^9Be$  would provide an almost constant level of neutron flux from the source over the lifetime of the equipment ( $\sim 20$  years) the energetic neutrons are generated following an interaction (1.1) between the alpha particle and the target material's nucleus .



The alpha particles were emitted by Americium  ${}^{241}\text{Am}$  decay, impinge on a  ${}^9\text{Be}_4$  target, producing neutrons over a broad range of energies with an average energy around 4.2 MeV and a maximum around 10 MeV [17, 18, 19].

### ***1.7 Applications of SSNTDs***

Polymeric materials find several applications in different fields from everyday life to high technology engineering, especially solid state nuclear track detectors - SSNTDs which are used in different applications and many articles are studied to understand and modify these polymers. One of the most important ways to promote progress in science and technology is to constantly explore new measurement means. Currently, the research in this area is rather active both at home and abroad [20, 21] Application of SSNTDs in many fields, as environments, accident and general fields as show in figure (1-2).

### ***1.8 Techniques used with SSNTDs***

Studies show that nuclear track evaluations using the recent developed methods based on the theoretical and practical aspects of modern optics can be accurate as well as the conventional methods (such as using the optical microscopes) but faster than using the traditional methods. These recent developed methods include application of fourier optics and also applying image processing techniques to improve track images. In fact, these methods are able to improve applications of SSNTDs, particularly when they are accompanied by image processing techniques [22].

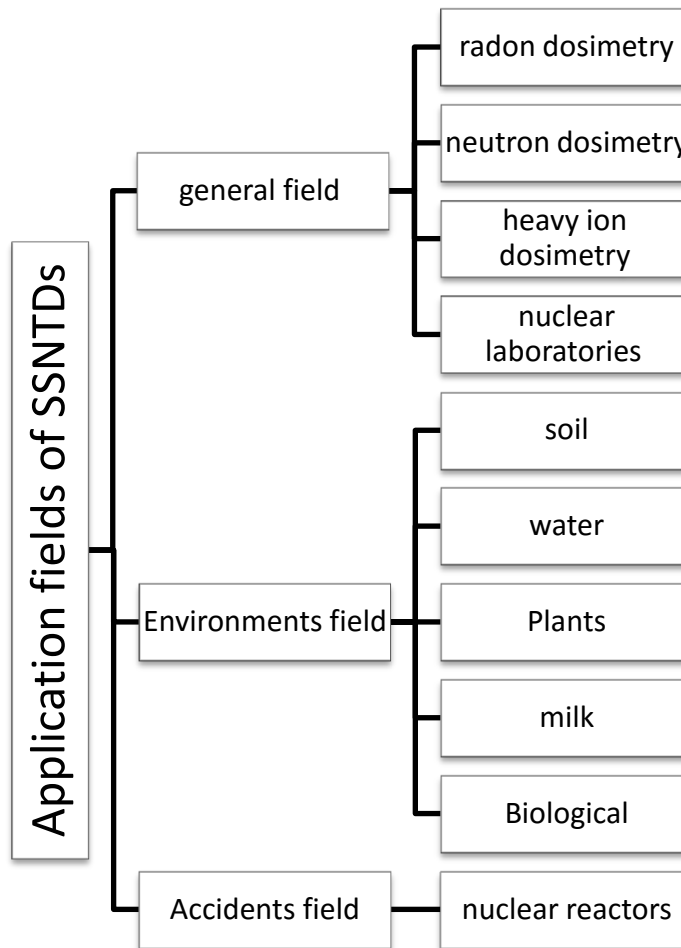


**Figure 1-2** Application fields of solid state nuclear track detector - SSNTDs

### ***1.8.1 Techniques used with SSNTDs in non-particle radiation***

Non-particle radiation such as gamma ray, x-ray, and UV radiation. UV-visible spectroscopy was used to determine the effect of pre-gamma irradiation on track density, bulk etch rate and light absorbance in CR-39 were investigated by IPE, et. al. (1985) [23]. Chong, et. al. (1997)[24] studied the UV- visible spectroscopy and Fourier Transform Infrared - FTIR spectroscopy of CR-39 plastics irradiated with 50 kVp tube x-rays. Shweikani, et. al. (2002)[25] determined the alpha tracks diameters and tracks densities by using UV-visible spectroscopy, and FTIR spectroscopy to show the effects of solar ultraviolet - SUV and ultraviolet type A-UVA produced by a solar UV simulator on CR-39 detectors .

UV-visible spectroscopy technique also used to study the effects of the x-ray irradiation and chemical etching on the physical and optical properties of CR-39 plastic detectors irradiated by different doses of x-ray were studied by Nur Sha'dah, et. al. (2014) [26]. FTIR spectroscopy used to study the chemical and structural changes occurring in polymeric systems due to irradiation to gamma radiations at different doses by Meenakshi, et. al. in same year [27].

After these studies Hussain, et. al. (2012) [28] study the effect of x-ray radiation on electro-optical characteristics of CR-39 sheets by using FTIR spectroscopy technique. In (2013) Abdel Raouf [29] study the comparison between the effect of many types of radiation (gamma-rays and x-rays) on the sensitivity of CR-39 detector by using the FTIR spectrometer. Where in same year Emad [30], study the effect of low gamma absorbed positron annihilation lifetime - PAL in conjunction with Transmission Electron Microscopy-TEM and Thermo - Gravimetric Analysis-TGA on PM-355 detector.

Tse, et. al. (2006) used FTIR spectroscopy technique to study the effects of ultraviolet - UV photons at different wavelengths on the polyallyl diglycol carbonate-PADC [31]. UV-visible spectroscopy technique used by Zaki, (2008) [32] to study the effect of gamma irradiation on optical absorption spectral of nuclear track detectors. Zaki, et. al. (2012) studied the effects of He-Ne laser on the optical characteristics of cellulose nitrate, CN-85, and CR-39 detectors, by using photoluminescence - PL and UV-visible spectroscopy techniques [33]. Photoluminescence spectroscopy and UV-visible spectroscopy technique were used by Tayel, et. al. (2014) to obtaining information about the interaction of gamma rays with track detector type Makrofol-DE [34].

### ***1.8.2 Techniques used with SSNTDs in particle radiation***

Particle radiation such as alpha particle, beta particle, ions, protons, fast neutron and thermal neutron. There was many techniques used to processing particle radiation with SSNTDs. One of these techniques is Atomic Force Microscope - AFM which used by Nikezic, et. al. (2002) to investigate the characteristics of tracks of heavy charged particles in solid state nuclear track detectors - SSNTDs [35]. Where the long-term measurements of radon progeny was determined the concentrations by using solid state nuclear tract detector which are being actively explored, These measurements depend critically on the thickness of the removed layer during etching, Scanning Electron Microscope - SEM observations have identified irregularities in etched LR 115 detectors by [36]. In (2003) Ho, et. al. used Atomic Force Microscope - AFM to study these pits on the surface of the LR 115 detector after etching as well as genuine alpha tracks for short etching time in LR-115 [37] and for same detector used for measurements of concentrations of radon gas and/or radon progeny. These measurements depend critically on the removed thickness of the active layer during etching [38] .

Vlasova, et. al. (2004) developed the track analysis methods to locate micro distribution of  $^{239}\text{Pu}$  and  $^{235}\text{U}$  combined with the analysis of contaminated micro particles by scanning electron microscopy-SEM with energy-dispersed spectrometry-SEM-EDS [39]. FTIR Spectrophotometer technique was used also with SSNTDs by Basua, et. al. (2005) to study a particular brand of polymer, commonly used as overhead projector transparencies [40]. Then Sharma, et. al. [41] study the neutron - irradiation effects on optical absorption of solid state nuclear track detector type CR-39 by UV-visible spectroscopy .

While Nidhi, et. al. used UV-visible spectroscopy and FTIR spectroscopy to study the effect of thermal annealing on optical properties of CR-39 [42]. Photoluminescence-PL technique used with UV-visible and FTIR spectroscopy

techniques by Ghazaly, M. El. and Hassan, H. E. (2014) to study on alpha particle - irradiated CR-39 detector [43].

x-ray diffraction technique with FTIR spectroscopy and UV–visible spectroscopy techniques were used to study the effects of swift heavy ion beam irradiation on the structural, chemical and optical properties of Makrofol detector by Ambika et. al. [44]. The same study by Vijay, et. al. was determined the effect of 120 MeV Nion ions beam irradiations at various fluence [45].

Scanning Electron Microscopy - SEM was used in four different variants to investigate the trace distribution of alpha particles on CR-39 as well as the fission fragments on a mica muscovite solid state nuclear trace detectors-SSNTD which work by Costea, et. al. [46].

Optical microscope and a Scanning Electron Microscope - SEM used analyzed the solid state nuclear track detector type CR-39 which expose to DT neutrons by Mosier-Boss, et. al. [47]. Etched tracks at nano size scale was analysis By Atomic Force Microscope-AFM by Espinosa, and Golzarri, [48]. When the surface morphology characterization was determined by Scanning Electron Microscopy - SEM and optical microscope by Malinowska, et. al. (2013) [49].

### ***1.9 Image processing software for SSNTDs***

In (1976) Abmayr, et. al. used on-line TV-system for real time analysis of two-dimensional images is described which is being used for automatic evaluation of track detectors, histological cell analysis, and a number of other purposes. Results are reported for applications commonly encountered in dielectric track detector evaluation problems ; namely determination of the integral track density, of the spatial distribution of tracks, and of statistical distributions of geometrical features of tracks. Special emphasis is given to the region of low track densities [50] .

James and Adams (1980) [51] was provide automate certain aspects of data analysis in cosmic-ray experiments employing plastic track detectors. This is due to the discovery of a new track detector type CR-39, and the development of fast microprocessor-based image analyzers. Measurements of etch cones made by  $\alpha$ -particles and fission fragments in CR-39 are described. Estimates are made of the accuracy with which the etch-rate ratio incidence angle, and track location can be measured under a variety of conditions. Possible applications to cosmic-ray physics are discussed .

Guel, S. et. al. (1984) [52] used a real time pseudo coloring technique for nuclear tracks on CR-39 detectors is proposed. The technique basis is track illumination from different directions with different colors. The track themselves diffusely reflect the colored light, giving color images that, when seen simultaneously, allow easy identification and measurements .

Radomirand and Mitja in (1990) [53] used a physical model of image formation in solid state nuclear track detectors has been formulated. Using this model the large area signal function (optical density over a large area) is calculated. The theoretical calculations are verified by experiments with LR-115, CA-8015 and CR-39 detectors using the  $^{10}\text{B} (n, \alpha) ^7\text{Li}$  reaction.

A Boukhair et. al. used a code for the numerical analysis of images from a CCD camera, including correction of acquisition system defects, has been written and applied to the visualization of  $\alpha$ -particle tracks in the solid state nuclear track detectors CR-39 and LR-115. A standard mask having different diameter holes permitted the calibration of the imaging system [54] .

In (2007) Patiris et.al. [55] used A computer program named TRIAC written in MATLAB has been developed for track recognition and track parameters measurements from images of the solid state nuclear track detectors CR39. The program using image analysis tools counts the number of tracks for dosimetry proposes and classifies the tracks according to their radii for the spectrometry of

alpha-particles as used same computer program named TRIAC II has been developed for recognition and parameters measurements of particles' tracks from images of solid state nuclear track detectors .

Fuminobu et. al. in (2007) [56] used observation system was developed to record time-lapse images of etch pits formed on the surface of a solid-state nuclear track detector - SSNTD CR-39. Pit-evolution images were constructed by digital image processing of the data of the time-lapse images. In addition, a finite element model of SSNTD was used to simulate the etch pit formation. Pit-evolution image analysis and computational simulation were performed to reveal the etch pit formation obtained via the incidence angle of energetic particles on a CR-39. Where Pugliesi et. al. [57] was study the comparison of the results together with the feasibility and rapidness in data acquisition have demonstrated the viability of the digital system to characterize SSNTD.

After that in (2008) Mostofizadeh et. al. [58] used MATLAB software as method to study edge detection, all measurements carried out in two cases of before and after improvement of track images. Considering the overlapping phenomenon –including double and triple tracks- experimental and statistical results showed that not only each particular edge detection method affects the accuracy of measurements.

Law et. al. in (2008) used TRACK\_TEST computer program to explained differentiation among recorded tracks for which the grey levels, major and minor axes values were used as inputs and from which the angle and energy of the incident alpha particles were given as the outputs [59] .

Nikezic and Yu in (2009) [60] used a computer program was developed to calculate the light scattered from an assembly of alpha particle tracks in a CR-39 detector. The tracks were randomly seeded on the film to simulate the irradiation by alpha particles emitted by the naturally occurring radon gas and its short-lived progeny. The ray-tracing method was applied to simulate light propagation through the tracks. The total amount of scattering increased linearly with the track density and

quadratically with the removed layer during chemical etching of the irradiated CR-39 detector.

Palacios et. al. (2010) [61] used STATISTICA software to analyze and correction of track overlapping on nuclear track detectors - SSNTD by A model for the track overlapping process. While Hadad et. al. (2011) [62] used of an automated counting system which was based on a high resolution scanner and related image processing software. Once the electrochemical etching was performed, the etched CR-39 films were scanned and counted by developed software (called NTC) with high accuracy .

SRIM software used by Zylstra et. al. [63] to study track formation process is explored with a Monte Carlo code, which shows that the track formation difference between frontand. When Felice et. al. (2012) [64] used the novel ENEA-INMRI image analyzer system has been tested in semi-automated mode for a computer-assisted alpha track counting of electro-chemically etched-ECE and chemically etched CR-39 solid state nuclear track detector - SSNTD chips .

In (2013) Osinga et. al. [65] used  $\text{Al}_2\text{O}_3:\text{C},\text{Mg}$ -based fluorescent nuclear track detectors-FSSNTDs and confocal laser scanning microscopy as a semiautomatic tool for fluence measurements in clinical ion beams. Then Firas et. al. (2013) [66] used MATLAB software to determined parameters of nuclear track detector, such as nuclear track diameter  $D_T(\mu\text{m})$ , number of track-N and area of track- $A_T$  .

### ***1.10 The aim of study***

The main purpose of the present work is to analysis of nuclear track detectors – SSNTDs parameters as total numbers, diameters and areas of tracks for CR-39 and CN-85 detectors after irradiated by thermal neutrons from ( $^{241}\text{Am}-^9\text{Be}$ ) source. The analysis included the image processing of these irradiated detectors by using of two programs, first was MATLAB program and second Image-J program. The possibility of using this technique in an accurate diagnosis of the particle radiation

effect on SSNTDs and take advantage of this study in the areas of nano- technology researches .



*Chapter Two*  
*Materials and Methods*

## ***Chapter Two***

### ***Materials and Methods***

#### ***2.1 Materials***

This chapter describes the use of two types for solid state nuclear track detectors-SSNTDs CR-39 and CN-85 and expresses the methods to preparation of samples (boric acid) in addition to the apparatus and material.

##### ***2.1.1 Nuclear track detector***

In this study two types for solid state nuclear track detectors-SSNTDs CR-39, and CN-85 were used, manufactured by TASTRAK Pershore Moulding ,Track Analysis System Ltd., UK and Kodak-Pathe - France respectively.

##### ***2.1.2 Sensitive balance***

A very sensitive balance for a little weights, readability of 0.0001 g and maximum weight of 200 g manufactured in Switzerland type of Mettler AC100 were be used in this study for weighting samples.

##### ***2.1.3 Pressing***

Piston used to press samples of boric acid, it is the type of Carver manufactured in USA, weight it 0.5 g under force 2000 kg for 30s of time with diameter 1.5 cm and thickness 1 mm.

##### ***2.1.4 Boric acid***

Boric acid ( $\text{H}_3\text{BO}_3$ ) is a boron compound which is soluble, colorless, water-soluble and salt-like white powder. Boric acid used as pellets to show thermal neutron tracks as  $^{10}\text{B}(n,\alpha)^7\text{Li}$ .

### ***2.1.5 Thermal neutron***

The thermal neutron irradiation system consists of a rod of  $^{241}\text{Am-}^9\text{Be}$  source surrounded by a paraffin wax. The paraffin wax was used to moderating the fast neutrons to thermal neutrons energies. The source of thermal neutron was  $^{241}\text{Am-}^9\text{Be}$  with activity 12Ci, neutron flux  $10^5 \text{ n.cm}^{-2}.\text{s}^{-1}$ . It was found in department of Physics - College of Education for Pure Sciences - Ibn Al-Haitham - Baghdad University

### ***2.1.6 Water bath***

Water bath was used to regulate the etchant solution temperature. It is the type of Memmert manufactured in Germany, it included a thermostat operating over a range of 20 °C to 110 °C and temperature regulation accuracy better than  $\pm 0.2$  °C. The chemical etching was carried out at 60 C°. Distilled water was used as the bath liquid.

### ***2.1.7 Optical microscope***

The counting of chemically etched tracks was carried out using optical microscope (type Motic, Malaysia). It is capable of giving magnifications of 400x and eyepiece 10x to measure the number of tracks, and eye piece type scalar to calculate the number of tracks.

### ***2.1.8 Digital eyepiece for microscope***

Digital camera which used in this study have 1.3 Mega pixel high resolution USB 2.0 color digital image system. It captures microscope images and displays live video on the PC screen. It offers full-screen-size display and the same resolution as your computer screen. This microscope image system comes with a 1280 x 1024 pixel digital camera, user-friendly software, compatible

with Windows 2000 / XP / Vista, and adapters for microscopes. As well as a real time video or capture still images and save them as JPG file.

### ***2.1.9 Image analysis programs***

There are many program of image analysis, in this work two programs are adopted with SSNTDs, the first one is MATLAB and the second one was Image-J programs.

#### ***2.1.9.1 MATLAB program***

MATLAB is the high-level language and interactive environment used by millions of engineers and scientists worldwide. It lets you explore and visualize ideas and collaborate across disciplines including signal and image processing, communications, control systems, and computational finance. used MATLAB in projects such as modeling energy consumption to build smart power grids, developing control algorithms for hypersonic vehicles, analyzing weather data to visualize the track and intensity of hurricanes, and running millions of simulations to pinpoint optimal dosing for antibiotics. The version of MATLAB program was R2013b (8.2.0.701) for 64bit (win 64).

#### ***2.1.9.2 Image-J program***

Image-J is written in Java language, which allows it to run on Linux, Mac OS X and Windows, in both 32-bit and 64-bit modes. Image-J and its Java source code are freely available and in the public domain. No license is required. Image-J has a large and knowledgeable worldwide user community. In analysis Measure area, mean standard deviation, min and max of selection or entire image. Measure lengths and angles. Use real world measurement units such as millimeters. Generate histograms and profile plots. In this study used version Image-J 1.48 bundled with 64-bit Java.

## **2.2 Methods**

### **2.2.1 Preparation of SSNTDs**

Two types of solid state nuclear track detector SSNTDs which are CR-39 and CN-85 in the form of sheets with thickness 1 mm and 0.1 mm for CR-39 and CN-85 respectively were used, These sheets were cut into eight small pieces, four pieces for each detector with dimensions 1cm × 1cm.

### **2.2.2 Preparation the boric acid pellets**

Prepared eight samples of boric acid powder, four samples for each detector, each sample has weight 0.5 g. pressed samples of boric acid in piston for 30s under 150 par of the force in steel piston with thickness 1mm and diameter 2cm. The pellet was covered with CR-39 and CN-85 detectors.

### **2.2.3 Thermal neutron irradiation**

CR-39 and CN-85 detectors covered with pellets of boric acid ( $\text{H}_3\text{BO}_3$ ) to convert free neutrons into charge-particle by equation  $^{10}\text{B}(n,\alpha)^7\text{Li}$ , put a pellet around the paraffin wax and irradiation samples with thermal neutron at a distance of 5 cm from neutron source  $^{241}\text{Am}-^9\text{Be}$  with flounce of thermal neutron  $10^5 \text{ n.cm}^{-2}.\text{s}^{-1}$ . The irradiation times -  $T_D$  were 4h, 8h, 16h and 24h for CR-39 and CN-85 detector as show in figure (2-1).

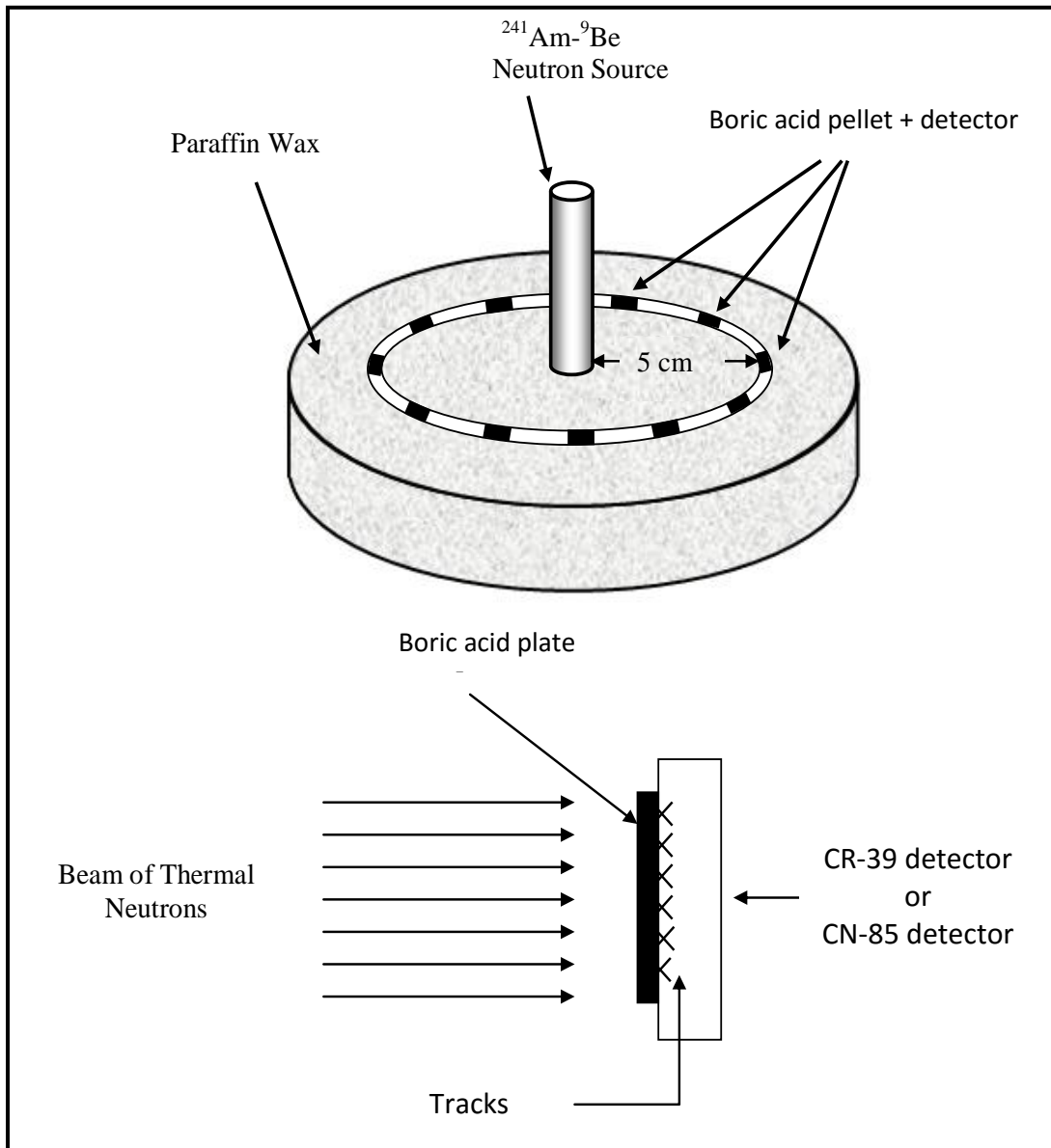


**Figure 2-1** The irradiation by thermal neutron on CR-39 or CN-85 detector which covered with boric acid pellets

### 2.2.4 Chemical etching

After irradiation and remove pellets of boric acid from the prepared detectors chemical etching solution, Sodium hydroxide NaOH solution with 6.25N, 2.5N has been used for the etching process for CR-39 and CN-85 respectively. The etchant solution was prepared using volumetric flask and applying the following equation:

$$W = W_{eq} \times N \times V \quad (2.1)$$

where:

W: weight of NaOH needed to prepare the given normality.

$W_{eq}$ : equivalent weight of NaOH.

N: normality and equals to 6.25 N, and 2.5 N for CR-39 and CN-85 respectively.

V: volume of distilled water (250 ml).

Molecular weight of NaOH is sum of the atomic weight of sodium, oxygen and hydrogen,

$$W_{eq} = 22.98977 + 15.9994 + 1.00794 = 39.99711 \text{ g/mol}$$

The information of chemical etching for CR-39 and CN-85 as shown in table (2-1)

**Table 2-1** Information about chemical etching for detectors

Detector	Normality (N)	Weight (g)	Etching time (min)	Temperature (C°)
CR-39	6.25	62.5	30	60
CN-85	2.5	25	15	50

### ***2.2.5 Preparation of images***

After chemical etching processes the detectors were put under optical microscope and install the digital camera on the microscope and defined it on computer, then take image for detectors which contain on the nuclear tracks, and store these images (pixel unit) in computer at the form (jpg) and has special name, after that insert these images to image processing programs for analysis, where the one pixel in these images was equal to converting factor 0.4225  $\mu\text{m}$  which calculated by using of role scale in optical microscope and take into account in the image processing of

MATLAB program. Figure (2-2) shows digital system which it consist of optical microscope, digital camera, and computer.

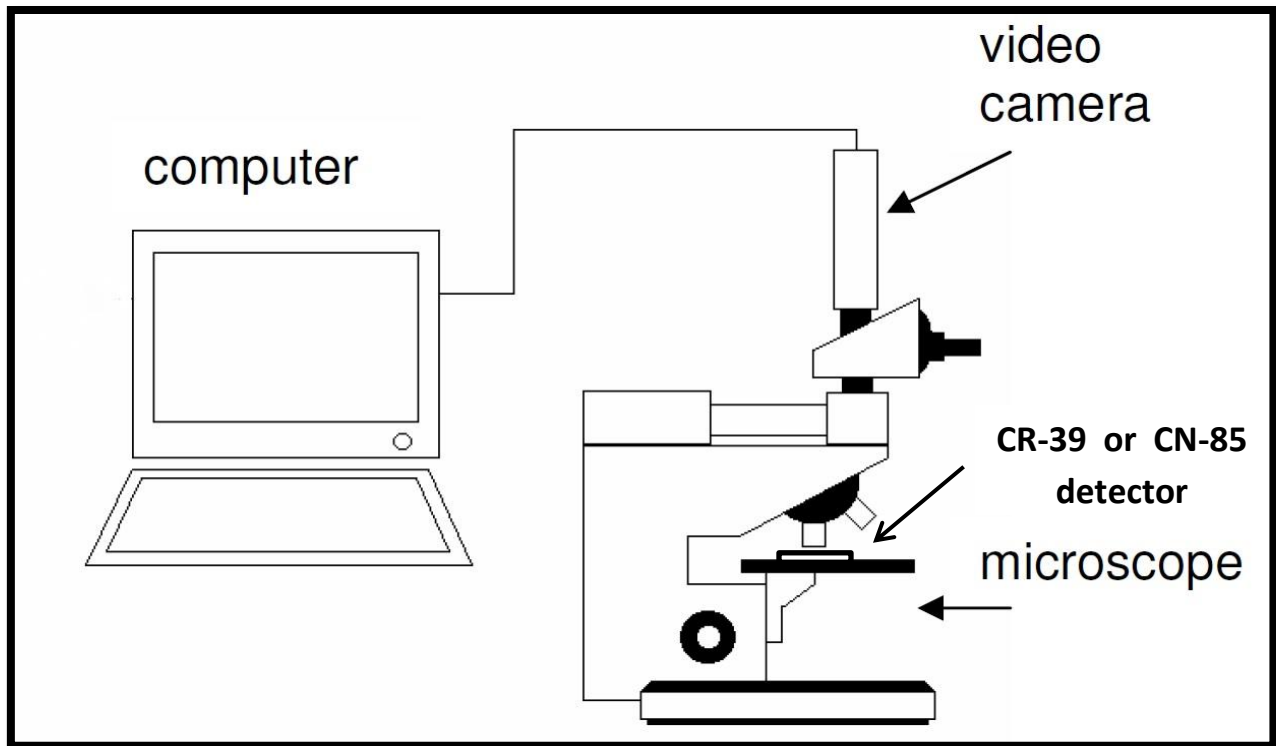


**Figure 2-2** Sketch of digital system which show optical microscope, video camera and personal computer

### ***2.2.6 Preparation programs***

There were many programs used in image processing and analysis. The program which used in this study were MATLAB and Image-J, Image-J one of the designed program, and contain on full options we use any option in processing and analysis. While MATLAB is programming language contain on special tools in image processing, after sum the tools to insert in programming steps to get data of image.

Figure (2-3) shows the flowchart to analysis in MATLAB after take image from microscope and save it at form (jpg) file in computer starting from open program → appear image → remove background → real image for tracks in binary → count of track → distribution of tracks between intensity and radius → get on color map →

histogram between number -  $N$  and track diameter -  $D_T \rightarrow$  histogram between number and track area -  $A_T$ .

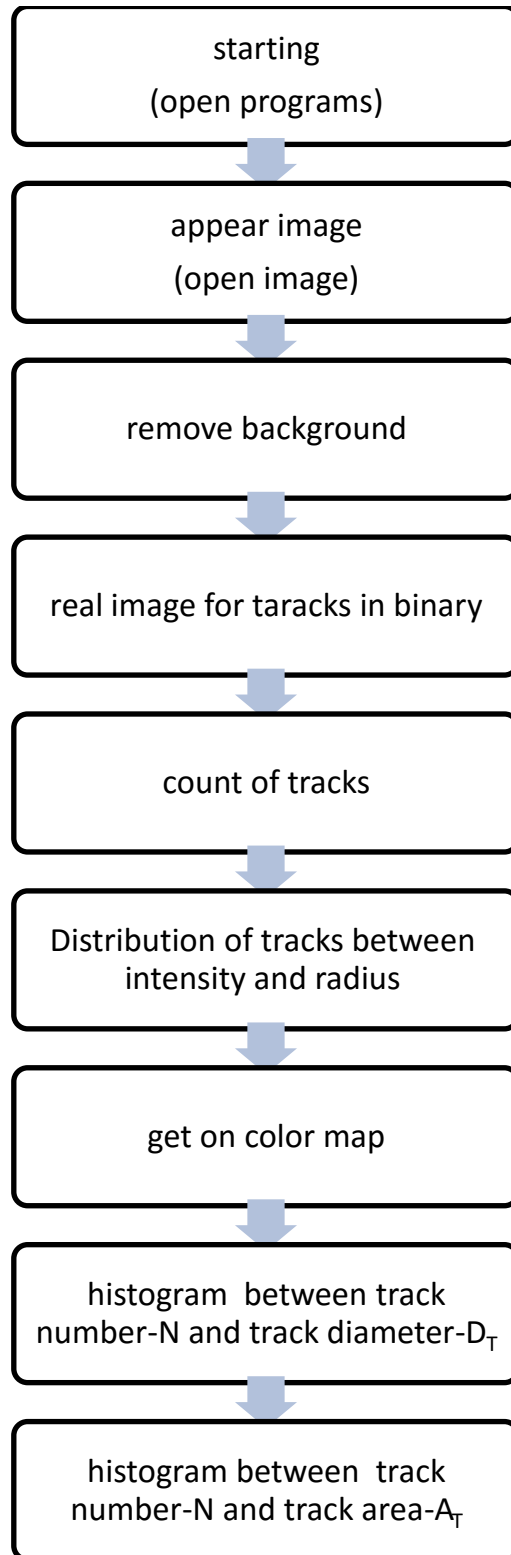


**Figure 2-3** Show the flowchart of image processing and analysis in MATLAB after take image from microscope



*Chapter Three*  
*Results and Discussion*

## Chapter Three

### Results and Discussion

#### *3.1 Image processing by using MATLAB program*

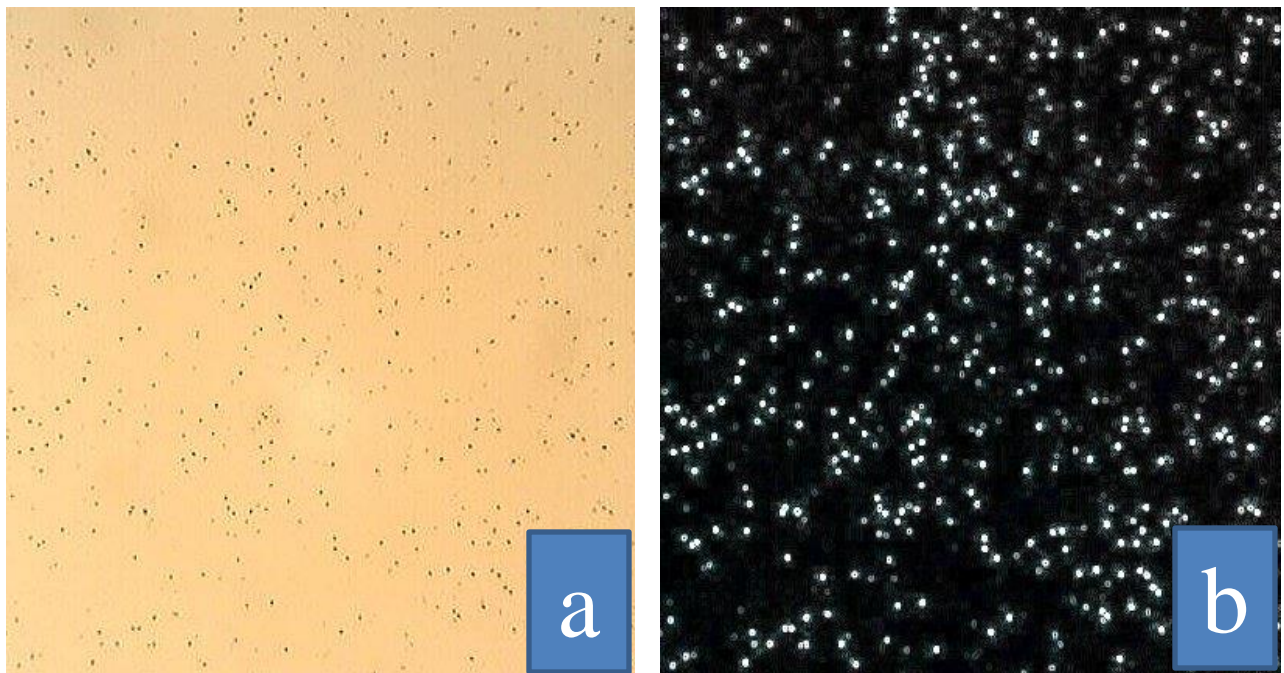
##### *3.1.1 For CR-39 detector*

Figure (3-1) shows the nuclear track detector type CR-39 irradiated by thermal neutron at different time 4h, 8h, 16h and 24h. From this figure shows increasing in the tracks with increasing of irradiation time -  $T_D$  comparison with un-irradiation detector.



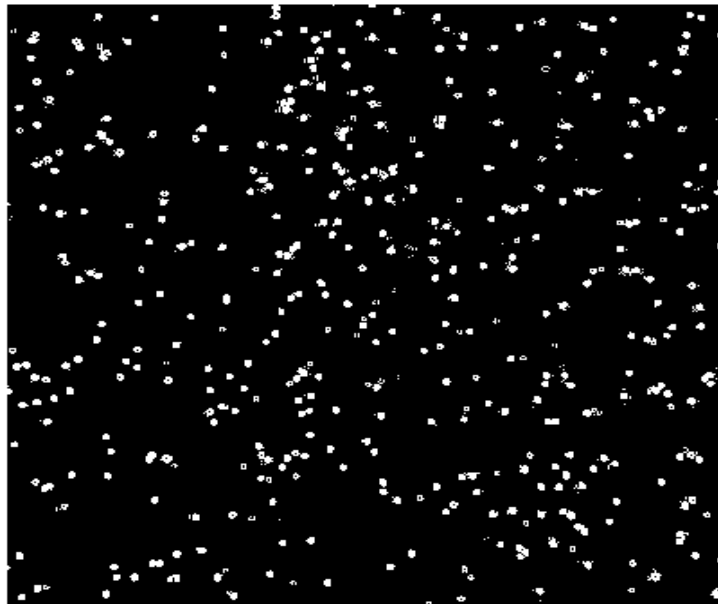
**Figure 3-1** Images by optical microscope of CR-39 detector irradiated with thermal neutrons for different irradiation times ( un-irradiated, 4h, 8h, 16h and 24h)

Figure (3-2:a) shows the first step from image processing of MATLAB program to image of tracks in CR-39 detector after 24h irradiation time -  $T_D$  by thermal neutron before image analysis. While figure (3-2:b) shows same image after image analysis and treatment the background of unwanted impurities and distortions on the detector.



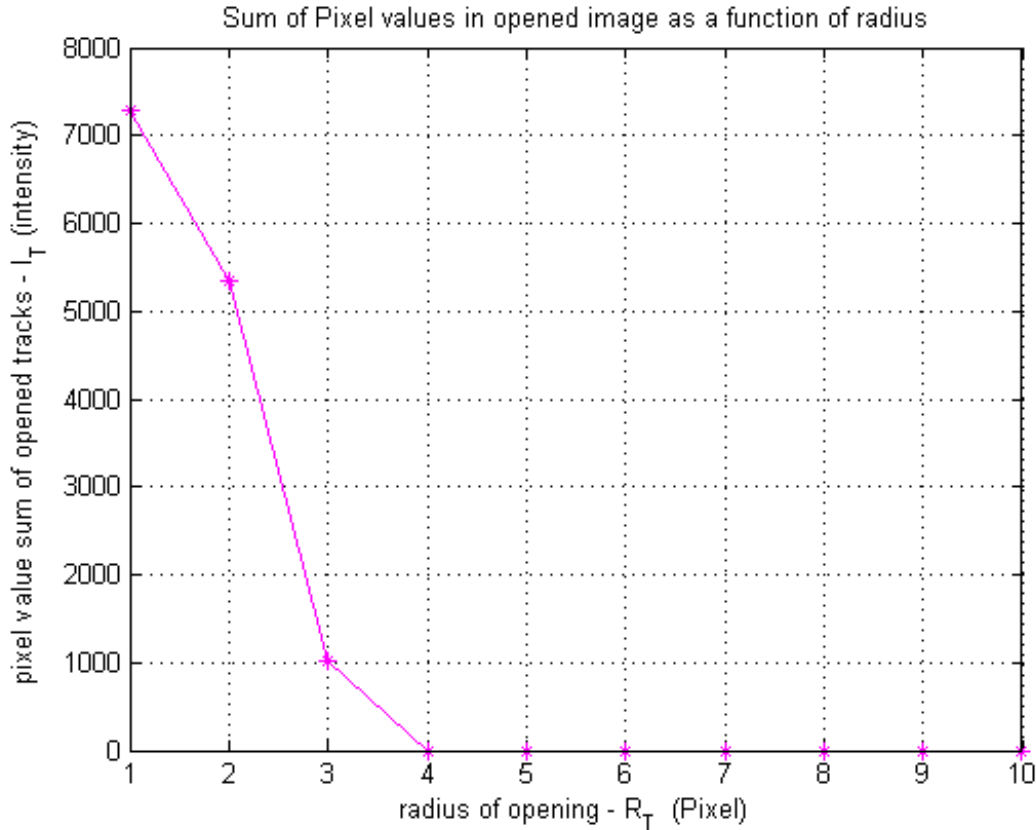
**Figure 3-2** First step from image processing of MATLAB program which obtained the track image in CR-39 detector after 24h irradiated time -  $T_D$   
 a) Before treated  
 b) After treated

Figure (3-3) shows the second step in image processing and shows the real image for tracks which convert from figure (3-2b) to binary system.



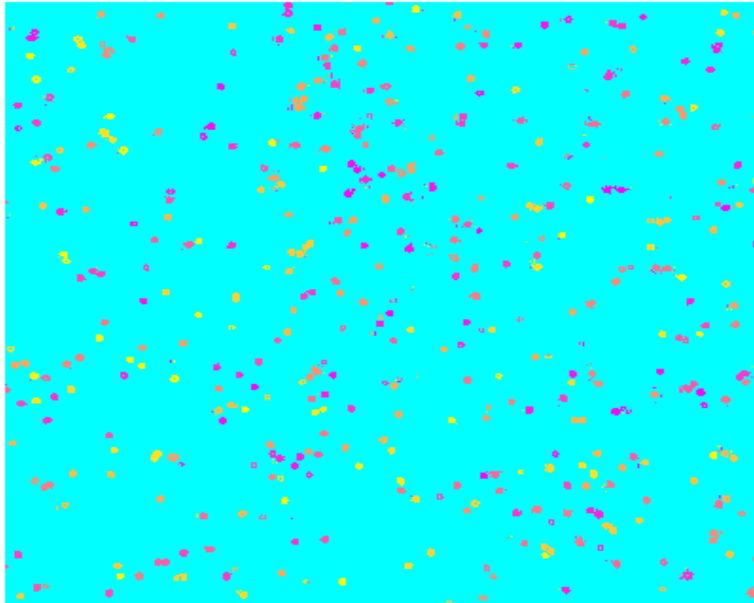
**Figure 3-3** Second step from image processing of MATLAB program which obtained the convert to binary system in CR-39 detector after 24h irradiated time -  $T_D$

Then figure (3-4) shows the third step in image processing for CR-39 detector and determined the relationship between pixel value sum of opened tracks (intensity) -  $I_T$  with track radius -  $R_T$  (in pixel). From this figure obtained increase in the  $R_T$  with decrease in the track intensity -  $I_T$  until to track radius -  $R_T$  at the value 4 pixel ( $1.69\mu\text{m}$ ), and the maximum track intensity was 7290 pixel at the radius track -  $R_T$  equal to the value 1 pixel ( $0.4225\mu\text{m}$ ).



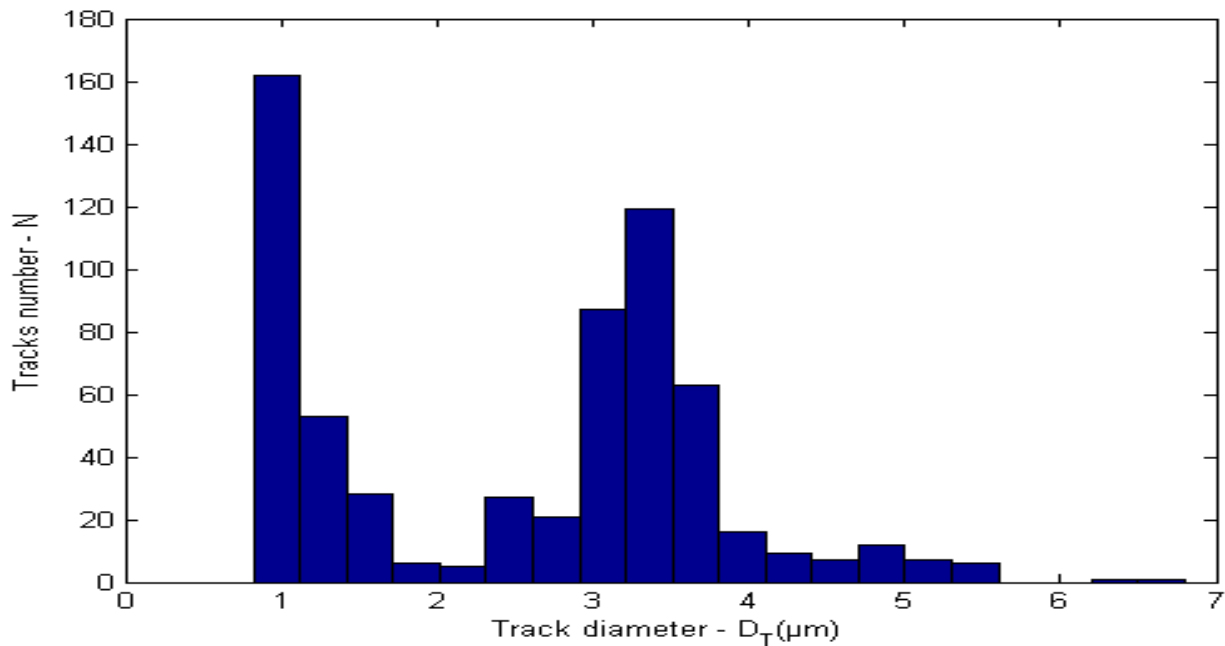
**Figure 3-4** Third step from image processing of MATLAB program which obtained the track intensity -  $I_T$  (in pixel) varies with track radius -  $R_T$  (in pixel) for CR-39 detector after 24h irradiated time -  $T_D$

The forth step in figure (3-5) appear pseudo coloring map for tracks of CR-39 detector, the color of track dependent on the track diameter -  $D_T$  or area track -  $A_T$ .



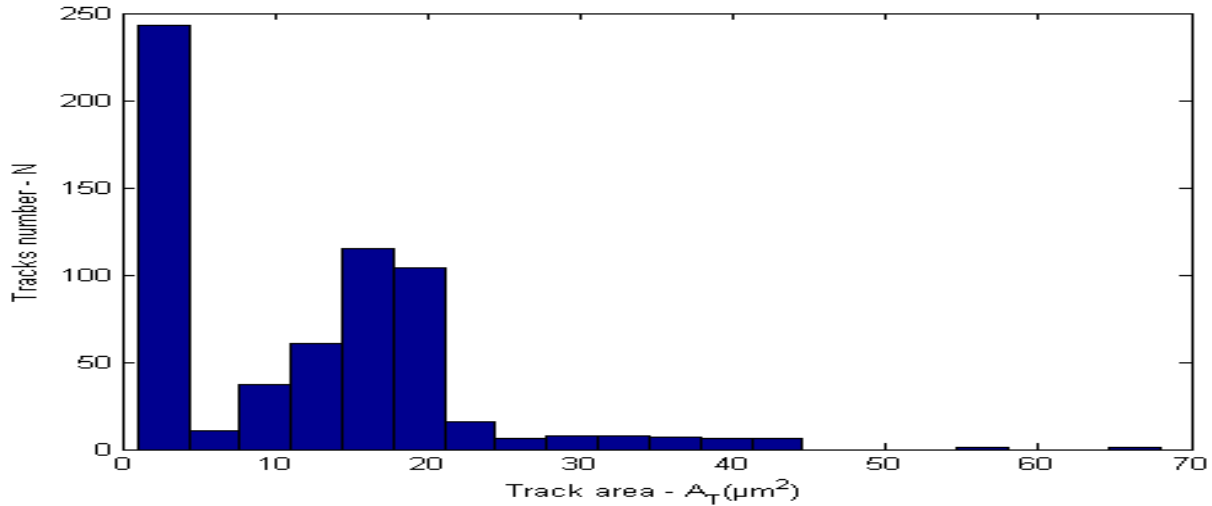
**Figure 3-5** Forth step from image processing of MATLAB program which appear the pseudo coloring map for tracks of irradiated CR-39 detector at 24h

Figure (3-6) shows the varp between the track number -  $N$  and track diameter -  $D_T$  as the histogram shape for fifth step to CR-39 detector, from this figure obtained the maximum track number -  $M_{RD}$  (relative to track diameter -  $D_T$ ) appear in 0.973, 3.36, 3.06, 3.66 and 1.27  $\mu\text{m}$ .



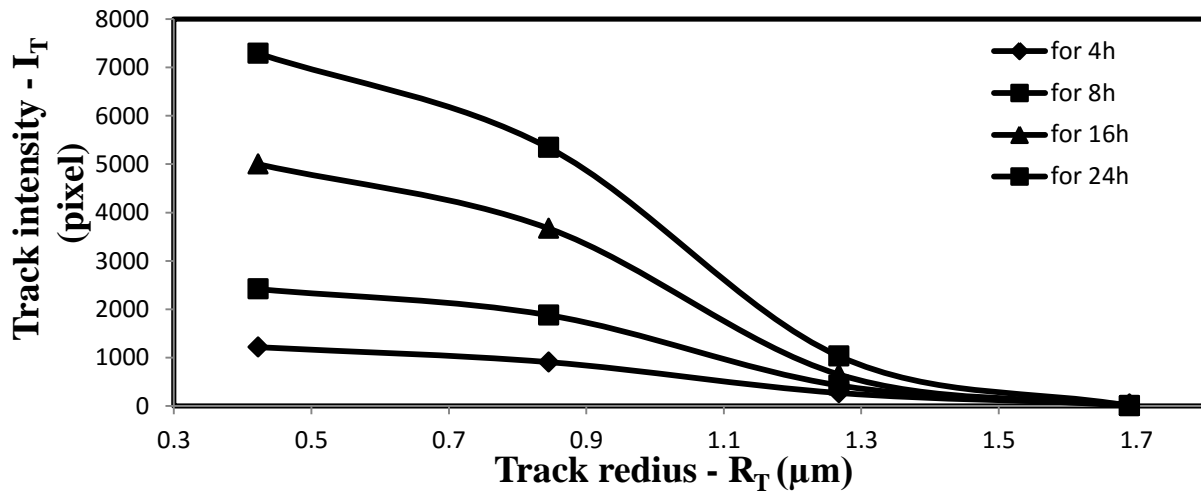
**Figure 3-6** Fifth step from image processing of MATLAB program which obtained the histogram between the tracks number -  $N$  and the tracks diameter -  $D_T$  for irradiated CR-39 detector at 24h

The relationship between track number –  $N$  and track area -  $A_T$  ( $\mu\text{m}^2$ ) obtained in figure (3-7) as the histogram shape, from this figure shows the maximum track number-  $M_{RA}$  (relative to track area -  $A_T$ ) appear at  $2.64 \mu\text{m}^2$ , and at range of track area -  $A_T$   $12.7 - 19.4 \mu\text{m}^2$ .



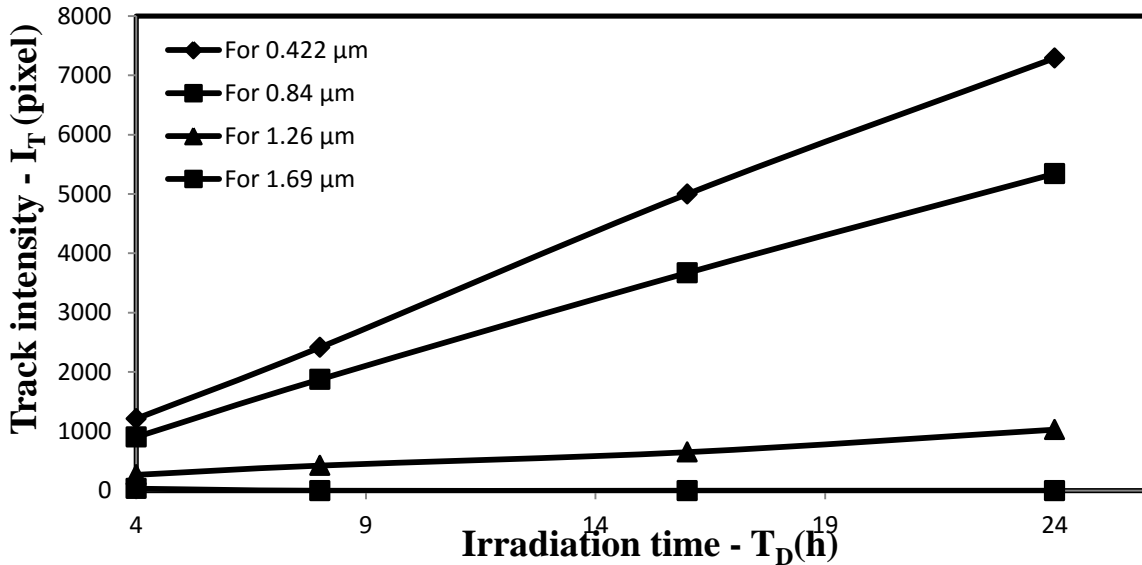
**Figure 3-7** Six step from image processing of MATLAB program which obtained the histogram between the tracks number -  $N$  and the tracks area -  $A_T$  for irradiated CR-39 detector at 24h

Figure (3-8) shows comparison for the relations between track intensity -  $I_T$  for CR-39 with track radius -  $R_T$  for different irradiation time -  $T_D$ , which calculate from figure (3-4) for 24h and same method for 4h, 8h and 16h and obtained from this figure there was increase in track intensity -  $I_T$  with increase of irradiation time -  $T_D$ .



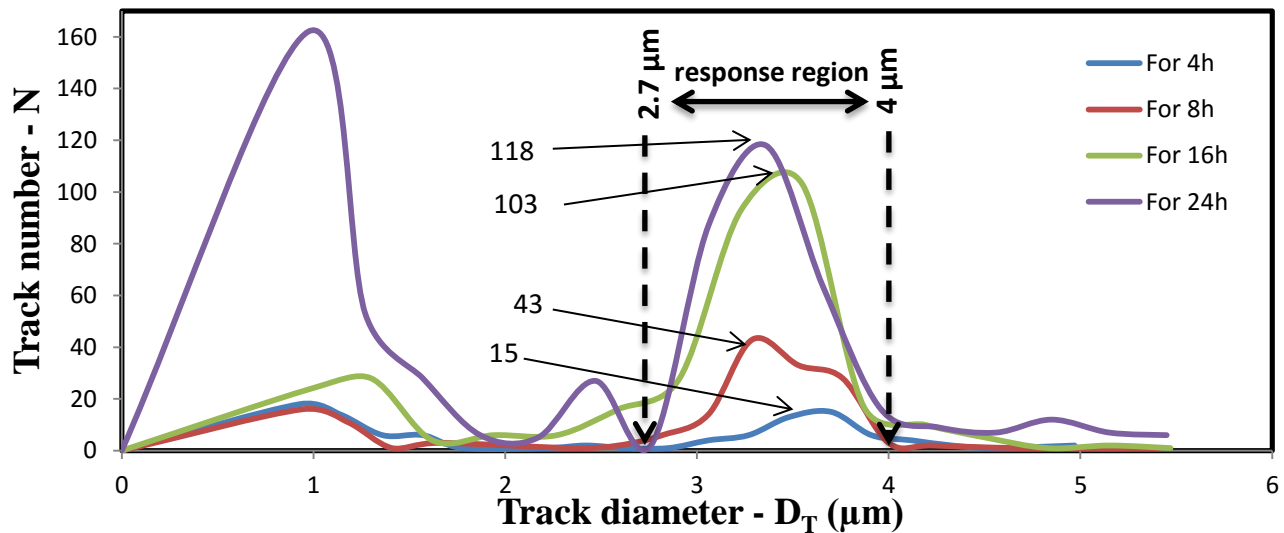
**Figure 3-8** Relation between track intensity -  $I_T$  (pixel) for CR-39 with track radius -  $R_T$  ( $\mu\text{m}$ ) at different irradiation time -  $T_D$  (h) for 4h, 8h, 16h and 24h

The figure (3-9) shows linearly relationship between track intensity -  $I_T$  and irradiation time -  $T_D$  at different track radius -  $R_T$  which calculate from figure (3-8).



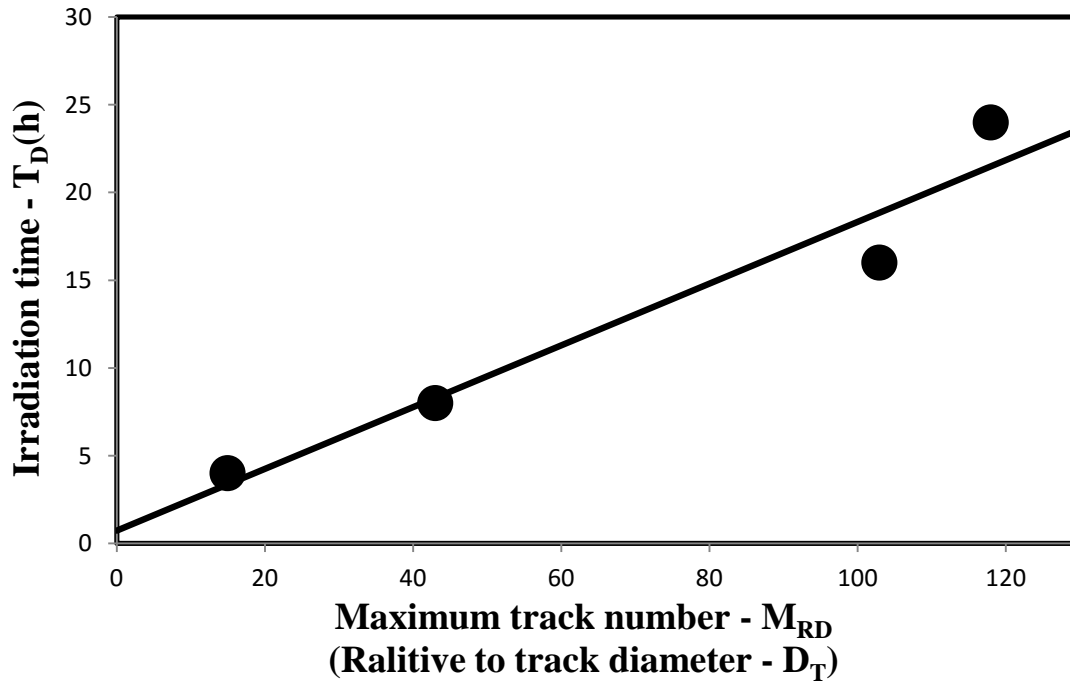
**Figure 3-9** Relation between track intensity -  $I_T$  for CR-39 with irradiation time -  $T_D$  for different track radius -  $R_T$  (0.4225, 0.845, 1.2675 and 1.69)  $\mu\text{m}$

Figure (3-10) shows the relation of the track number -  $N$  with track diameter -  $D_T$  ( $\mu\text{m}$ ) for different value of irradiation time -  $T_D$ . This figure shows that increase in the value of maximum track number -  $M_{RD}$  (relative to track diameter -  $D_T$ ) with increase of irradiation time -  $T_D$ . These increasing of  $M_{RD}$  was limited at the response region of track diameter -  $D_T$  from 2.7  $\mu\text{m}$  to 4  $\mu\text{m}$ .



**Figure 3-10** Relation between the tracks number -  $N$  for CR-39 with tracks diameter -  $D_T$  ( $\mu\text{m}$ ) at irradiation time -  $T_D$  (h) 4h, 8h, 16h and 24h

From figure (3-11) shows relationship between irradiation time -  $T_D$  with maximum track number -  $M_{RD}$  at response region of track diameter -  $D_T$  from  $2.7 \mu\text{m}$  to  $4 \mu\text{m}$  which equal to values 15, 43, 103 and 118 track (relative to track diameter -  $D_T$ ) which calculated from figure (3-10).



**Figure 3-11** Calibration curve between irradiation time -  $T_D$  (h) with maximum track number -  $M_{RD}$  (relative to track diameter -  $D_T$ ) for limited response region between  $2.7 \mu\text{m}$  to  $4 \mu\text{m}$ .

The mathematical relation between irradiation time -  $T_D$  and maximum track number -  $M_{RD}$  (relative to track diameter -  $D_T$ ) which obtained from figure (3-11) was behavior as linear relationship written by following equation:

$$T_D \text{ (h)} = 0.1759 M_{RD} + 0.7321 \quad (3.1)$$

Equation (3.1) can be used to calculate directly the value of irradiation time -  $T_D$  for each effect of thermal neutron after determine the value of maximum track number -  $M_{RD}$  at response region between  $2.7 \mu\text{m}$  to  $4 \mu\text{m}$  (relative to track diameter -  $D_T$ ).

The relation between irradiation time -  $T_D$  with maximum track number -  $M_D$  (without depending on track diameter -  $D_T$ ) which equal to 16, 43, 103 and 162 track from figure (3-10) was determined in figure (3-12). The relation behavior between irradiation time -  $T_D$  with maximum track number -  $M_D$  (without depending on track diameter -  $D_T$ ) was liner relationship.

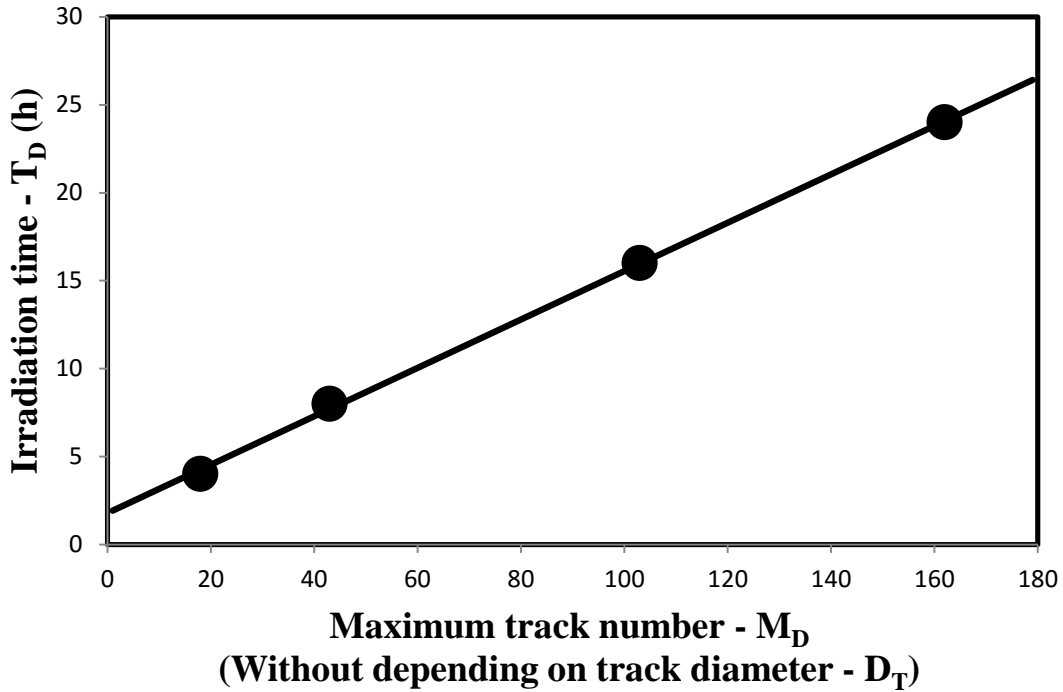


**Figure 3-12** Linear relationship between maximum track number -  $M_D$  (without depending on track diameter -  $D_T$ ) with irradiation time -  $T_D$  (h)

The mathematical equation which reflect the behavior of irradiation time -  $T_D$  with maximum track number -  $M_D$  (without depending on track diameter -  $D_T$ ) in figure (3-12) calculated by fallowing equation:

$$T_D \text{ (h)} = 0.1376 M_D + 1.7861 \quad (3.2)$$

While in figure (3-13) shows the relation of the number of track -  $N$  with track area -  $A_T$  ( $\mu\text{m}^2$ ) for different irradiation time -  $T_D$ . From this figure obtained increase in the value of maximum track number -  $M_{RA}$  (relative to track area -  $A_T$ ) with increase in irradiation time -  $T_D$ . These increasing of maximum track number -  $M_{RA}$

was limited at the response region of track area -  $A_T$ , from  $7 \mu\text{m}^2$  to  $23 \mu\text{m}^2$  which equal to 12, 44, 107 and 115 track.

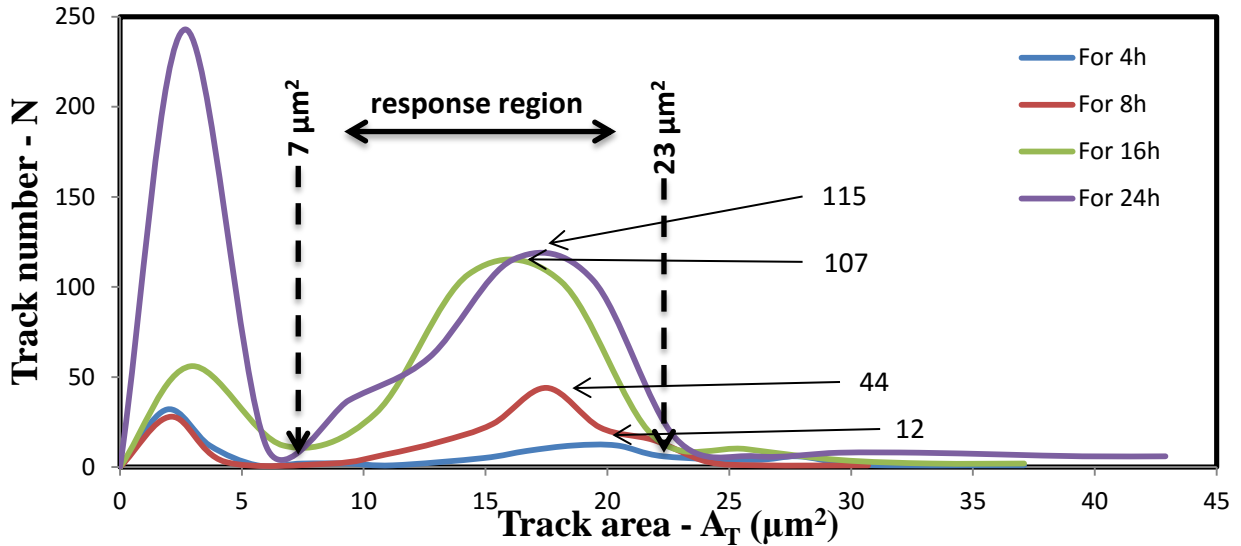


**Figure 3-13** Relation between the track number -  $N$  for CR-39 detector with area of track-  $A_T (\mu\text{m}^2)$  at irradiation time -  $T_D$  (h) 4h, 8h, 16h and 24h

Figure (3-14) shows relation between irradiation time -  $T_D$  with maximum track number -  $M_{RA}$  at response region of track area -  $A_T$ . Which starting from track area -  $A_T$   $7 \mu\text{m}^2$  to  $23 \mu\text{m}^2$  which equal values 12, 44, 107 and 115 track (relative to track area -  $A_T$ ) which calculated from figure (3-13).

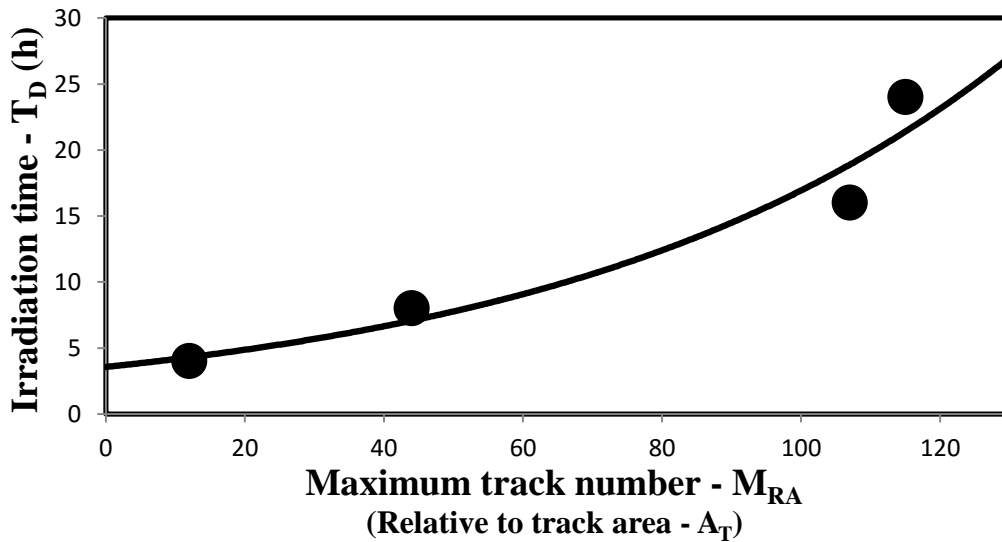


**Figure 3-14** Calibration curve between irradiation time -  $T_D$  (h) with maximum count of track -  $M_{RA}$  (relative to track area -  $A_T$ ) at limited response region of  $A_T$ , starting from track area -  $A_T$   $7 \mu\text{m}^2$  to  $23 \mu\text{m}^2$

The mathematical relation between irradiation time -  $T_D$  and maximum track number -  $M_{RA}$  (relative to track area -  $A_T$ ) which obtained from figure (3-14) was behavior as exponential relationship written by following equation:

$$T_D (h) = 3.5644 e^{0.0156 M_{RA}} \quad (3.3)$$

From equation (3.3) may be used to calculate directly the value of irradiation time -  $T_D$  for the effect of thermal neutron after determine the value of maximum track number -  $M_{RA}$  at response region from track area -  $A_T$   $7 \mu m^2$  to  $23 \mu m^2$  (relative to track area -  $A_T$ ).

From figure (3-13) present the relation between maximum track number -  $M_A$  (without depending on track area -  $A_T$ ) with irradiation time -  $T_D$ , and that relation was behavior as logarithmic relationship as shown in figure (3-15).

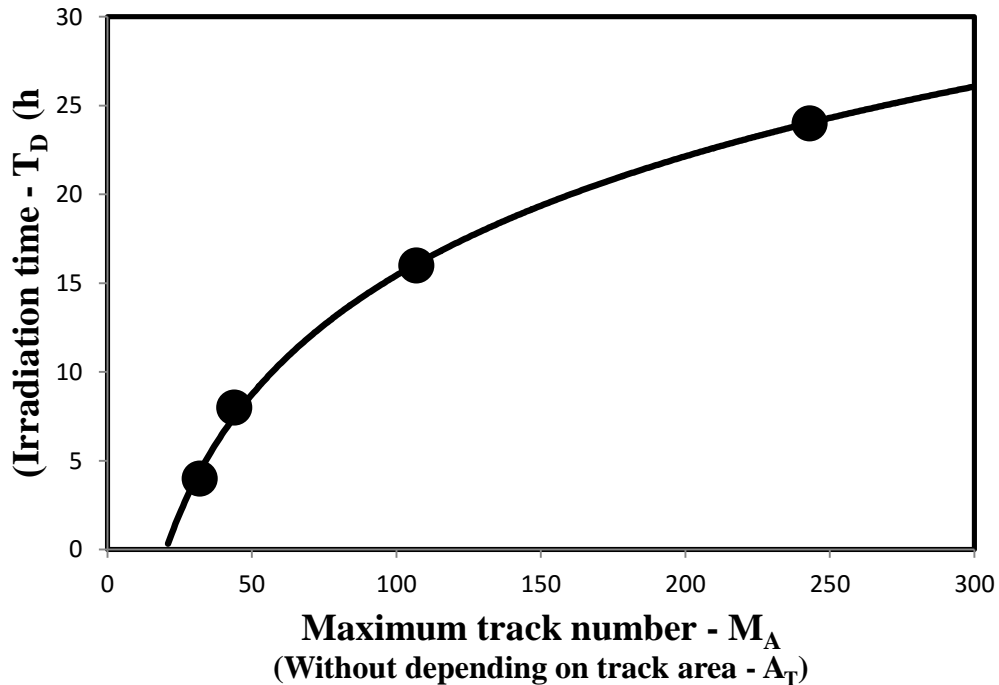


**Figure 3-15** Relation between maximum value for track number -  $M_A$  (without depending on area of track -  $A_T$ ) with irradiation time  $T_D$  (h)

The mathematical relation which reflect the behavior of irradiation time -  $T_D$  with maximum track number -  $M_A$  (without depending on track area -  $A_T$ ) in figure (3-15) calculated by the following equation:

$$T_D (h) = 9.6822 \ln(M_A) - 29.156 \quad (3.4)$$

Figures (3-10) and (3-13) reflect the relation between track number -  $N$  with track diameter -  $D_T$  and track area -  $A_T$  respectively. While the total track number -  $N_T$  which reflect the value of maximum track number (without depending on the track diameter and track area -  $A_T$ ), was behavior as a linear relationship between irradiation time -  $T_D$  and total track number -  $N_T$  as shown in figure (3-16)

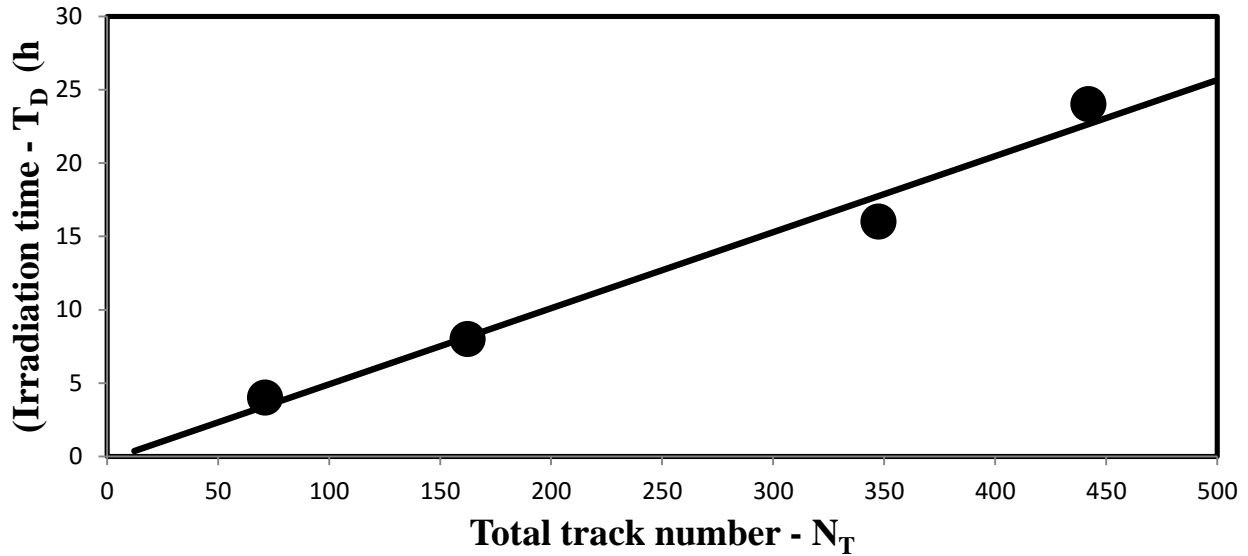


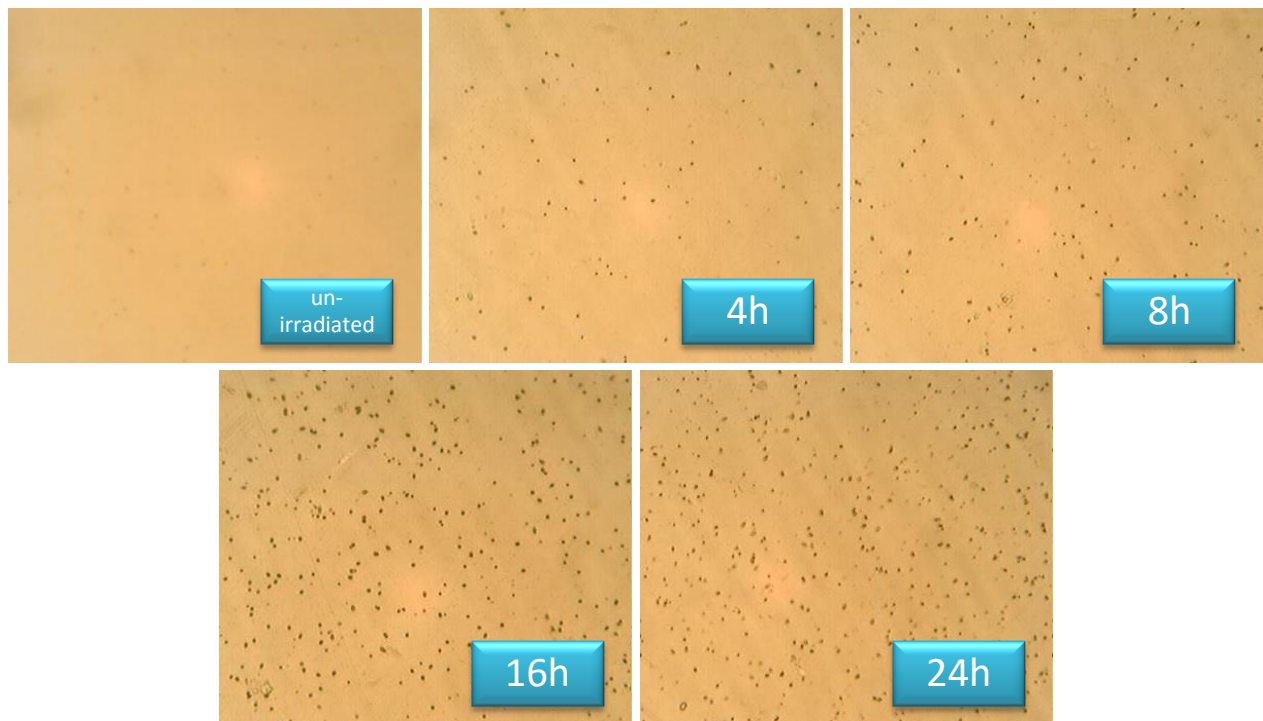
**Figure 3-16** Linear relation between the total track numbers- $N_T$  with irradiation time- $T_D$  (h)

The mathematical relation between irradiation time -  $T_D$  and total track number -  $N_T$  (without depended on track area -  $A_T$  or track diameter -  $D_T$ ) which obtained from figure (3-16) was behavior as following linear relationship equation (3-5):

$$T_D (h) = 0.0518 N_T - 0.2591 \quad (3.5)$$

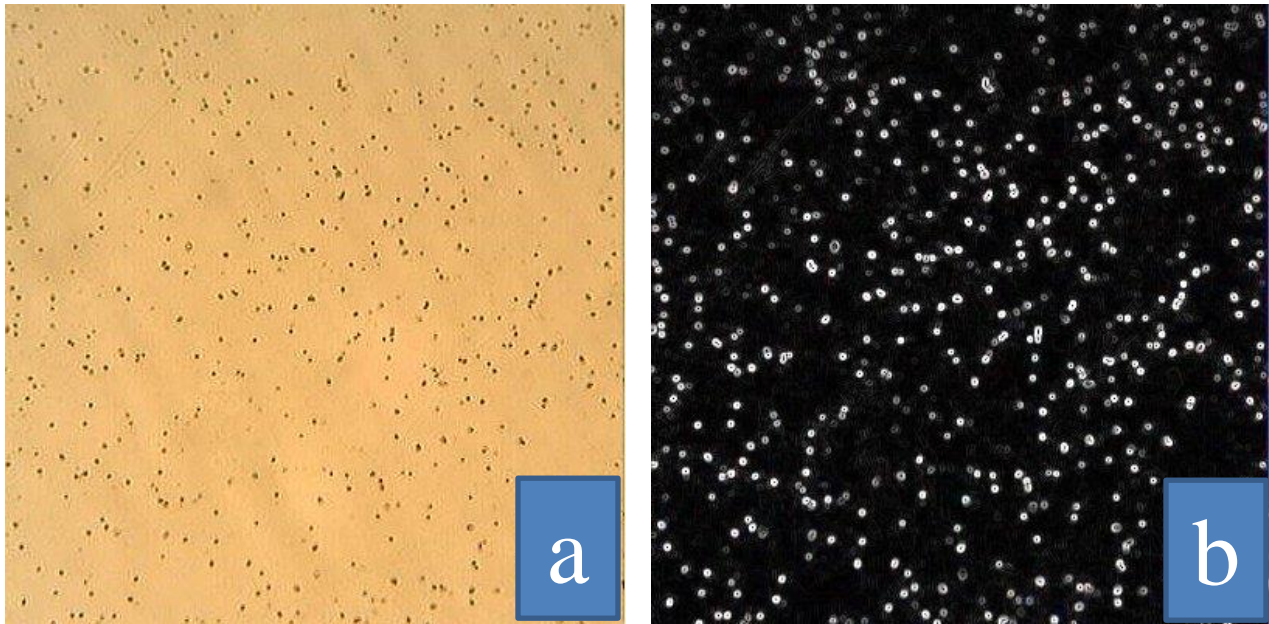
### 3.1.2 For CN-85 detector

Figure (3-17) shows the nuclear track detector type CN-85 irradiation by thermal neutron at different time 4h, 8h, 16h and 24h. From this figure shows increasing in the tracks with increasing of irradiation time -  $T_D$  comparison with un-irradiation detector.



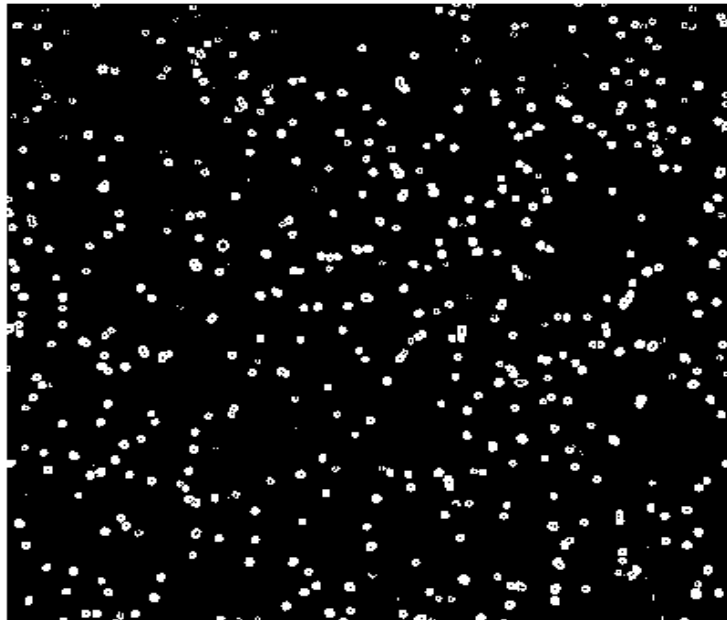
**Figure 3-17** Images by optical microscope of CN-85 detector irradiated with thermal neutrons for different irradiation times -  $T_D$  ( un-irradiated, 4h, 8h, 16h and 24h)

Figure (3-18:a) shows the first step from image processing of MATLAB program to image of tracks in CN-85 detector after 24h irradiation time -  $T_D$  by thermal neutron before image analysis. While figure (3-18:b) shows same image after image analysis and treatment the background of unwanted impurities and distortions on the detector.



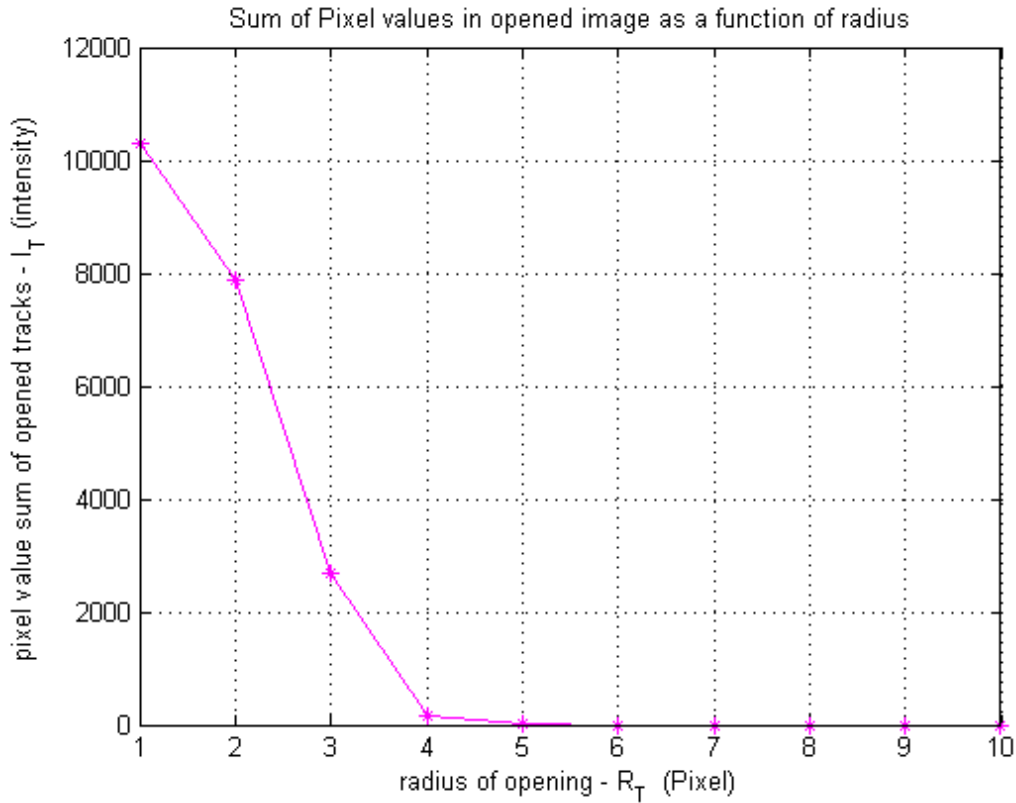
**Figure 3-18** First step from image processing of MATLAB program which obtained the track image in CN-85 detector after 24h irradiated time -  $T_D$   
a) Before treated  
b) After treated

Figure (3-19) shows the second step in image processing and shows the real image for tracks which convert from figure (3-18b) to binary system.



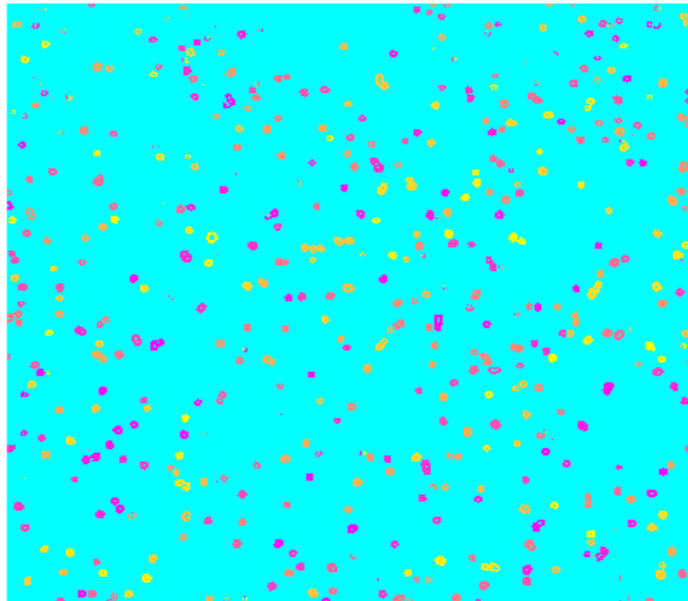
**Figure 3-19** Second step from image processing of MATLAB program which obtained the convert to binary system in CN-85 detector after 24h irradiated time -  $T_D$

Then figure (3-20) shows the third step in image processing for CN-85 detector and determined the relationship between pixel value sum of opened tracks (intensity) with track radius -  $R_T$  (in pixel). From this figure obtained increase in the  $R_T$  with decrease in the intensity track -  $I_T$  until to track radius -  $R_T$  which equal to 4 pixel ( $1.69\mu\text{m}$ ). And the maximum intensity track was 11170 pixel at the track radius -  $R_T$  equal to the value 1 pixel ( $0.4225\mu\text{m}$ ).



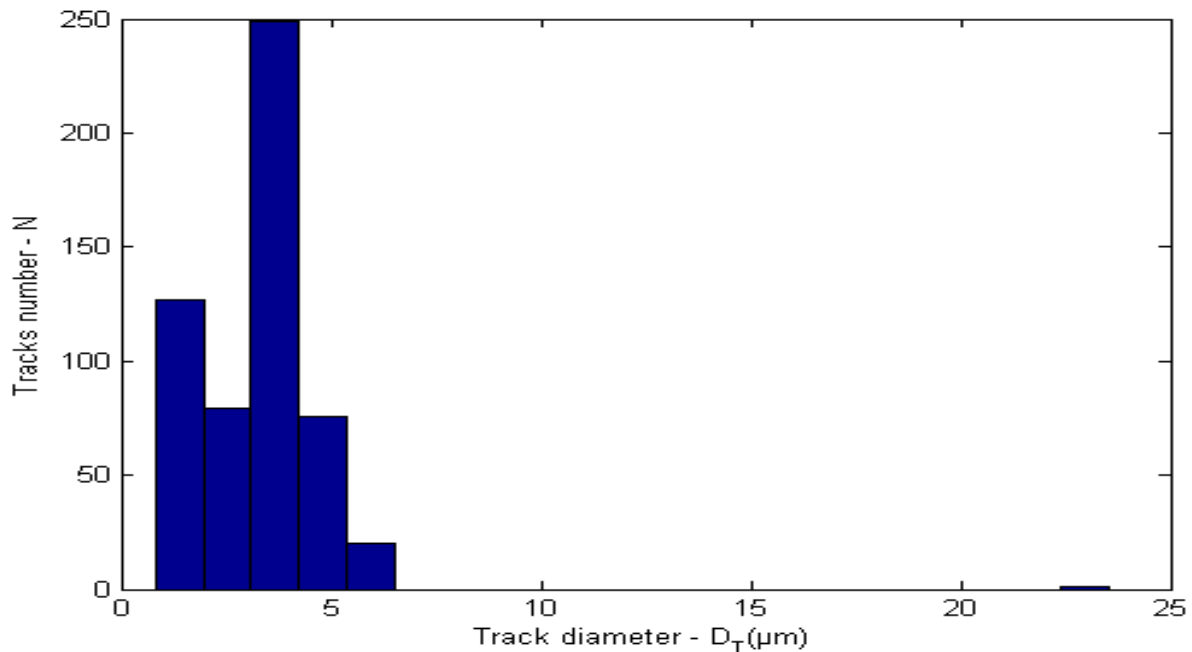
**Figure 3-20** Third step from image processing of MATLAB program which obtained the track intensity -  $I_T$  (in pixel) varies with track radius -  $R_T$  (in pixel) for CN-85 detector after 24h irradiated time -  $T_D$

The fourth step in figure (3-21) appear pseudo coloring map for tracks of CN-85 detector, the color of track dependent on the track diameter -  $D_T$  or area of track -  $A_T$ .



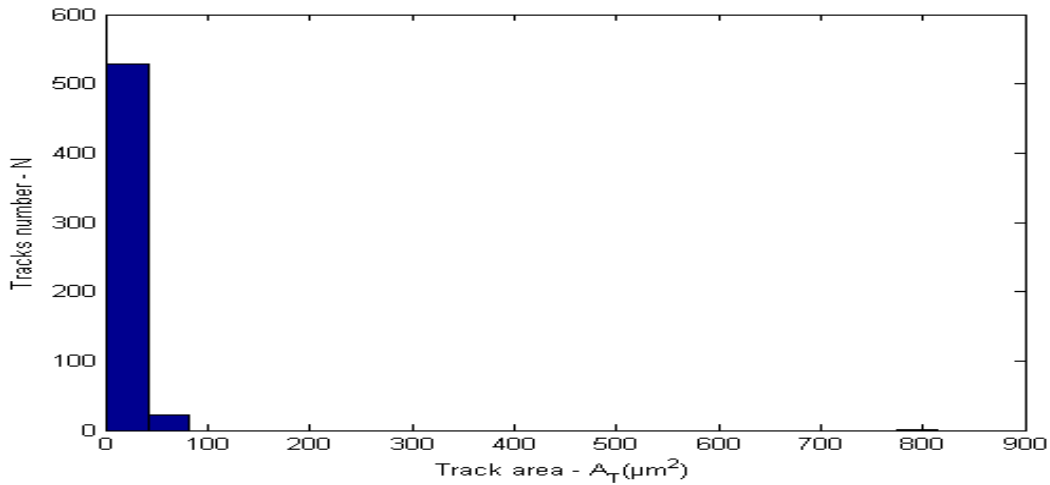
**Figure 3-21** Forth step from image processing of MATLAB program which appear the pseudo coloring map for tracks of irradiated CN-85 detector at 24h

Figure (3-22) shows the relationship between the tracks number -  $N$  and track diameter -  $D_T$  as the histogram shape for fifth step to CN-85 detector, from this figure obtained the maximum track number -  $M_{RD}$  (relative to track diameter -  $D_T$ ) appear in 3.66, 1.93, 2.53 and 4.8  $\mu\text{m}$ .



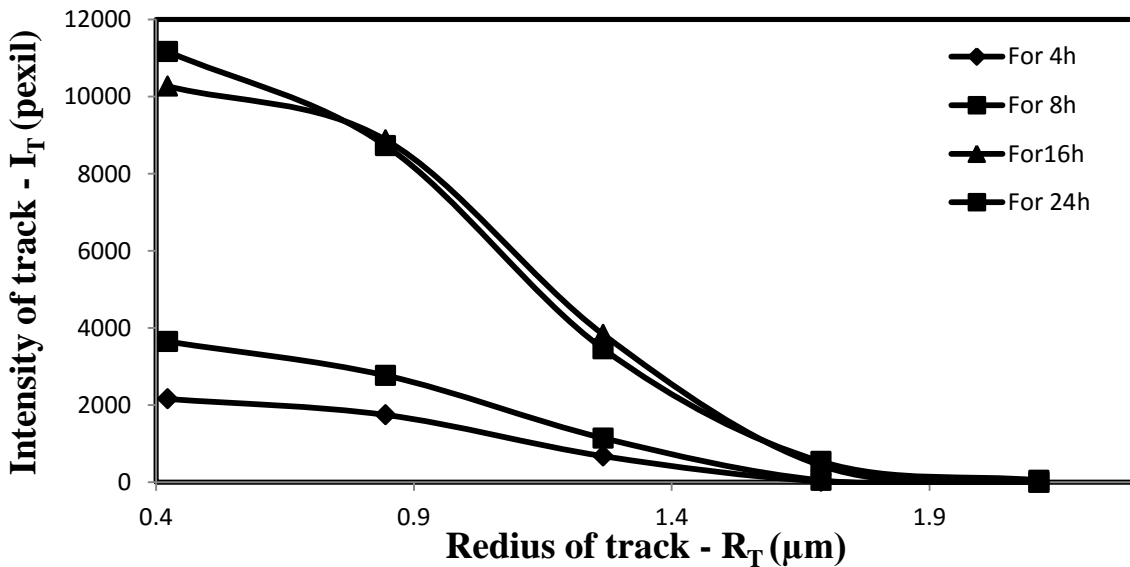
**Figure 3-22** Fifth step from image processing of MATLAB program which obtained the histogram between the tracks number -  $N$  and the track diameter -  $D_T$  for irradiated CN-85 detector at 24h

The relationship between track number-  $N$  and tracks area -  $A_T$  obtained in figure (3-23) as the histogram shape. From this figure shows the maximum track number -  $M_{RA}$  (relative to track area -  $A_T$ ) appear at track area -  $A_T$   $21.4 \mu\text{m}^2$ .



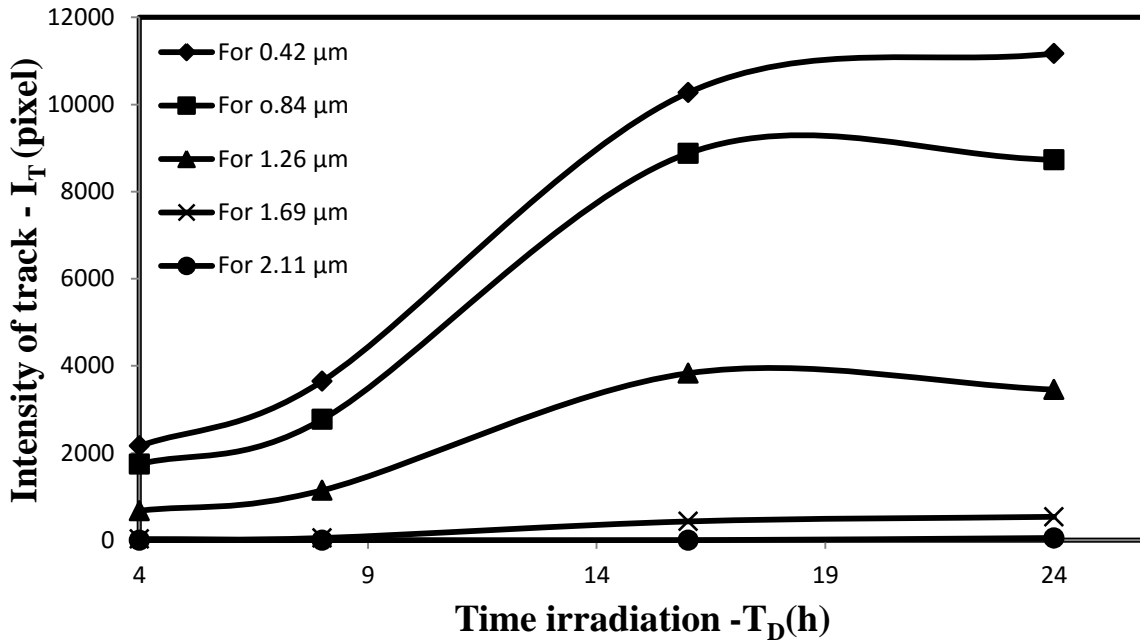
**Figure 3-23** Six step from image processing of MATLAB program which obtained the histogram between the track numbers -  $N$  and the area of tracks -  $A_T$  for irradiated CN-85 detector at 24h

Figure (3-24) shows comparison for the relations between track intensity -  $I_T$  for CN-85 with track radius -  $R_T$  for different irradiation track -  $T_D$  which calculated from figure (3-20) for 24h and same method for 4h, 8h and 16h. And obtained from this figure there was increase in track intensity -  $I_T$  with increase of  $T_D$ .



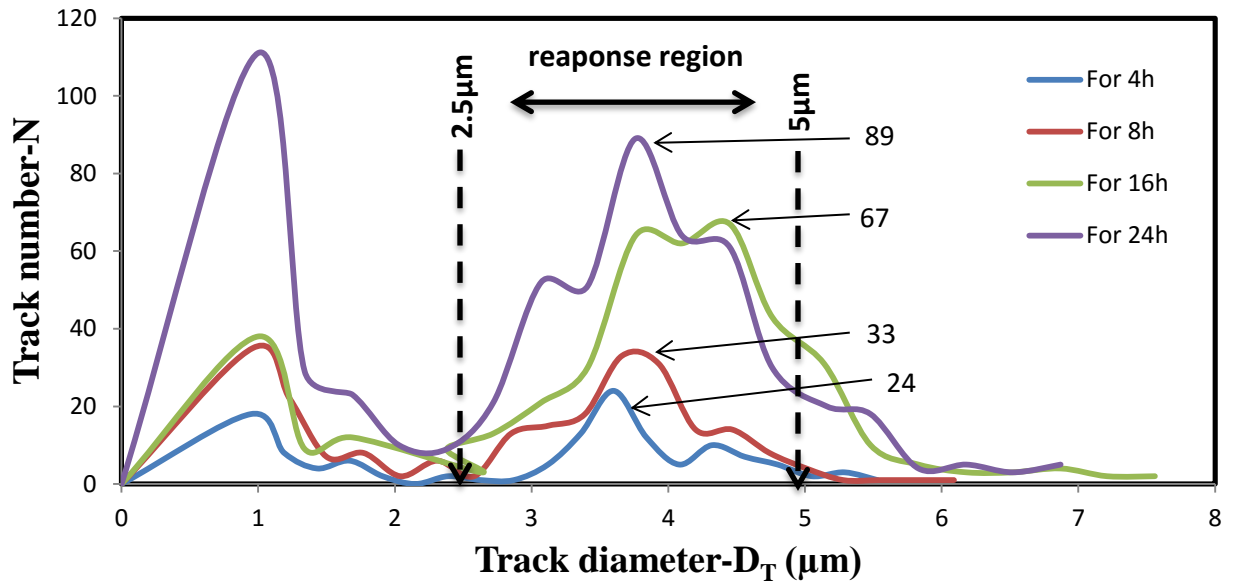
**Figure 3-24** Relation between track intensity -  $I_T$  (pixel) for CN-85 with track radius -  $R_T$  at different irradiation time -  $T_D$  for 4h, 8h, 16h and 24h

The figure (3-25) shows linearly relationship between  $I_T$  and  $T_D$  at different  $R_T$  which calculate from figure (3-24).



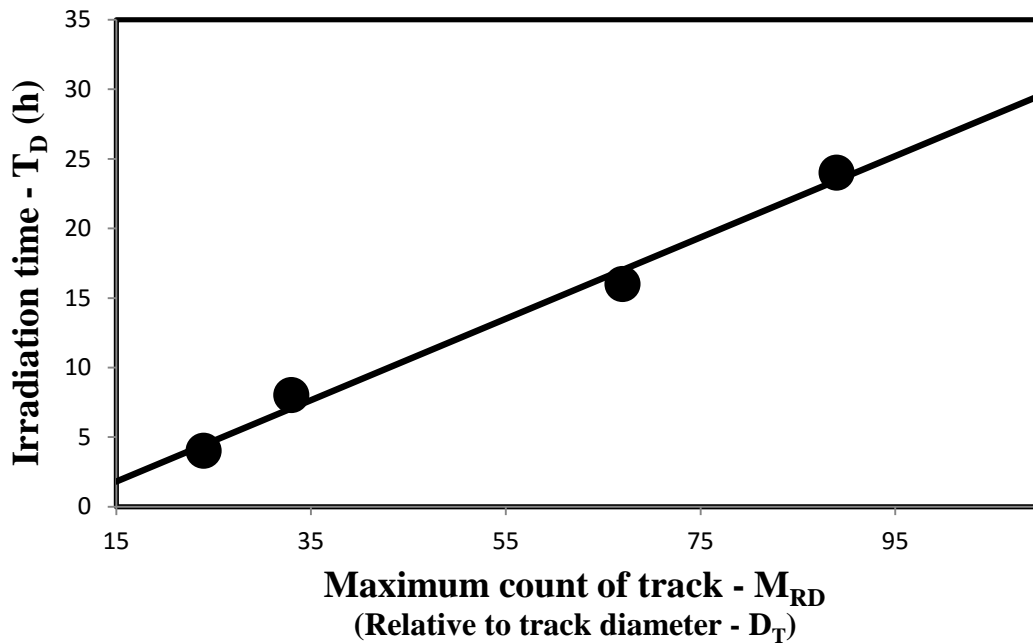
**Figure (3-25)** Relation between track intensity -  $I_T$  for CN-85 with irradiation time -  $T_D$  (h) for different radius of track -  $R_T$  ( $0.4225$ ,  $0.845$ ,  $1.2675$ ,  $1.69$  and  $2.11 \mu\text{m}$ )

Figure (3-26) shows the relation of the track number -  $N$  with track diameter -  $D_T$  ( $\mu\text{m}$ ) for different value of irradiation time -  $T_D$ . From this figure obtained increase in the value of maximum track number -  $M_{RD}$  (relative to track diameter -  $D_T$ ) with increase of irradiation time -  $T_D$ . These increasing of maximum track number -  $M_{RD}$  was limited at the response region of track diameter -  $D_T$  from the values  $2.5 \mu\text{m}$  to  $5 \mu\text{m}$ .



**Figure 3-26** Relation between the tracks number - N for CN-85 with track diameter -  $D_T$  ( $\mu\text{m}$ ) at irradiation time -  $T_D$  (h) 4h, 8h, 16h and 24h

From figure (3-27) shows relationship between irradiation time -  $T_D$  with maximum track number -  $M_{RD}$  at response region of track diameter -  $D_T$  from 2.5  $\mu\text{m}$  to 5  $\mu\text{m}$  which equal values to 24, 33, 67 and 89 track (relative to track diameter -  $D_T$ ) which calculated from figure (3-26).



**Figure 3-27** Calibration curve between irradiation time -  $T_D$  (h) with maximum count of track -  $M_{RD}$  (relative to track diameter -  $D_T$ ) for limited response region between track diameter values 2.5  $\mu\text{m}$  and 5  $\mu\text{m}$ .

The mathematical relation between irradiation time -  $T_D$  and maximum track number -  $M_{RD}$  (relative to track diameter -  $D_T$ ) which obtained from figure (3-27) was behavior as linear relationship in equation (3-6) :

$$T_D (h) = 0.2924 M_{RD} - 2.5692 \quad (3.6)$$

From equation (3.6) which used to calculate directly the value of irradiation time -  $T_D$  for each effect of thermal neutron after determine the value of maximum track number -  $M_{RD}$  (relative to track diameter -  $D_T$ ).

The relation between maximum track number -  $M_D$  (without depending on track diameter -  $D_T$ ) with irradiation time -  $T_D$  which equal to 24, 35, 67 and 111 track from figure (3-26) was determined in figure (3-28). The relation behavior between maximum track number -  $M_D$  (without depending on track diameter -  $D_T$ ) with irradiation time -  $T_D$  was liner relationship.

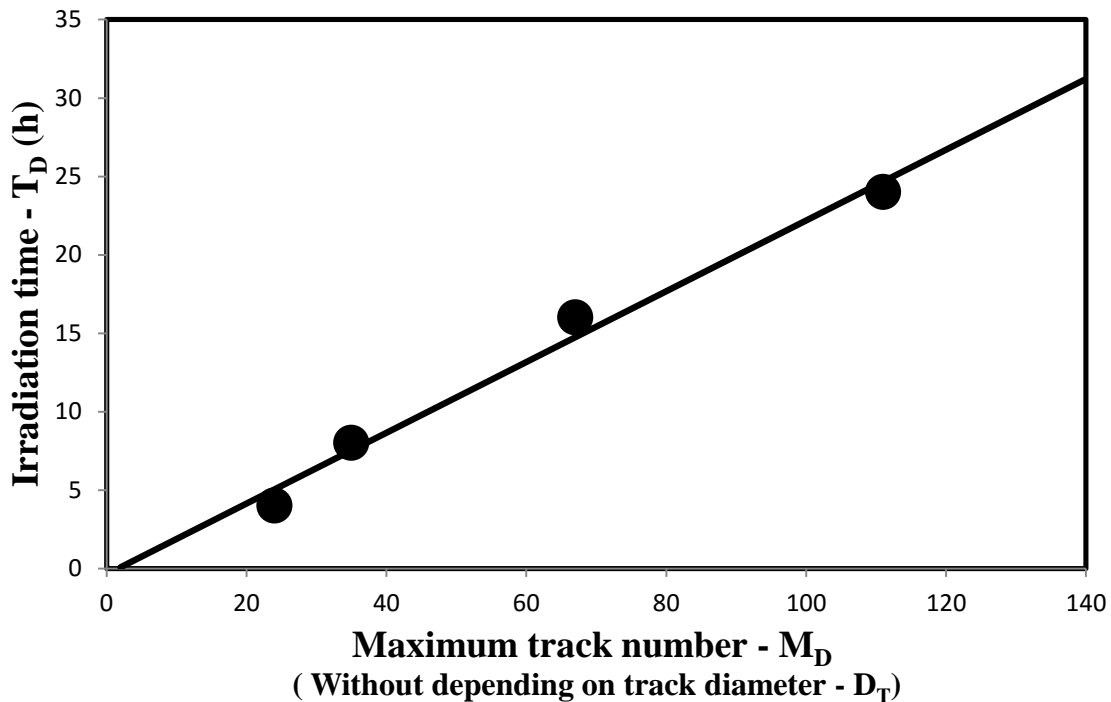


**Figure 3-28** Linear relationship between maximum value for track number-  $M_D$  (without depending on track diameter -  $D_T$ ) with irradiation time -  $T_D$  (h)

The mathematical equation which reflect the behavior of irradiation time -  $T_D$  with maximum track number -  $M_D$  (without depending on track diameter -  $D_T$ ) in figure (3-28) calculated by following equation:

$$T_D \text{ (h)} = 0.2257 M_D - 0.3706 \quad (3.7)$$

While in figure (3-29) shows the relation of the track number -  $N$  with track area -  $A_T$  ( $\mu\text{m}^2$ ) for different irradiation time -  $T_D$ . From this figure obtained increase in the value of maximum track number -  $M_{RA}$  (relative to track area -  $A_T$ ) with increase in irradiation time -  $T_D$ . And these increasing was limited at the response region of track area -  $A_T$ , starting from  $7 \mu\text{m}^2$  to  $35 \mu\text{m}^2$  which equal to 15, 40, 72 and 89 track.

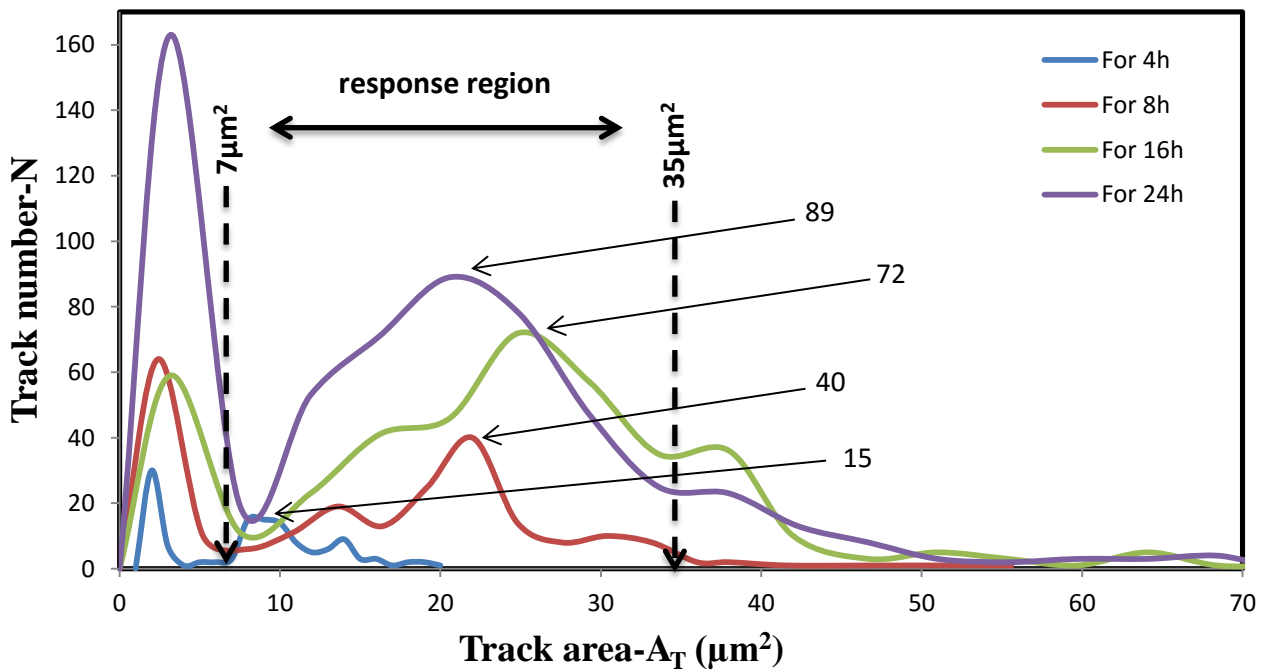


**Figure 3-29** Relation between the track number -  $N$  for CN-85 detector with track area -  $A_T$  ( $\mu\text{m}^2$ ) at irradiation time -  $T_D$  (h) 4h, 8h, 16h and 24h

From figure (3-30) shows relation between irradiation time -  $T_D$  with maximum track number -  $M_{RA}$  at response region of track area -  $A_T$  which starting from track area -  $A_T$   $7 \mu\text{m}^2$  to  $35 \mu\text{m}^2$  with values of 15, 40, 72 and 89 track (relative to track area -  $A_T$ ). These relation was calculated from figure (3-29).

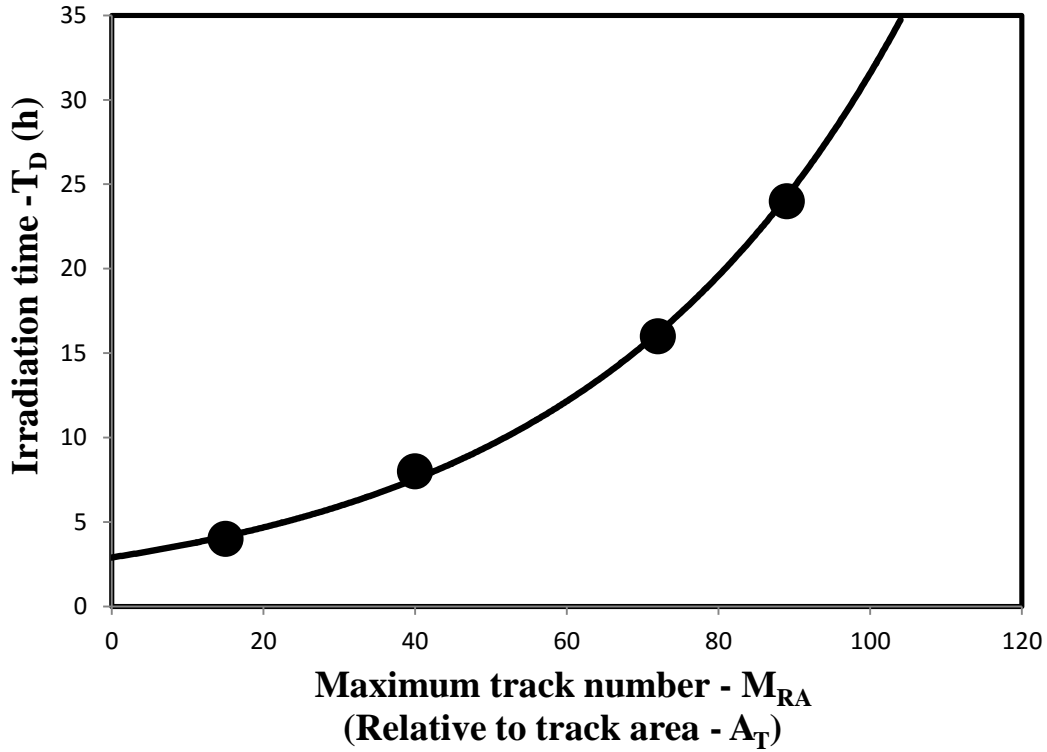


**Figure 3-30** Calibration curve between irradiation time -  $T_D$  (h) with maximum count of track -  $M_{RA}$  (relative to area track -  $A_T$ ) at limited response region of  $A_T$ , from  $7 \mu\text{m}^2$  and  $35 \mu\text{m}^2$

The mathematical relation between irradiation time -  $T_D$  and maximum track number -  $M_{RA}$  (relative to track area -  $A_T$ ) which obtained from figure (3-30), was behavior as exponential relationship written by following equation:

$$T_D \text{ (h)} = 2.9011 e^{0.0239M_{RA}} \quad (3.8)$$

From equation (3.8) which used to calculate the value of irradiation time -  $T_D$  for each effect of thermal neutron after determine the value of maximum track number -  $M_{RA}$  (relative to track area -  $A_T$ ).

From figure (3-29) determined the relation between irradiation time -  $T_D$  with maximum track number -  $M_A$  (without depending on track area -  $A_T$ ). And that relation was behavior as logarithmic relationship as shown in figure (3-31).

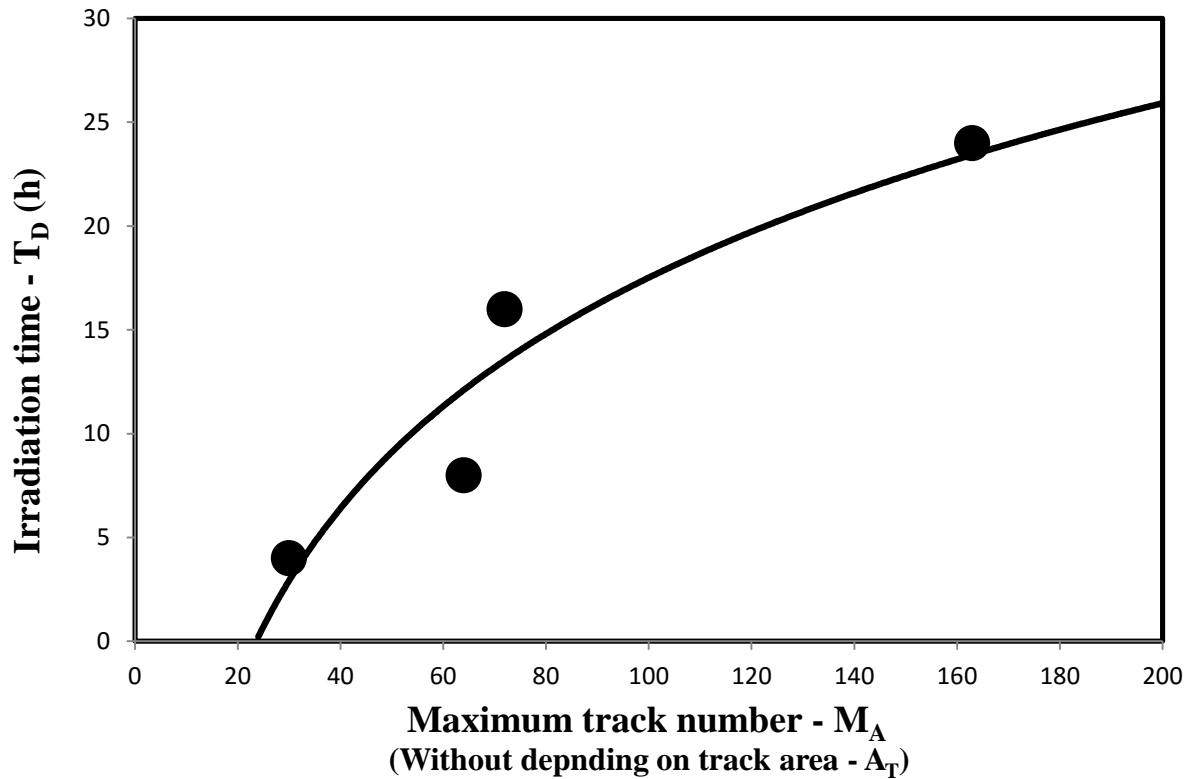


**Figure 3-31** Relation between maximum count of track -  $M_A$  with irradiation time -  $T_D$  (h)

The mathematical equation which reflect the behavior of irradiation time -  $T_D$  with maximum track number -  $M_A$  (without depending on track area -  $A_T$ ) in figure (3-31) calculated by following equation:

$$T_D \text{ (h)} = 12.121 \ln(M_A) - 38.302 \quad (3.9)$$

Figure (3-26) and figure (3-29) reflect the relation between track number -  $N$  with track diameter -  $D_T$  and track area -  $A_T$  respectively. While the total track number -  $N_T$  which reflect the value of maximum track number (without depending on the track diameter -  $D_T$  and track area -  $A_T$ ), was behavior as a linear relationship between irradiation time -  $T_D$  and total track number -  $N_T$  as shown in figure (3-32)

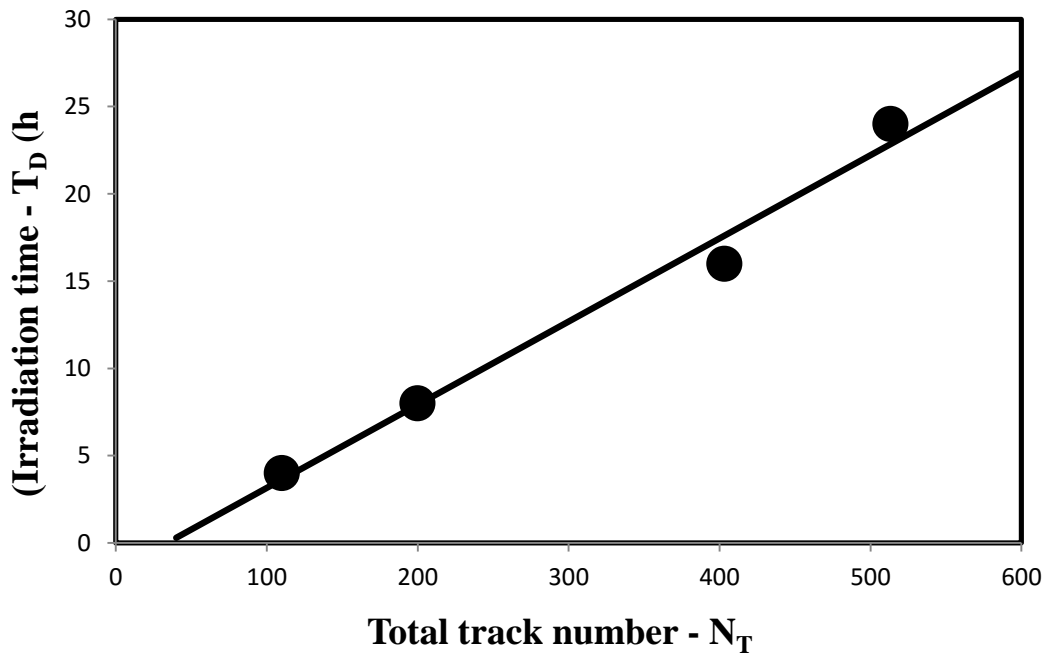


**Figure 3-32** Linear relation between the total track numbers- $N_T$  with irradiation time- $T_D$  (h)

The mathematical relation between irradiation time -  $T_D$  and total track number -  $N_T$  (without depended on track area- $A_T$  or track diameter -  $D_T$ ) which obtained from figure (3-16), was behavior as following linear relationship equation (3-10) :

$$T_D \text{ (h)} = 0.0477 N_T - 1.6187 \quad (3.10)$$

The final relations equations for CR-39 detector and CN-85 detector between the nuclear track detector parameters irradiation time -  $T_D$ , maximum count of track -  $M_{RD}$  (depend on track diameter -  $D_T$ ), maximum count of track -  $M_{RA}$  (depend on track area -  $A_T$ ), maximum track number -  $M_D$  (without depended on track diameter -  $D_T$ ), maximum track number -  $M_A$  (without depended on track area -  $A_T$ ), and total number of track -  $N_T$ , which calculated by MATLAB program were collected as shown in table (3-1).

**Table 3-1** The final equation which calculated by output of MATLAB program for the relation between irradiation time- $T_D$  for CR-39 and CN-85 detectors with  $M_{RD}$  (deepened on track diameter - $D_T$ ),  $M_{RA}$  (deepened on track area -  $A_T$ ), maximum track number -  $M_D$  (without depended on track diameter -  $D_T$ ), maximum track number -  $M_A$  (without depended on track area -  $A_T$ ), and total number of track -  $N_T$ .

Type of detector	Type of measurement	Equation	Range
CR-39	Track Diameter - $D_T$ ( $\mu\text{m}$ )	$T_D (h) = 0.1759 M_{RD} + 0.7321$	(2.5-4) $\mu\text{m}$
		$T_D (h) = 0.1376 M_D + 1.7861$	
	Track Area - $A_T$ ( $\mu\text{m}^2$ )	$T_D (h) = 3.5644e^{0.0156 M_{RA}}$	(7-24) $\mu\text{m}^2$
		$T_D (h) = 9.6822 \ln(M_A) - 29.156$	
	Total - $N_T$	$T_D (h) = 0.0518 N_T - 0.2591$	
CN-85	Track Diameter - $D_T$ ( $\mu\text{m}$ )	$T_D (h) = 0.2924 M_{RD} - 2.5692$	(2.5-5) $\mu\text{m}$
		$T_D (h) = 0.2257 M_D - 0.3706$	
	Track Area - $A_T$ ( $\mu\text{m}^2$ )	$T_D (h) = 2.9011e^{0.0239 M_{RA}}$	(9-35) $\mu\text{m}^2$
		$T_D (h) = 12.121 \ln(M_A) - 38.302$	
	Total - $N_T$	$T_D (h) = 0.0477 N_T - 1.6187$	

Figure (3-33) shows the relations behavior of irradiation time -  $T_D$  (h) for nuclear track detector type CR-39 and CN-85 with following nuclear track parameters which calculated by using MATLAB program, maximum track number -  $M_D$  (without depended on track diameter -  $D_T$ ), maximum track number -  $M_A$  (without depended on track area -  $A_T$ ), and total number of track -  $N_T$ .

Figure (3-33:a) shows relation of irradiation time -  $T_D$  with maximum track number -  $M_D$  (without depended on track diameter -  $D_T$ ), when the relation of irradiation time -  $T_D$  with maximum track number -  $M_A$  (without depended on track area -  $A_T$ ) was shown in figure (3-33:b). While the relation of irradiation time -  $T_D$  with total number of track -  $N_T$  was shown in figure (3-33:c).

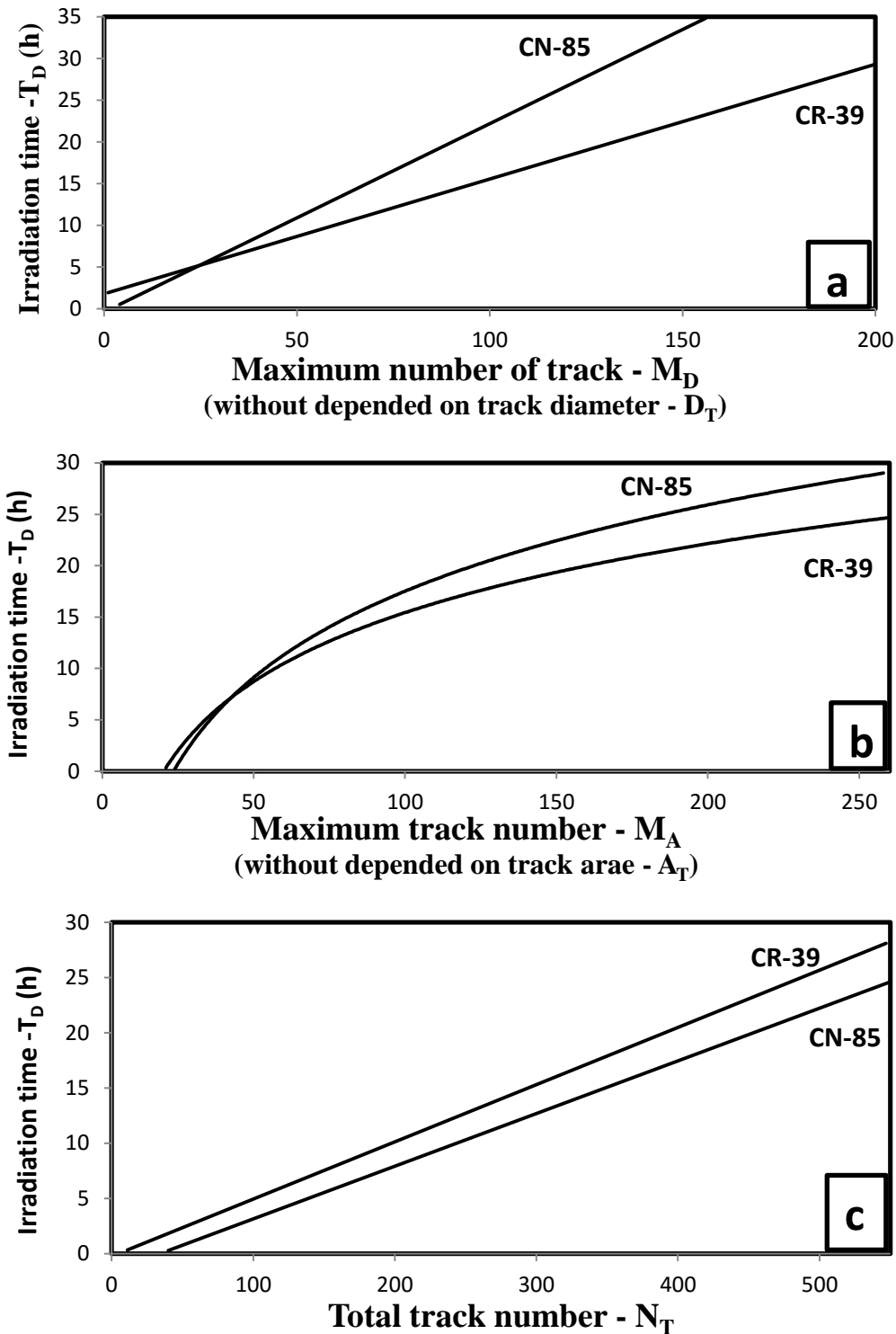


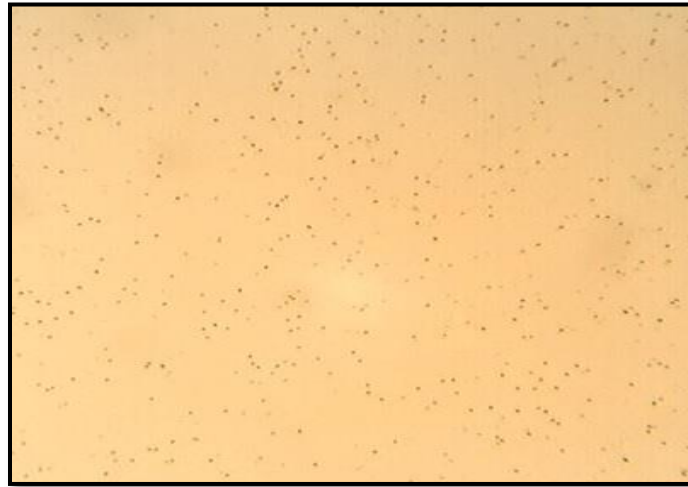
**Figure 3-33** Final relation of irradiation time -  $T_D$  for nuclear track detector type CR-39 and CN-85 with following nuclear track parameter which calculated by MATLAB program,  
 a) Maximum track number -  $M_D$  (without depended on track diameter -  $D_T$ )  
 b) Maximum track number -  $M_A$  (without depended on track area -  $A_T$ )  
 c) Total number of track -  $N_T$

From figure (3-33:a) shows the relation behavior of irradiation time -  $T_D$  with maximum track number -  $M_D$  (without depended on track diameter -  $D_T$ ) for CR-39 detector and CN-85 detector. This relation have response in CR-39 detector better than CN-85 detector. Also in figure (3-33:b) shows the relation behavior of irradiation time -  $T_D$  with maximum track number -  $M_A$  (without depended on track area -  $A_T$ ) for CR-39 detector and CN-85 detector. And this relation have response in CR-39 detector better than CN-85 detector. While in figure (3-33:c) shows the relation behavior of irradiation time -  $T_D$  with total track number -  $N_T$  for CR-39 detector and CN-85 detector, which have the response of CN-85 was better than CR-39 detector.

## 3.2 Image processing and analysis by using Image-J program

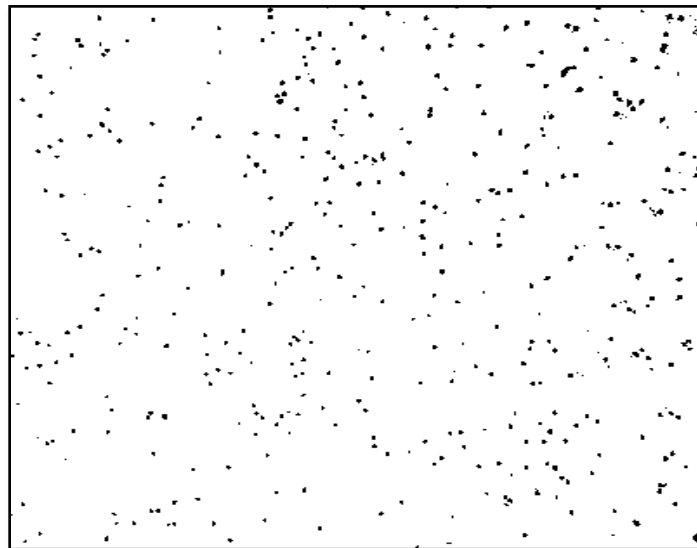
### 3.2.1 For CR-39 detector

This program is simplest from MATLAB because it has available options and don't need programming. The first step in this program was opened the image which will process as shows in figure (3-34).



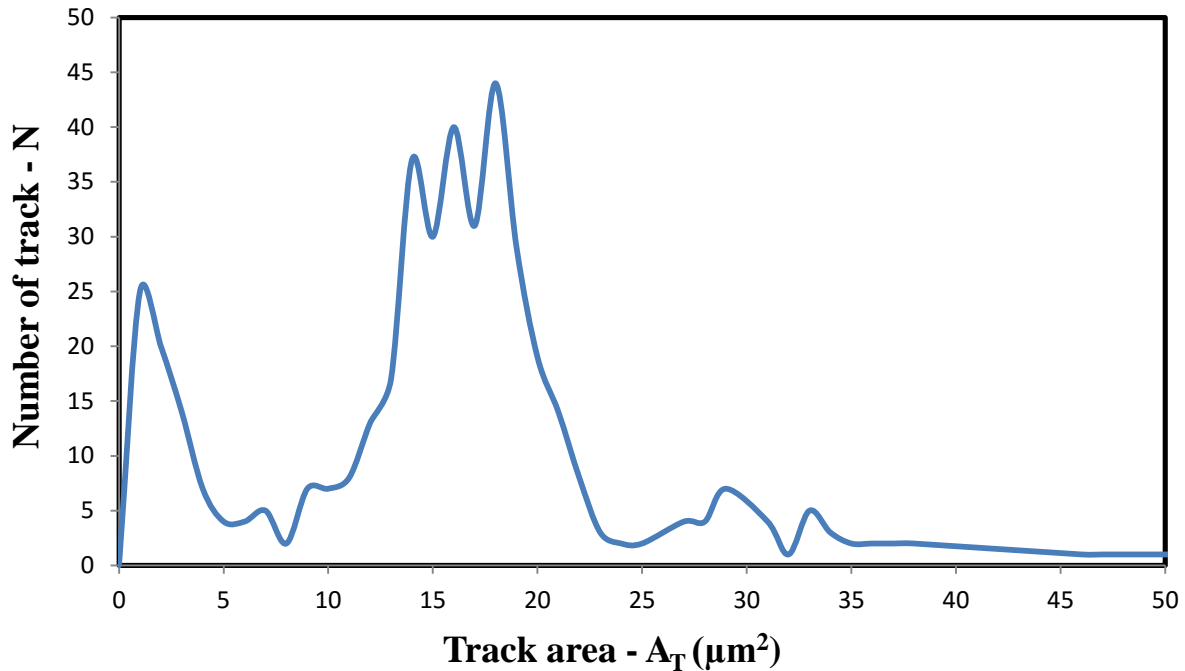
**Figure 3-34** First step from image processing of Image-J program which obtained the track image in CR-39 detector after 24h irradiated time -  $T_D$

Figure (3-35) shows the image in binary system after convert the image in figure (3-34) to the second step of this program.



**Figure 3-35** Second step from image processing of Image-J program which obtained the convert to binary system in CR-39 detector after 24h irradiated time -  $T_D$

The relationship between track number -  $N$  and track area -  $A_T$  for irradiated CR-39 detector at 24h which obtained in figure (3-36). This figure shows the maximum track number -  $M_{RA}$  (relative to track area -  $A_T$ ) appear at less than  $5 \mu\text{m}^2$ , and at the range of track area -  $A_T$  from  $10 \mu\text{m}^2$  to  $24 \mu\text{m}^2$ .



**Figure 3-36** Third step from image processing of Image-J program between the track number -  $N_T$  and the tracks area- $A_T$  for irradiated CR-39 detector at 24h

While in figure (3-37) shows the relation of the track number -  $N$  with track area -  $A_T$  ( $\mu\text{m}^2$ ) for different  $T_D$ . From this figure obtained increase in the value of maximum track number -  $M_{RA}$  (relative to track area -  $A_T$ ) with increase in irradiation time -  $T_D$ , the increasing was limited at the response region of track area -  $A_T$ , from  $12 \mu\text{m}^2$  to  $22 \mu\text{m}^2$ .

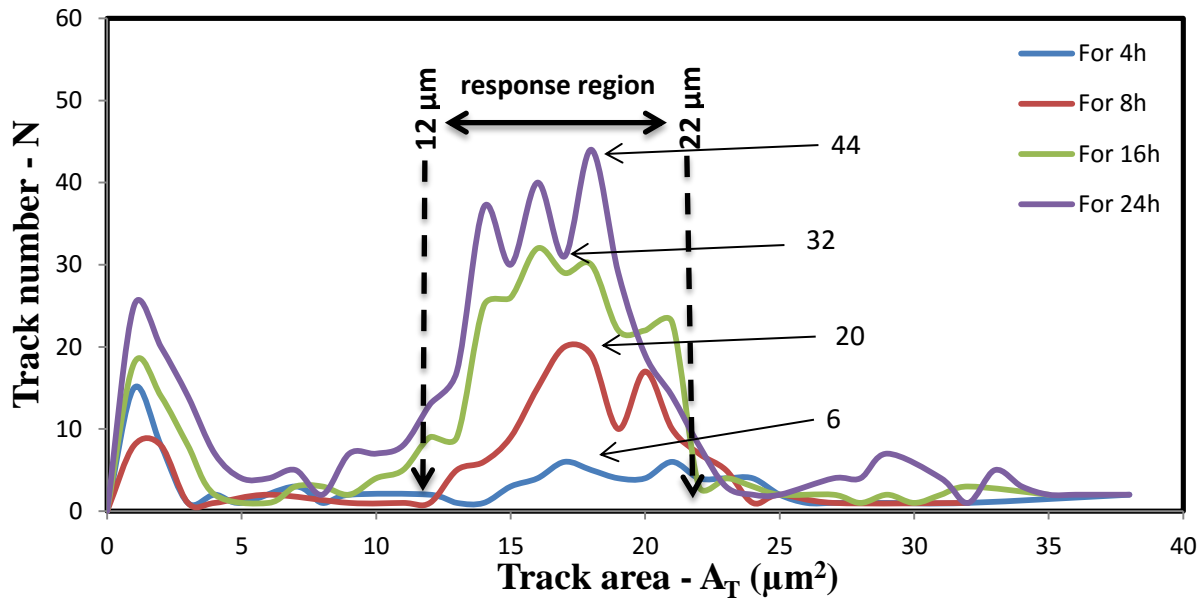


**Figure 3-37** Relation between the track number -  $N$  for CR-39 with track diameter -  $D_T$  at irradiation time -  $T_D$  4h, 8h, 16h and 24h

Figure (3-38) shows relation between irradiation time -  $T_D$  with maximum track number -  $M_{RA}$  (relative to track area -  $A_T$ ) at response region, the values of track area -  $A_T$  which start from  $12 \mu\text{m}^2$  to  $22 \mu\text{m}^2$  with values 6, 20, 32 and 44 track (relative to track area -  $A_T$ ) which calculated from figure (3-37).

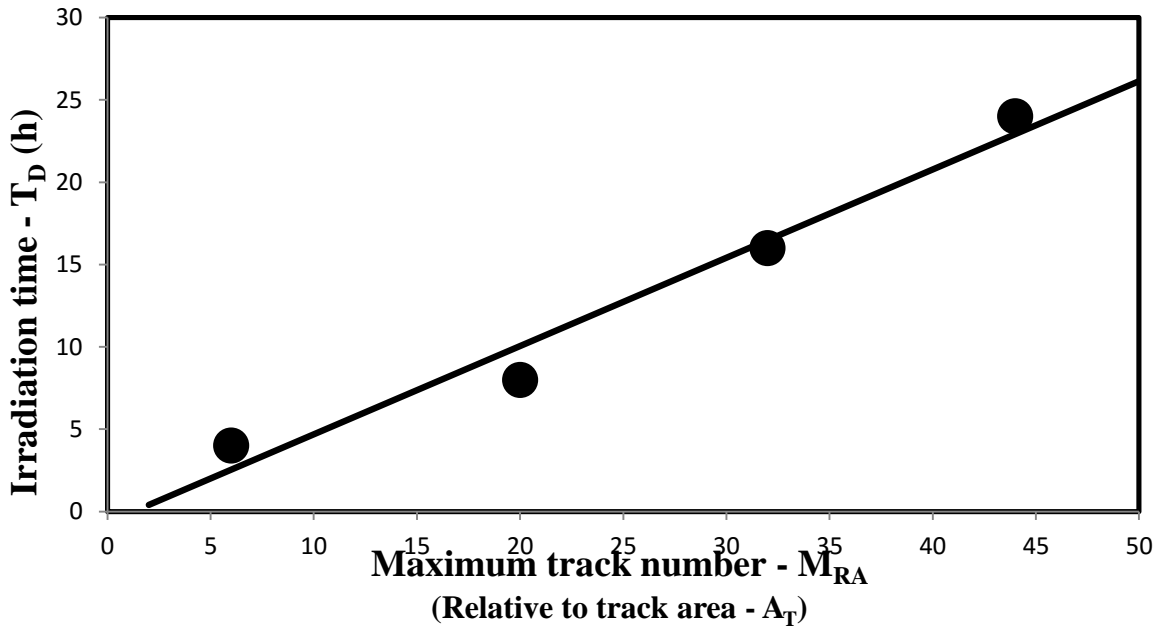


**Figure 3-38** Calibration curve between irradiation time -  $T_D$  with maximum count of track -  $M_{TA}$  (relative to track area -  $A_T$ ) at limited response region of  $A_T$ , from  $12\mu\text{m}^2$  to  $22\mu\text{m}^2$

The mathematical relation between irradiation time -  $T_D$  and maximum track number -  $M_{RA}$  (relative to track area -  $A_T$ ) which obtained from figure (3-38) was behavior as following linear relationship equation :

$$T_D \text{ (h)} = 0.5358 M_{RA} - 0.6642 \quad (3.11)$$

From equation (3.11) which used to calculate the value of irradiation time -  $T_D$  for each effect of thermal neutron after determine the value of maximum track number -  $M_{RA}$  (relative to track area -  $A_T$ ).

From figure (3-37) determined the relation between irradiation time -  $T_D$  with maximum track number -  $M_A$  (without depending on track area -  $A_T$ ). And that relation was behavior as linear relationship as shown in figure (3-39).

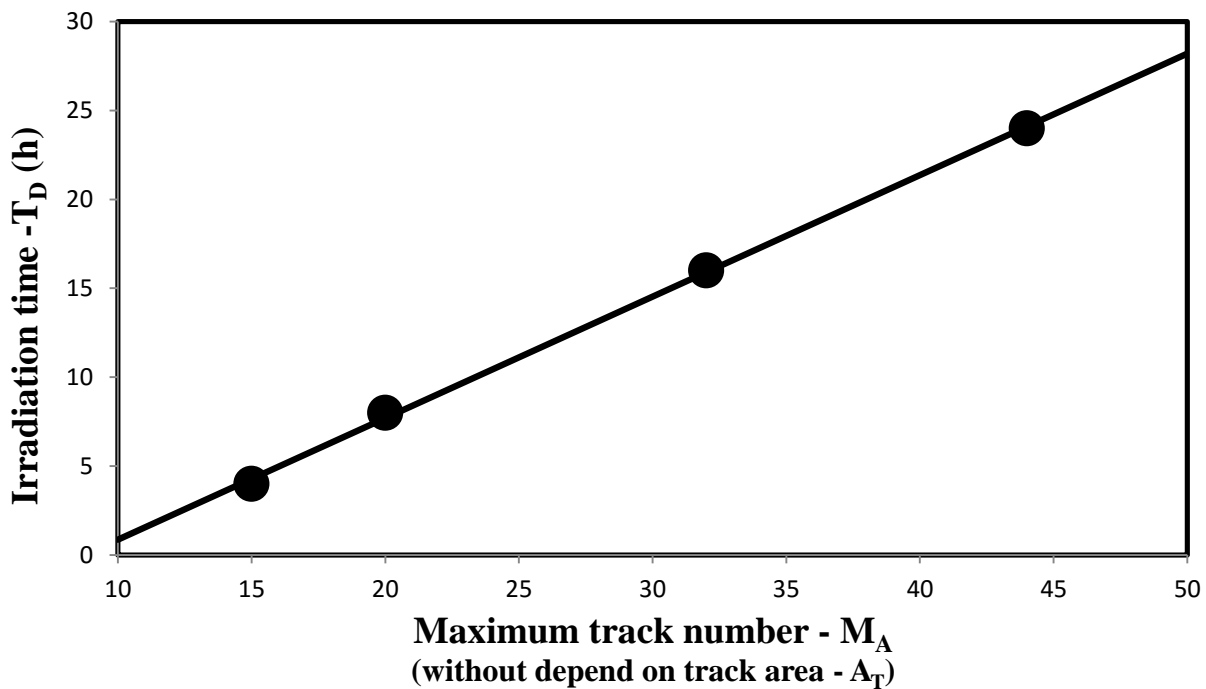


**Figure 3-39** Relation between maximum track number -  $M_T$  for each irradiation time -  $T_D$  with irradiation time -  $T_D$

The mathematical relation which reflect the behavior of irradiation time -  $T_D$  with maximum track number -  $M_A$  (without depending on track area -  $A_T$ ) in figure (3-39) calculated by following equation:

$$T_D (h) = 0.6835 M_A - 5.9673 \quad (3.12)$$

The total track number -  $N_T$  which reflect the value of maximum track without depending on the track diameter -  $D_T$  and track area -  $A_T$  of tracks, was behavior as a linear relationship between irradiation time -  $T_D$  and total track number -  $N_T$  as shown in figure (3-40).

The mathematical relation between irradiation track -  $T_D$  and total number -  $N_T$  (without depended on track area -  $A_T$  or track diameter -  $D_T$ ) which obtained from figure (3-40) was behavior as following linear relationship equation :

$$T_D = 0.0519 N_T - 0.2773 \quad (3.13)$$

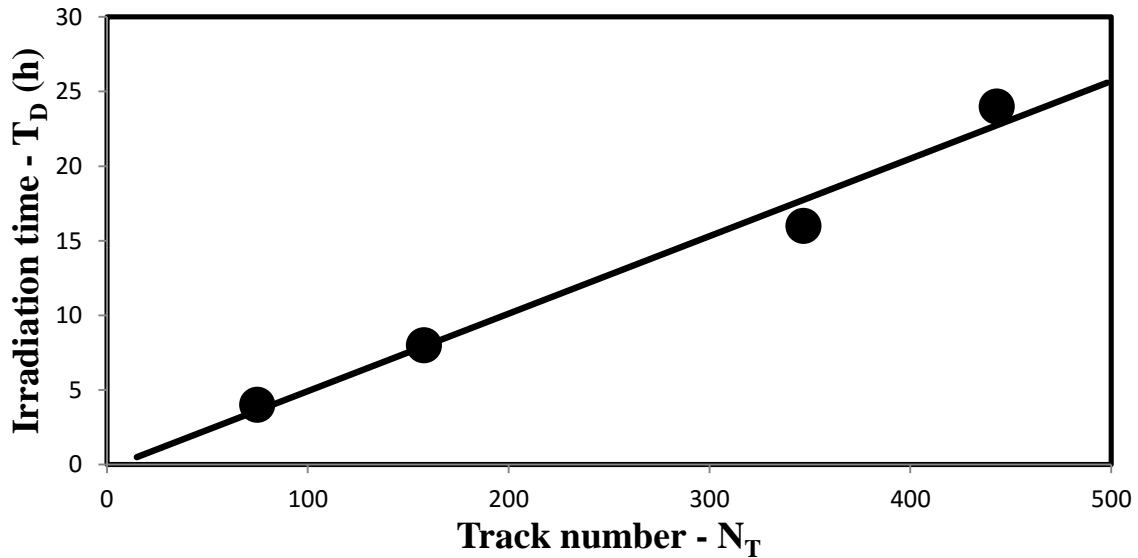


**Figure 3-40** Linear relation between the total track numbers -  $N_T$  with irradiation time -  $T_D$

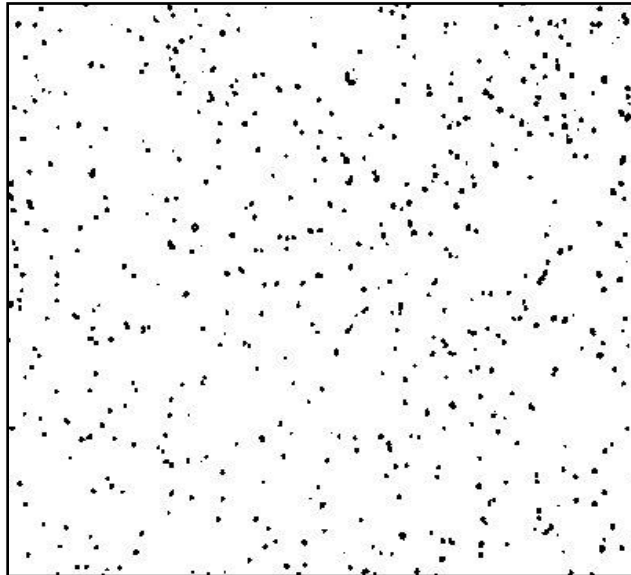
### 3.2.1 For CN-85 detector

Figure (3-41) also obtained the image which will process for CN-85 detector.



**Figure 3-41** First step from image processing of Image-J program which obtained the track image in CN-85 detector after 24h irradiated time -  $T_D$

In figure (3-42) shows the image in binary system after convert the image in figure (3-41) in second step of this program.



**Figure 3-42** Second step from image processing of Image-J program which obtained the convert to binary system in CN-85 detector after 24h irradiated time -  $T_D$

The relationship between track number -  $N$  and track area -  $A_T$  for irradiated CR-39 detector at 24h which obtained in figure (3-43). From this figure shows the maximum track number -  $M_{RA}$  appear at less than  $4 \mu\text{m}^2$ , and at the range of track area -  $A_T$  from the values  $15 \mu\text{m}^2$  to  $28 \mu\text{m}^2$ .

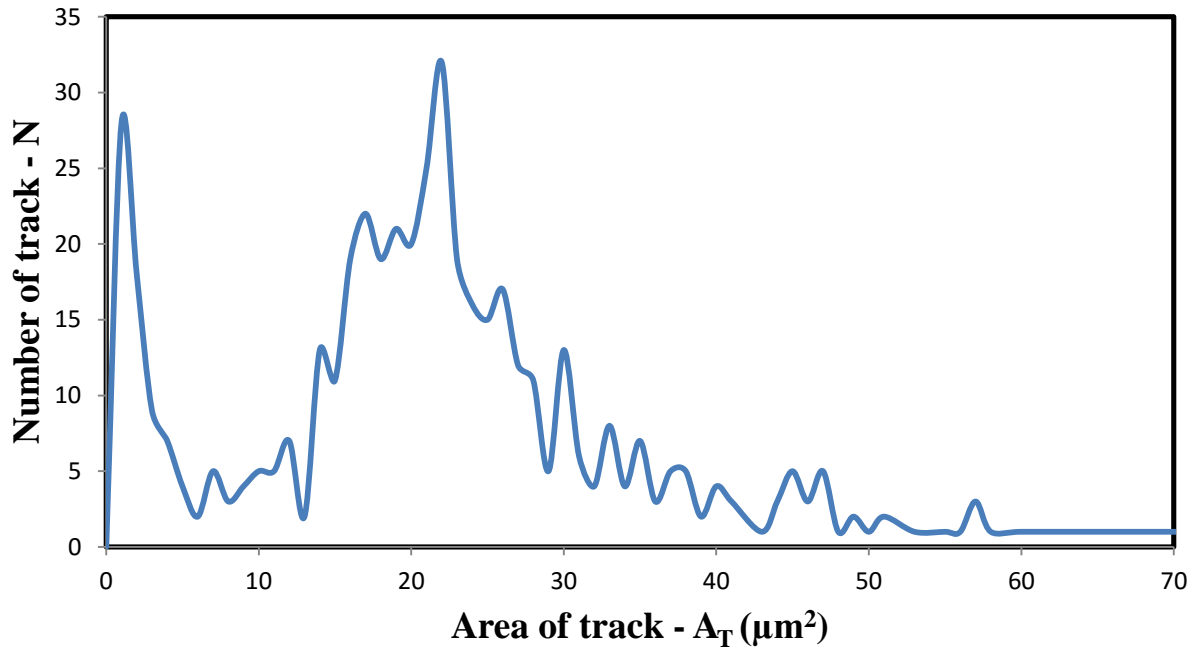


**Figure 3-43** Third step from image processing of Image-J program between the track numbers -  $N$  and the track area -  $A_T$  for irradiated CN-85 detector at 24h

While in figure (3-44) shows the relation of the track number -  $N$  with track area -  $A_T$  ( $\mu\text{m}^2$ ) for irradiation time -  $T_D$  4h, 8h, 16h and 24h. From this figure obtained increase in the value of maximum track number -  $M_{RA}$  (relative to track area -  $A_T$ ) with increase in irradiation time -  $T_D$ . The increasing of number of track- $N$  was limited at the response region of track area -  $A_T$ , from  $5 \mu\text{m}^2$  to  $27 \mu\text{m}^2$ .

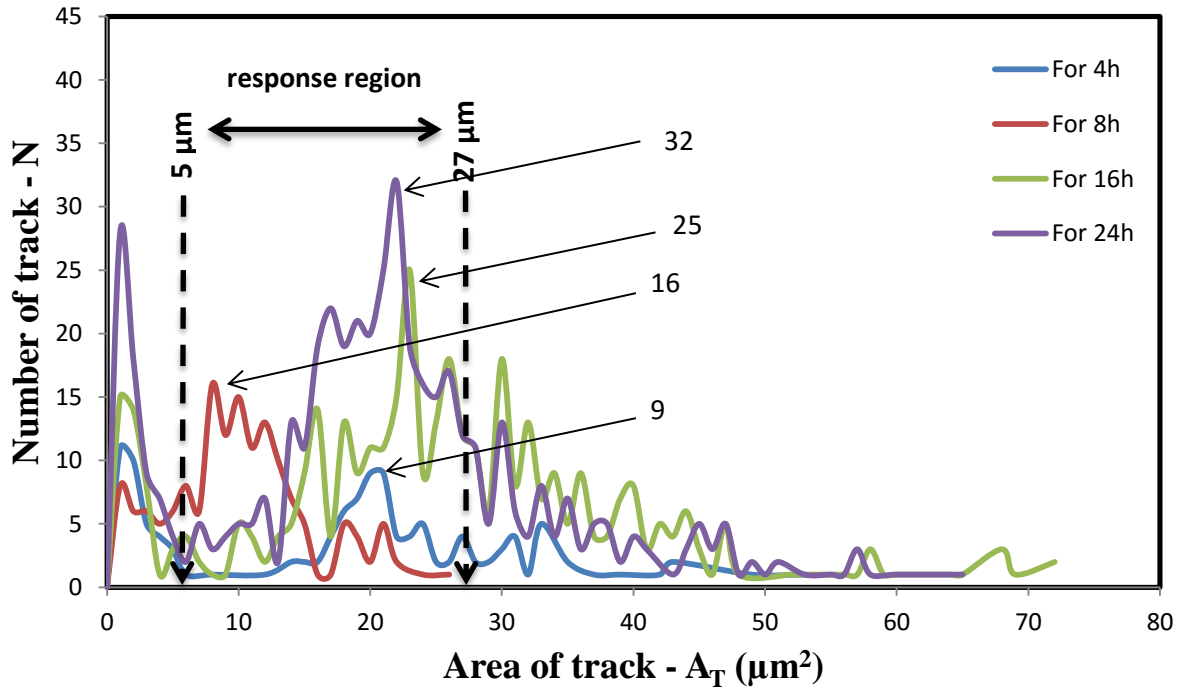


**Figure 3-44** Relation between the track number -  $N$  for CR-39 with track area -  $A_T$  at irradiation time -  $T_D$  for 4h, 8h, 16h and 24h

Figure (3-45) shows relation between irradiation time -  $T_D$  with maximum track number -  $M_{RA}$  (relative to track area -  $A_T$ ) at limited response region of track area -  $A_T$ , from  $5 \mu\text{m}^2$  to  $27 \mu\text{m}^2$ .

And the mathematical relation between irradiation time -  $T_D$  and maximum track number -  $M_{RA}$  (relative to track area -  $A_T$ ) which obtained from figure (3-45), was behavior as following linear relationship equation (3-14) :

$$T_D \text{ (h)} = 0.8721 M_{RA} - 4.8787 \quad (3.14)$$

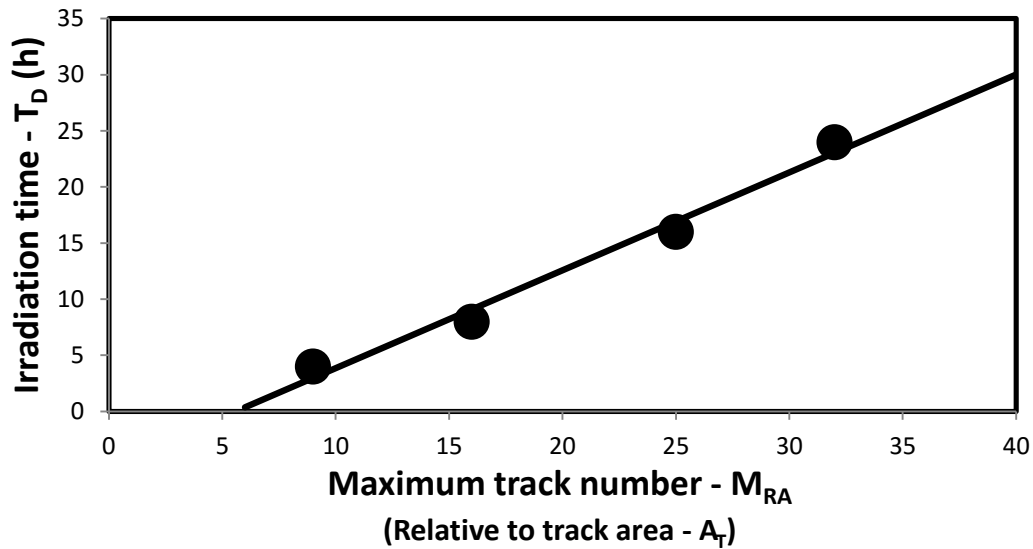


**Figure 3-45** Calibration curve between irradiation time -  $T_D$  (h) with maximum track number -  $M_{RA}$  (relative to track area) at limited response region of  $A_T$ , starting from  $5 \mu\text{m}^2$  to  $27 \mu\text{m}^2$

Equation (3.14) which used to calculate the value of irradiation track -  $T_D$  for each effect of thermal neutron after determine the value of maximum track number -  $M_{RA}$  (relative to track area -  $A_T$ ).

From figure (3-44) present the relation between irradiation time -  $T_D$  with maximum track number -  $M_A$  (without depending on area of track -  $A_T$ ). And that relation was behavior as linear relationship as shown in figure (3-46)

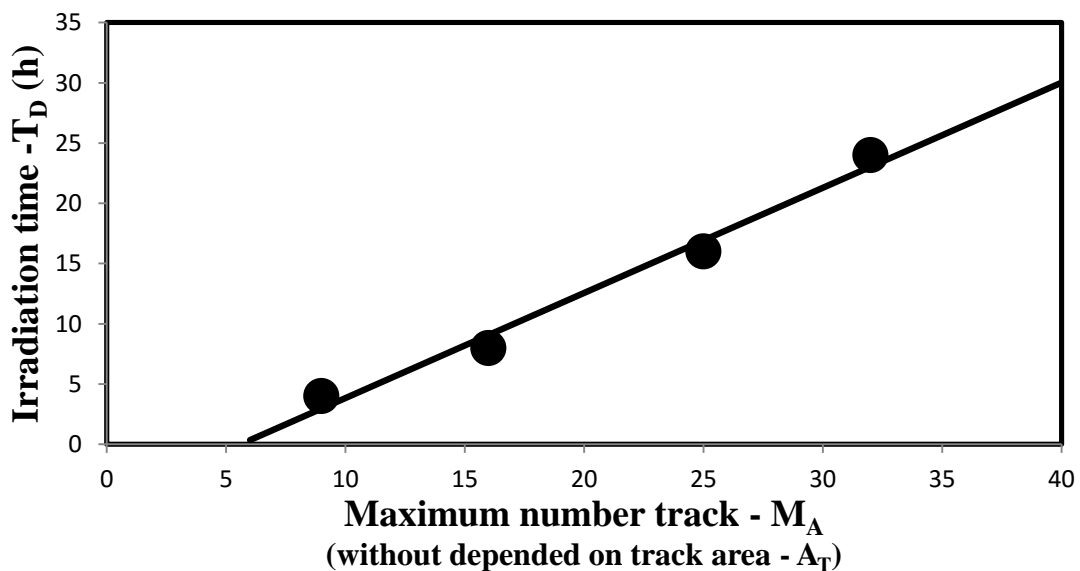


**Figure 3-46** Relation between maximum track number -  $M_A$  with irradiation time -  $T_D$  (h)

The mathematical equation which reflect the behavior of irradiation time -  $T_D$  with maximum track number -  $M_A$  (without depending on track area -  $A_T$ ) in figure (3-46) calculated in following equation :

$$T_D (h) = 0.8721 M_A - 4.8787 \quad (3.15)$$

The total track number -  $N_T$  which reflect the value of maximum track number (without depending on the track diameter -  $D_T$  and area track -  $A_T$ ) was behavior as a linear relationship between irradiation time -  $T_D$  and total track number -  $N_T$  as showsn in figure (3-47).

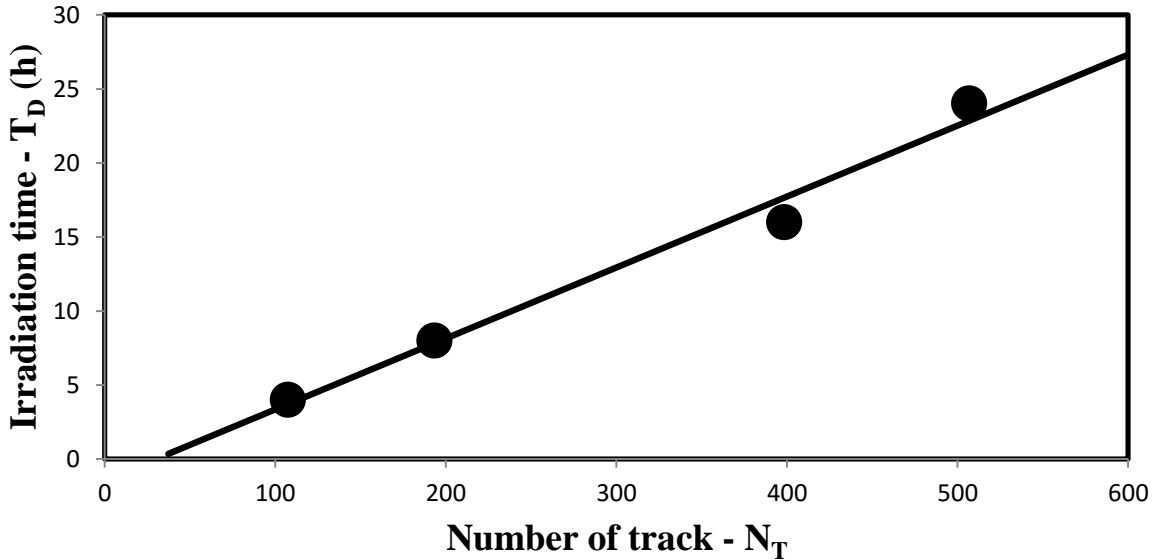


**Figure 3-47** Linear relation between the total track numbers -  $N_T$  with irradiation time- $T_D$

The mathematical relation between irradiation track -  $T_D$  and total track umber -  $N_T$  (without depended on track area -  $A_T$  or track diameter -  $D_T$ ) which obtained from figure (3-47) was behavior as following linear relationship equation (3-16) :

$$T_D (h) = 0.0479 M_T - 1.452 \quad (3.16)$$

The final relations and equations for CR-39 detector and CN-85 detector between the nuclear track detector parameters irradiation time -  $T_D$ , maximum track number -  $M_{RA}$  (depend on track area -  $A_T$ ), maximum track number -  $M_A$

(without depended on track diameter -  $D_T$  or track area -  $A_T$ ), and total number of track -  $N_T$ , which calculated by Image-J program were collected as showsn in table (3-2).

**Table 3-2** The final equations which calculated by output of Image-J program for the relation between irradiation time -  $T_D$  for CR-39 and CN-85 detector with maximum track number -  $M_{RA}$  (deepened on track area -  $A_T$ ), maximum track number -  $M_A$  (without depended on track diameter-  $D_T$  or track area -  $A_T$ ), and total number of track -  $N_T$

Type of detector	Type of measurement	Equation	Range
CR-39	Track Area ( $\mu\text{m}^2$ )	$T_D = 0.5358 M_{TA} - 0.6642$	(12-24) $\mu\text{m}^2$
		$T_D = 0.6835M_T - 5.9673$	
	Total	$TD = 0.0519N_T - 0.2773$	
CN-85	Track Area ( $\mu\text{m}^2$ )	$T_D = 0.8721M_{TA} - 4.8787$	(5-27) $\mu\text{m}^2$
		$T_D = 0.8721M_T - 4.8787$	
	Total	$T_D = 0.0479N_T - 1.452$	

Figure (3-48) shows the relations behavior of irradiation time -  $T_D$  (h) for nuclear track detector type CR-39 and CN-85 with following nuclear track parameter, maximum track number -  $M_A$  (without depended on track area -  $A_T$ ), and total number of track -  $N_T$ .

From figure (3-48:a) shows relation of irradiation time -  $T_D$  with maximum track number -  $M_A$  (without depended on track area -  $A_T$ ), while the relation of irradiation time -  $T_D$  with total number of track -  $N_T$  was showsn in the figure (3-48:b).

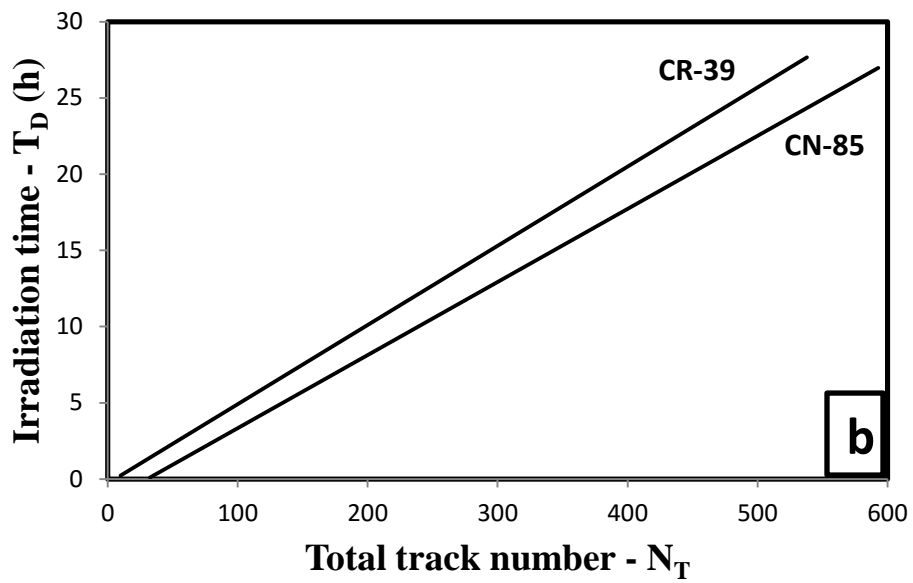
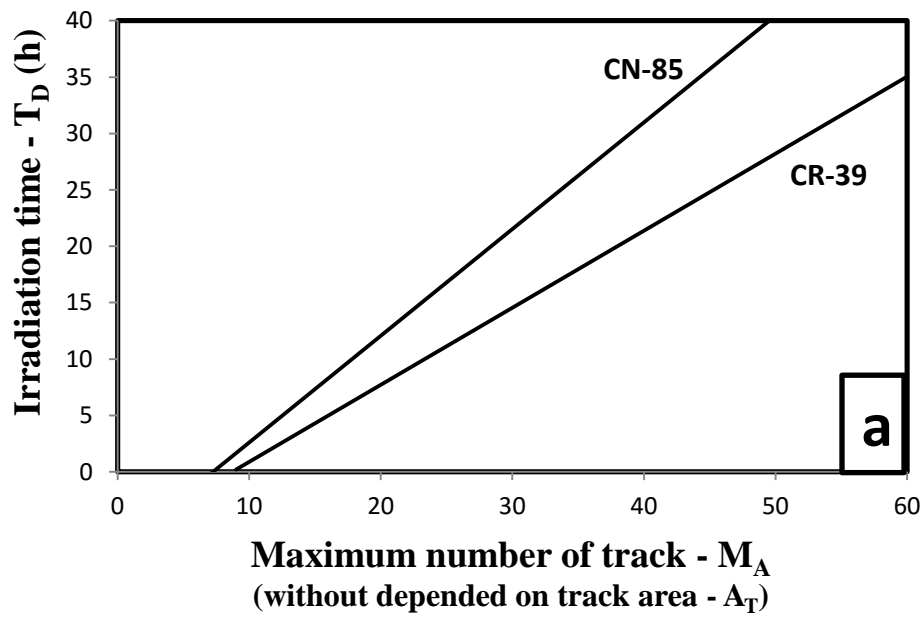


**Figure 3-48** Final relation of irradiation time -  $T_D$  for nuclear track detector type C R-39 and CN-85 with following nuclear track parameters which calculated by Image-J program,  
 a) Maximum track number -  $M_A$  (without depended on track area)  
 b) Total number of track -  $N_T$

Also in figure (3-48:a) obtained relation behavior of irradiation time -  $T_D$  and maximum track number -  $M_A$  (without depended on track area -  $A_T$ ) for CR-39 detector and CN-85 detector which obtained the irradiation response of CR-39

detector was better than CN-85 detector. While in figure (3-48:b) shows relation behavior of irradiation time -  $T_D$  and Total track number -  $N_T$  for CR-39 detector and CN-85 detector which obtained the irradiation response of CN-85 detector was better than CR-39 detector.

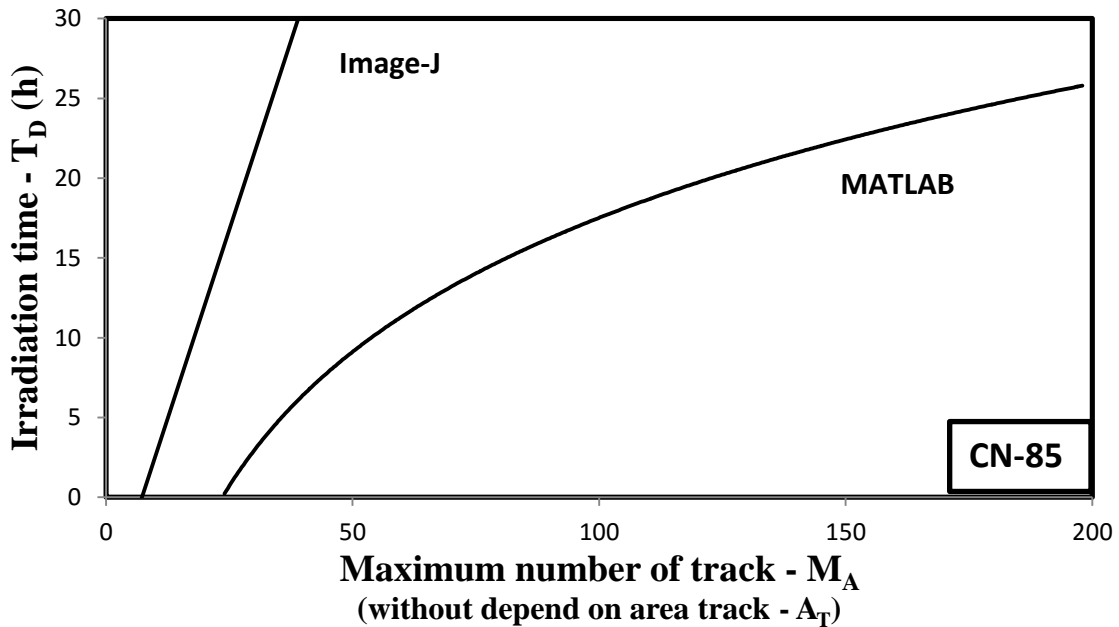
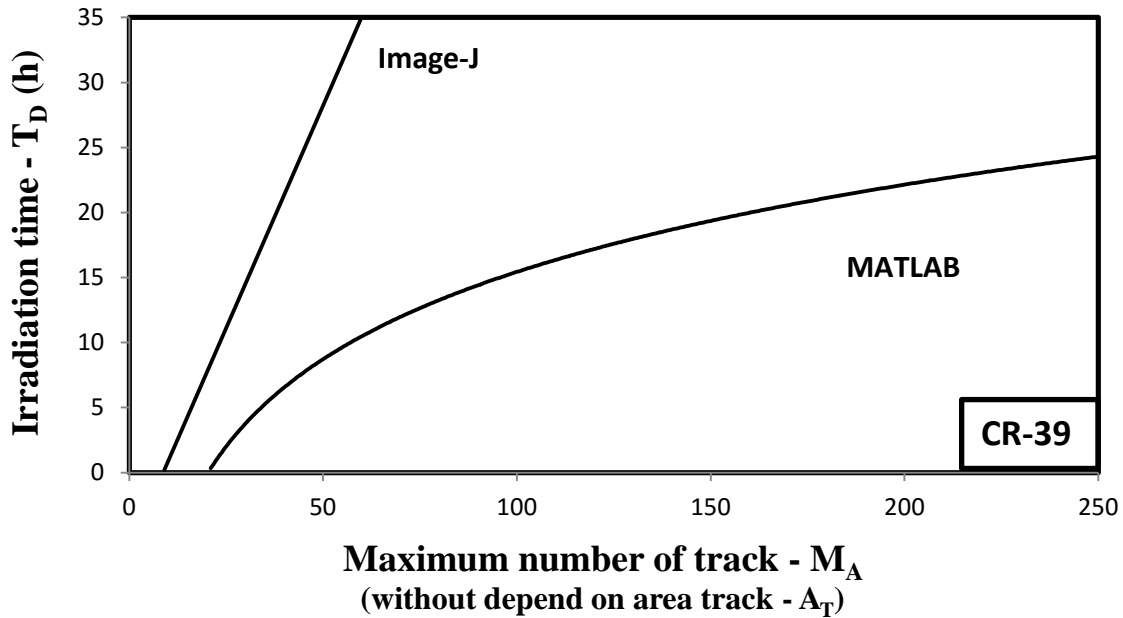


**Figure 3-49** Relation between irradiation time -  $T_D$  with maximum number of track -  $M_A$  (without depended on track area –  $A_T$ ) for nuclear track detector type CR-39 and CN-85 detectors by using of MATLAB program and Image-J programs

The comparison between MATLAB and Image-J programs for relation between irradiation time -  $T_D$  and maximum track number -  $M_A$  (without depended on track area -  $A_T$ ) was shown in figure (3-49). And obtained the output calculation of nuclear track parameters from MATLAB was better than these calculation in Image-J at CR-39 detector. And the slop of equation (3-12) was 0.6835 from Image-J program when the slop of equation (3-4) was 9.6822 from MATLAB program with logarithmic relation. That mean the different in the value of slop which calculated by equation (3-12) and equation (3-4) reflected the output data analysis for MATLAB program was better than Image-J program.



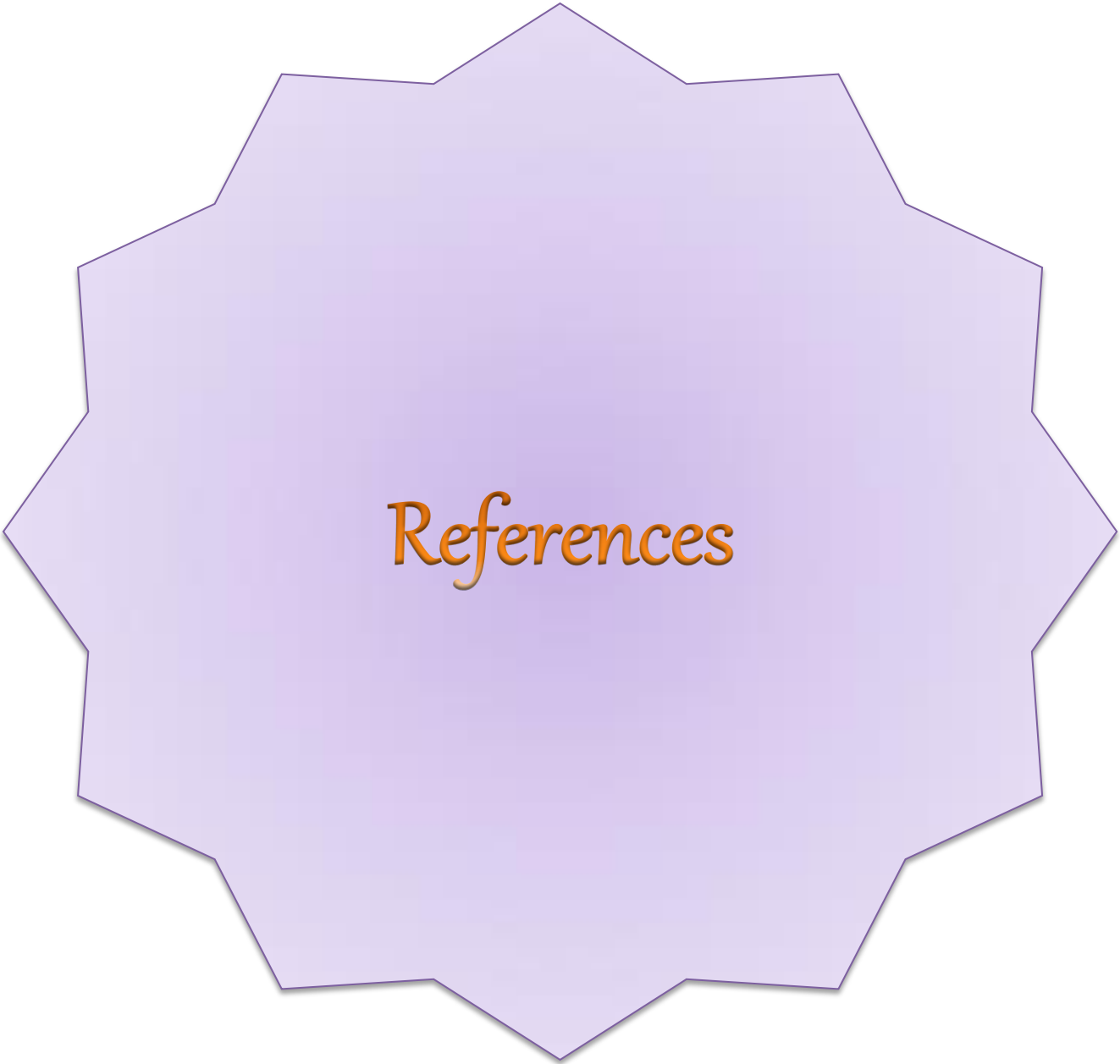
*Chapter Four*  
*Conclusions*

**Chapter Four**

## **Conclusions**

- 1- In this study obtained by image processing and analysis technique in MATLAB and Image-J programs at scanning time of less than a few minute per image analyzed, and better option for personnel monitoring where large numbers of samples are to be processed and analyzed. And the determination of nuclear track detector parameters which calculated in CR-39 and CN-85 detectors by using image processing technique, (MATLAB and Image-J programs) can be using for other detectors.
- 2- There was another methods in image program in MATLAB program from options (image processing toolbox - enhancement – correction nonuniform illumination) which using the determination of shape and depth of tracks -  $D_p$  depending on coloring of track as obtained in effect of the thermal neutron as M. Akram et. al. in (2013). Also can use image processing in MATLAB program to solve and process the overlap of track by option in program (image processing toolbox - image segmentation - marker - controlled watershed segmentation).
- 3- The relation equations which calculated by MATLAB program for nuclear track diameter -  $D_T$  with irradiation time -  $T_D$  can be used to obtained the amount of energy for  $\alpha$ -particle and the relation between energy of  $\alpha$ -particle with irradiation time -  $D_T$  which used to determine the type of  $\alpha$ -particle emitters.
- 4- The data analyses which calculate by MATLAB program for the relations of nuclear track detectors, specialized nuclear track diameter -  $D_T$  can used in the nanotechnology studies. Where the preparation of nanofilters and nonomembrane from NTDs take into account the nuclear track diameter - $D_T$  as the indicator to reach the require of nanofilters and nonomembrane.

- 5- Image processing analysis by another methods can used also, for the images which photo by polarized optical microscope – POM or scanning electron microscope –SEM. These images include the picture of NTDs etch solution after alpha particle irradiation.
- 6- The relations which calculated by this study between nuclear track diameter -  $D_T$  with another nuclear track parameters, can conclusion by the next studies of the relations between track core radius-  $dc$  ( which depend on the track diameter -  $D_T$  ) and energy loss rate ( $\frac{dE}{dx}$ ) of alpha particle.
- 7- The inferred results from images processing for NTDs , It could give a clear picture for the amount of irradiation contamination by alpha emitters sources in fields of environmental radiation accidents.



# *References*

## *References*

- [1] Malinowska, A., Szydłowski, A., Jaskóła, M., Korman, A., Sartowska, B., Kuehn, T. and Kuk, M. "Investigations of protons passing through the CR-39 / PM-355 type of solid state nuclear track detectors", *Review of Scientific Instruments* 84, p 1-6, (2013).
- [2] Nikezic, D. and Yub, K.N. "Formation and growth of tracks in nuclear track materials", *Materials Science and Engineering* 46, p 51–123, (2004).
- [3] Nikezic, D. and Yu, K.N., "Optical characteristics of tracks in solid state nuclear track detectors studied with ray tracing method", Nova Science Publishers, Inc., p 1-19, (2009).
- [4] Shahid manzoor, "Improvements and calibration of nuclear track detector for rare particle searches and fragmentation studies", *facoltda de scienze matematiche fisiche naturali anno accademico*, Ms.c thesis, p 1, (2006/ 2007).
- [5] Al-Tememy, Lamyā' Tawfiq Ali, "Uranium concentration measurements of human blood samples using CR-39", AL-Nahrain University, Ms.c thesis, p 30, (2007).
- [6] Mohammed, Aamir Abdullah, "Concentration measurements of radon, uranium and background of gamma rays in air at the university of Baghdad – Al-Jadiriyah site", University of Baghdad, Ms.c thesis, p 46, (2013).
- [7] "Introduction to Radiation", Canadian Nuclear Safety Commission (CNSC), p 7, (2012).
- [8] "Radiation and Radioactive Materials" National Law Enforcement and Corrections Technology Center
- [9] "Radiation: Facts, Risks and Realities", United state Environmental protection agency", April (2012).
- [10] Kwan-Hoong Ng, "Non-ionizing radiations–sources, biological effects, emissions", the International Conference on Non-ionizing Radiation at UNITEN, October (2003).
- [11] [http://www.windows2universe.org/physical\\_science/physics/atom\\_particle/](http://www.windows2universe.org/physical_science/physics/atom_particle/)

- [12] Al – Rubyie, Atheer Qassim Muryoush, "Radioactive detection on the blood samples of cancer patients diseases by using CR-39 detector and its effect on cytogenetic", AL-Nahrain University, Ms.c thesis, p 7, (2004).
- [13] Saja Faaiz hassen, "Measurement of uranium concentration in human blood samples from some governorates of Iraq With using CR-39 nuclear track detector", AL-Nahrain University, Ms.c thesis, p 39, (2006).
- [14] Fala Hatem Taha, "Radiation dose assessment for ionizing and ultraviolet radiations using CR-39, lexan and LR-115 nuclear track detectors", AL-Nahrain University, Ms.c thesis, p 23, (2011).
- [15] Durrani, S. A. and Bull, R. K., "Solid state nuclear track detector", Pergamonn press Oxford, (1987).
- [16] Fathi, firas mohammed ali, "Electromagnetic radiation dosimetry using nuclear track detectors and determination of their intrinsic efficiencies with invocation computer image processing in measurement of nuclear track parameters", University of Mosul, Ds.c dissertation, p 20, (2009).
- [17] Peeples, Cody Ryan, "Alternatives to the americium-beryllium neutron sourcefor the compensated neutron porosity log raleigh", North Carolina University, Ms.c thesis, (2007).
- [18] Kakavand, T., Haji-Shafeieha, M. AND Ghafourian, H., "STUDY of neutron yield for the  $^{241}\text{Am}$ - $^9\text{Be}$  source", Iranian Journal of Science and Technology, Transaction 33, p. 277 -280, (2009).
- [19] Taner Uckan, José March-Leuba, Danny Powell, James D. White and Joseph Glaser, " $^{241}\text{AmBe}$  sealed neutron source assessment studies for the fissile mass flow monitor", OAK RIDGE National Laboratory, (2003).
- [20] Zaki, M. F., Hegazy, Tarek M. and Taha, Doaa. H., "Investigation of the effect of He-Ne Laser on the optical properties through etched CN-85 and CR-39 containing alpha tracks", Arab Journal of Nuclear Science and Applications, 46 (3), p. 201-210, (2013).

- [21] Shao Rong HB, "Measurement of solid state nuclear tracks in apatite by thermal analysis method", *shines in science bulltin*, Springer, (2009).
- [22] A. Mostofizadeh, X. Sun and M. R. Kardan, "Improvement of Nuclear Track Density Measurements Using Image Processing Techniques", *American Journal of Applied Sciences* 5 (2), p. 71-76, (2008).
- [23] IPE, N. E. and Ziemer, P. L. "Effect of pre-gamma irradiation on CR-39", SLAC - PUB - October (1985).
- [24] Chong, C.S., Ishak, I., Mahat, R. H. and Amin, Y. M., "UV-vis and FTIR spectral studies of CR-39 plastics irradiated with x-ray", *Radiation Measurements* 28, p.119-122, (1997).
- [25] Shweikani, R., Raja, G. and Sawaf, A. A., "The possibility of using plastic detectors CR-39 as uv dosimeters", *Radiation Measurements* 35, p. 281-285, (2002).
- [26] Nur Sha'dah, Z., Iskandar, S.M., Azhar, A.R., Suhaimi, M.J., Nur Lina, R. and Halimah, M.K., "UV-VIS Spectral Evaluation of CR-39 Detector Exposed with Diagnostic Dosage", *Sains Malaysiana* 43, p. 953–958, (2014).
- [27] Meenakshi Choudhary, Sangeeta Prasher and Mukesh kumar, "Structural analysis of gamma induced modification in Cr-39 polymers", *International Journal of Innovative Research in Science, Engineering and Technology* 3, Issue 7, July (2014).
- [28] Al-Jobouri, Hussain Ali, Sulaiman, Jameel M. A. and Jarallah, Ahamed S., "Effect of x-ray radiation on electro-optical characteristics of CR-39 sheets by using microwave and FTIR spectroscopy techniques", *Journal of Al-Nahrain University* 15, December, pp.318-343, (2012).
- [29] Abdel Raouf, Kh. M. , "Study of CR-39 SSNDs irradiated with different types of radiation by FTIR spectroscopy and  $\alpha$ -range determination", *American Journal of Environmental Protection* 2, p. 53-57, (2013).
- [30] Emad Hassan Aly, "microstructural investigation of PM-355 nuclear track detector subjected to low-dose gamma irradiation: a positron annihilation lifetime study", *Materials Sciences and Applications* 4, p. 622-629, (2013).

- [31] Tse, K.C.C., Ng, F.M.F. and Yu, K.N., "Photo-degradation of PADC by UV radiation at various wavelengths", *Polymer Degradation and Stability* 91, p. 2380-2388, (2006).
- [32] Tayel, A., Zaki, M.F., El Basaty, A.B. and Hegazy, Tarek M., "Modifications induced by gamma irradiation to makrofol polymer nuclear track detector", *Journal of Advanced Research*, p.1-6, (2014).
- [33] Zaki, M. F., "Gamma-induced modification on optical band gap of CR-39 SSNTD", *Brazilian Journal of Physics*, 38, p. 558-562, December, (2008).
- [34] Zaki, M. F., Hegazy, Tarek M. and Taha, Doaa. H., "Investigation of the effect of He-Ne laser on the optical properties through etched CN-85 and CR-39 containing alpha tracks", *Arab Journal of Nuclear Science and Applications* 36 , p. 201-210, (2013).
- [35] Nikezic, D., Ho, J.P.Y., Yip, C.W.Y., Koo, V.S.Y. and Yu, K.N., "Feasibility and limitation of track studies using atomic force microscopy", *Nuclear Instruments and Methods in Physics Research B* 197 , p. 293–300, (2002).
- [36] Yip, C.W.Y., Ho, J.P.Y., Nikezic, D. and Yu, K.N., "Study of inhomogeneity in thickness of LR 115 detector with SEM and form talysurf ", *Radiation Measurements* 36, p. 245 -248, (2003).
- [37] Ho, J.P.Y., Yip, C.W.Y., Nikezic, D. and Yu, K.N., "differentiation between tracks and damages in SSNTD under the atomic force microscope", *Radiation Measurements* 36, p.155 - 159, (2003).
- [38] Ng, F.M.F., Yip, C.W.Y., Ho, J.P.Y., Nikezic, D. and Yu, K.N., "non-destructive measurement of active-layer thickness of LR 115 SSNTD", *Radiation Measurements* 38, p. 1 - 3, (2004)
- [39] Vlasova, I.E., Kalmykov, S.N., Kashkarov, L.L. ,Clark, S. B. and Aliev, R.A., "plutonium spatial distribution in soils studied by track analysis and SEM-EDS", *Electronic Scientific Information Journal* 1, p.1-3, (2004).
- [40] B. Basua, B. Fischerb, A. Mazumdar, S. Rahaa, S. Sahad, S.K. Sahaa, and D. Syame, " Characterization of a polymer as a heavy ion detector", 29th International Cosmic Ray Conference Pune 9, p. 279-282, (2005).

- [41] Sharma, Vishal, Diwan, P K, Pratibha, Tanu Sharma, Shyam Kumar and Avasthi, D K, "Energy loss of light ions in polypropylene absorber foils", *Indian J. Phys.* 83 (7), p. 937-941, (2009).
- [42] Nidhi, Renu Gupta, Tanu Sharma, Sanjeev Aggarwal and Kumar, S, "Effect of thermal annealing on optical properties of CR-39 polymeric track detector", *Indian J. Phys.* 83 (7), p. 921-926, (2009).
- [43] M. El Ghazaly and H.E. Hassan, " Spectroscopic studies on alpha particle-irradiated PADC (CR-39 detector)", *Results in Physics*, 4, p. 40-43, (2014).
- [44] Ambika Negi, Hariwal, R V, Anju Semwal, Sonkawede, R G, Kanjilal, D, Jmsrana and Ramola, R C, "Opto-chemical response of makrofol-kg to swift heavy ion irradiation", *journal of physics Indian Academy of Sciences* 77, p. 707–714 , October (2011).
- [45] Vijay Kumar, Sonkawade R G, Yasir Ali and Dhaliwal A.S, "Study of chemical, optical and structural properties of 120 MeV Ni<sup>11+</sup> ions beam irradiated poly (ethylene terephthalate) film", *International Journal of Applied Engineering Research* 2, p. 419-430, (2011).
- [46] Costea, C., Dului, O.G., Danis, A., Szobotka, S., "SEM investigations of CR-39 and mica-muscovite solid state nuclear track detectors", *Romanian Reports in Physics* 63, P. 86–94, (2011).
- [47] Mosier-Boss, Forsley, L.P.G., Carbonnelle, P., Morey, M.S., Tinsley, J.R., Hurley, J.P. and Gordon, F.E., "Comparison of SEM and optical analyses of DT neutron tracks in CR-39 detectors" ,*Radiation Measurements* 47, p. 57-66, (2012).
- [48] Espinosa, G. and Golzarri, J.I., "Ageing effects on polymeric track detectors: studies of etched tracks at nanosize scale using atomic force microscope", *Radiation Physics Revista Mexicana de F´ısica* 58, p. 215–219, (2012).
- [49] Malinowska, A., Szydłowski, A., Jaskóła, M., Korman, A., Sartowska, B., Kuehn, T. and Kuk, M. "Investigations of protons passing through the CR-39 / PM-355 type of solid state nuclear track detectors", *Review of Scientific Instruments* 84, (2013).

- [50] Abmayr R., [W.](#), Gais, [P.](#), Paretzke, [H.G.](#), Rodenacker, [K.](#) and Schwarzkopf, [G.](#), "Real-time automatic evaluation of solid state nuclear track detectors with an on-line TV-device", Nuclear Instruments and Methods 147, p. 79–81, 1977.
- [51] James H., Adams Jr. "Automated track measurements in CR39 " , Nuclear Tracks 4, p. 67-76, (1980).
- [52] Guel, S., Moreno, A., Berriel, L.R., Espinosa, G. and Golzarri, J.I., "Nuclear track pseudo coloring by illumination wave front angle variation ", Nuclear Tracks and Radiation Measurements 8, p. 219-222, (1982).
- [53] Radomir Ilić and Mitja Najžer, " Image formation in track-etch detectorsThe large area signal transfer function", Nuclear Tracks and Radiation Measurements 17, Pages 453-460
- [54] Boukhair, A, Haessler, A, Adloff, J.C and Nourreddine, A, "New code for digital imaging system for track measurements", Nuclear Instruments and Methods in Physics Research Section B: Beam Interactions with Materials and Atoms 160, p. 550-555, (2000).
- [55] Patiris, D.L. and Ioannides, K.G., "Discriminative detection of deposited radon daughters on CR-39 track detectors using TRIAC II code", Nuclear Instruments and Methods in Physics Research Section B: Beam Interactions with Materials and Atoms 267, p. 2440-2448, (2009).
- [56] Fuminobu Sato, Takahiro Kuchimaru, Yushi Kato and Toshiyuki Iida, "Digital image analysis of etch pit formation in CR-39 track detector", Japanese Journal of Applied Physics 47, p. 269-272, (2008).
- [57] Mostofizadeh, A., Sun, X. and Kardan, M. R., "Improvement of nuclear track density measurements using image processing techniques", American Journal of Applied Sciences 5, p.71-76, (2008).
- [58] Pugliesi, F., Sciani, V., Pereira, M.A. Stanojev and Pugliesi, R., "Digital system to characterize solid state nuclear track detectors", Brazilian Journal of Physics 37, p.446-449, (2007).

- [59] Law, Y.L., Nikezic, D. and Yu, K.N., "Optical appearance of alpha-particle tracks in CR-39 SSNTDs", *Radiation Measurements* 43, p.128-131, (2008).
- [60] Nikezic, D. and Yu, K.N., "Light scattering from an assembly of tracks in a PADC film", *Nuclear Instruments and Methods in Physics Research Section A: Accelerators, Spectrometers, Detectors and Associated Equipment* 602, p. 545-551, (2009).
- [61] Palacios, D., L. Sajo-Bohusa, Barrosa, H., Fusellab, E. and Avilaa, Y. "Analysis and correction of track overlapping on nuclear track detectors (SSNTD)", *Revista Mexicana DE F'isica* 57 p. 34–39, (2011).
- [62] Hadad, K., Hakimdavoud, M.R. and M. Hashemi-Tilehnoee, "Indoor radon survey in Shiraz-Iran using developed passive measurement method", *Iran. J. Radiat. Res.* 9, p.175-182, (2011).
- [63] Zylstra, A. B., Rinderknecht, H. G., Sinenian N., Rosenberg, M. J., Manue, M., Séguin, F. H., Casey, D. T., Frenje, J. A., Li, C. K., and Petrasso, R. D., "Increasing the energy dynamic range of solid-state nuclear track detectors using multiple surfaces", *Review Of Scientific Instruments* 82, (2011).
- [64] Felice, P. DE, Cotellessa, G., Capogni, M., Cardellini, F., Pagliari, M. and Sciocchetti, G., "The novel track recording apparatus from ssntd for radon measurement", *First East European Radon Symposium* 58, p.115-125, *Rom. Journ. Phys.* (2012).
- [65] Osinga, J. M., Akselrod, M.S., Herrmann, R., Hable, V., Dollinger, G., Jäkel, O. and Greilich, S., "High-accuracy fluence determination in ion beams using fluorescent nuclear track detectors", *Radiation Measurements* 56, p. 294-298, (2013) .
- [66] Al-Jomaily, Firas M., Al-jobouri, Hussain A. and Mheemeed, Ahmed K., "Determination of nuclear track parameters for Ir-115 detector by using of MATLAB software technique", *Journal of Al-Nahrain University* 16, p.117-124, (2013).

## Appendix

"Image processing program for MATLAB software"

```
I = imread('D:1.JPG');
figure(1),imshow(I)
background = imopen(I,strel('disk',100));
I2 = imsubtract(I,background);
figure(2),imshow(I2)
level = graythresh(I2);
bw = im2bw(I2,level);
figure(3),imshow(bw)
[labeled,numtracks] =bwlabel(bw,4); % 4-connected
numtracks % Count all distinct tracks in the image.
for counter = 0:9
    remain = imopen(bw, strel('disk', counter));
    intensity_area(counter + 1) = sum(remain(:));
end
figure(4),plot(intensity_area, 'm - *'), grid on;
title('Sum of Pixel values in opened image as a function of radius');
xlabel('radius of opening (Pixel)');
ylabel('pixel value sum of opened tracks (intensity)');
% rect = [105 125 10 10];
% grain = imcrop(labeled,rect)
RGB_label = label2rgb(labeled, @spring, 'c', 'shuffle');
figure(5), imshow(RGB_label)
trackdata = regionprops(labeled,'basic')
trackdata(20).Area
alltracks = [trackdata.Area];
max_area = max(alltracks)
bigtrack = find(alltracks==max_area)
A=mean(alltracks)
D=sqrt(A/3.14)*0.4225*2
A1=(alltracks);
D1=sqrt(A1/3.14)*0.73*2;
nbins=20;
figure(6),hist(D1,nbins);
xlabel("Track diameter-D_T(μm)"),ylabel("Tracks number-N")
figure(7),hist(alltracks,nbins);
xlabel("Track area-A_T(μm^2)"),ylabel("Tracks number-N")
```

## الملخص

تم استخدام تقنية المعالجة الصورية الحاسوبية في الكثير من الدراسات والبحوث العلمية و استنتجت منها عدد من العلاقات الرياضية . في هذه الدراسة تم استخدام برنامجين للمعالجة الصورية البرنامج الاول هو MATLAB، والثاني Image-J . اعتمدت تلك البرامج في تحليل اثار جسيمات الفا-  $\alpha$  على كواشف الأثر النووي نوع CR-39 و CN-85 . حيث تم تشعيع الكواشف بالنيوترونات الحرارية من المصدر ( $^{241}\text{Am}-^9\text{Be}$ ) ذو نشاط اشعاعي 12Ci وفيض نيوتروني  $10^5 \text{ n} \cdot \text{cm}^{-2} \cdot \text{s}^{-1}$  . تم الحصول على جسيمات الفا-  $\alpha$  الساقطة على الكواشف من خلال تفاعل  $^{10}\text{B}(n, \alpha)^7\text{Li}$  بعد تغطيتها بأقراص حامض البوريك  $\text{H}_3\text{BO}_3$  . كانت فترات زمن التشعيع -  $T_D$  لكلا الكاشفين هي 4 ، 8 ، 16 و 24 ساعة .

من خلال تحليل نتائج مستخرجات برنامج الـ MATLAB عند الكواشف المشعة مسبقا وجدت العلاقات التالية :

- (أ) ان زمن التشعيع يتصرف بعلاقة خطية مع معاملات الأثر النووي التالية :
- العدد الكلي للأثار -  $N_T$
  - عدد الاقصى للأثار -  $M_{RD}$  (بالاعتماد على قطر الأثر -  $D_T$ ) وضمن مديات منطقة الاستجابة الإشعاعية ( $2.5 - 4 \mu\text{m}$ ) و ( $2.5 - 5 \mu\text{m}$ ) لكل من الكاشف CR-39 و الكاشف CN-85 على التوالي
  - العدد الاقصى للأثار -  $M_D$  (دون الاعتماد على قطر الأثر -  $D_T$ ).
- (ب) ان زمن التشعيع -  $T_D$  يتصرف بعلاقة أسية مع العدد الاقصى للأثار -  $M_{RA}$  (بالاعتماد على مساحة الأثر -  $A_T$ ) وضمن مديات منطقة الاستجابة الإشعاعية ( $7 - 24 \mu\text{m}$ ) و ( $9 - 35 \mu\text{m}$ ) لكل من الكاشف CR-39 و الكاشف CN-85 على التوالي .
- (ت) ان زمن التشعيع -  $T_D$  يتصرف بعلاقة لوغاريتمية مع العدد الاقصى للأثار -  $M_A$  (دون الاعتماد على مساحة الاثر -  $A_T$ ).

في حين من خلال تحليل نتائج مستخرجات برنامج الـ Image-J عند الكواشف المشعة مسبقا وجد ان زمن التشعيع -  $T_D$  يتصرف بعلاقات خطية مع معاملات الأثر النووي التالية :

- (أ) العدد الكلي للأثار -  $T_D$ .
- (ب) العدد الاقصى للأثار -  $M_{RA}$  (بالاعتماد على مساحة الأثر -  $A_T$ ) وضمن مديات منطقة الاستجابة الإشعاعية ( $12 - 24 \mu\text{m}$ ) و ( $5 - 27 \mu\text{m}$ ) لكل من الكاشف CR-39 و الكاشف CN-85 على التوالي .
- (ت) العدد الاقصى للأثار -  $M_A$  (دون الاعتماد على مساحة الاثر -  $A_T$ ) .

تبين من خلال دراستنا ان برنامج الـ MATLAB كان اكثر تحليلا ودقة من برنامج الـ Image-J وذلك من خلال السلوك اللوغاريتمي لكلا الكاشفين CR-39 و CN-85 بين زمن التشعيع -  $T_D$  واعلى قمة للأثر -  $M_A$  (دون الاعتماد على مساحة الأثر -  $A_T$ ).

وهناك امكانية استخدام برنامج الـ MATLAB مستقبلا في تحليل معاملات الأثر النووي الاخرى ومن ضمنها سرعة قشط الأثر النووي -  $V_T$  ، والزاوية الحرجة -  $\theta_T$  بالإضافة الى عمق الأثر النووي -  $D_p$  .

ان تقنية التحليل الصوري لكواشف الأثر النووي التي تم الحصول عليها في هذه الدراسة وخاصة تلك التي تتعلق بقطر الأثر النووي -  $D_T$  يمكن الاعتماد عليها في تشخيص بواعث جسيمات الفا ، بالإضافة الى إدخال هذه التقنية في تحضير الفلاتر والاعشبة النانوية في مجال بحوث النانو تكنولوجي .



جمهورية العراق  
وزارة التعليم العالي والبحث العلمي  
جامعة النهرين  
كلية العلوم  
قسم الفيزياء

# معالجة رقمية وتحليلية للأثار الناتجة من التشعيع بالمصدر النيوتروني $^{241}\text{Am}-^9\text{Be}$ على بعض كواشف الأثر النووي للحالة الصلبة

رسالة

مقدمه الى كلية العلوم/ جامعة النهرين  
كجزء من متطلبات نيل درجة الماجستير في علوم الفيزياء

من قبل

مصطفى يوسف رجب

بكالوريوس (٢٠١١)

إشراف

أ.م.د. حسين علي الجبوري